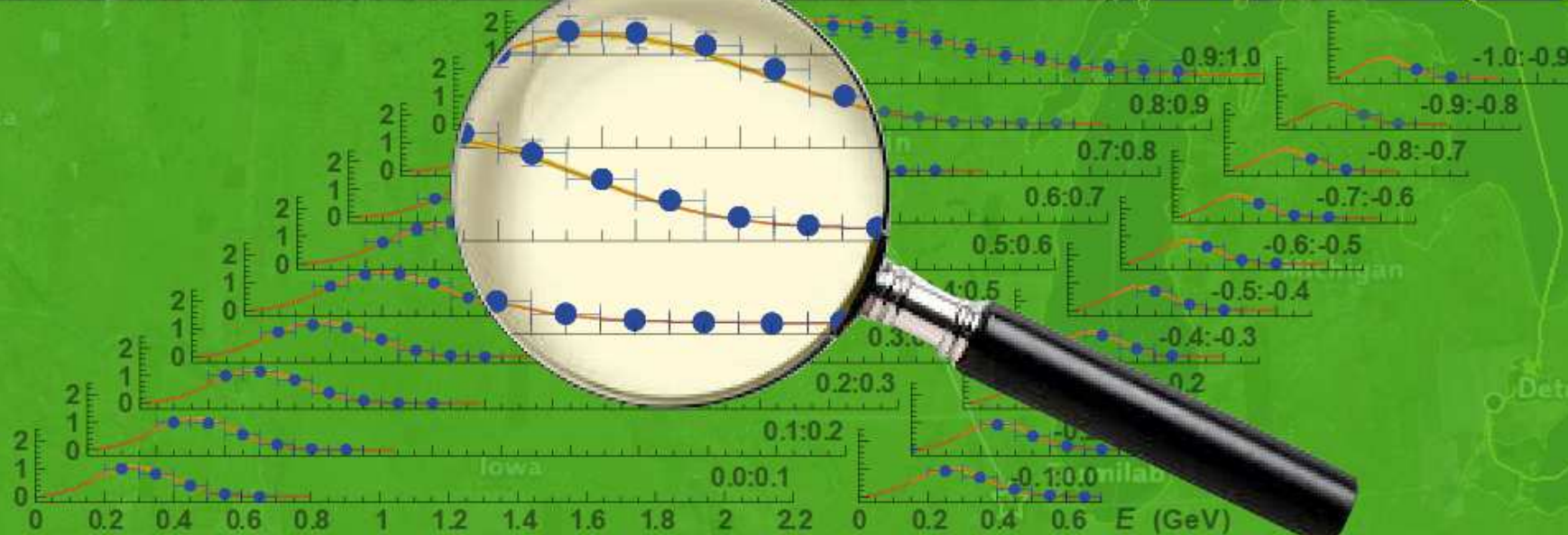


Running axial mass for CCQE neutrino-nucleus scattering

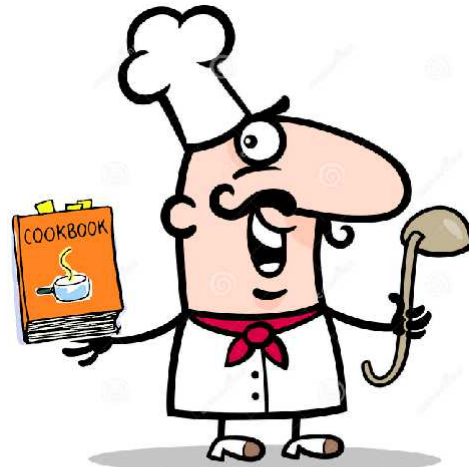
I. Kakorin, K. Kuzmin, & V. Naumov
JINR NOvA Group (Dubna)



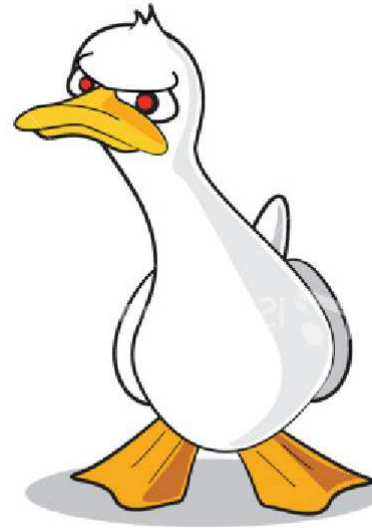
NOvA Collaboration Meeting at FNAL, October 20–23, 2016

Ohio

The aim of this report is to provide a simple “**cookbook recipe**” for a precise description of the CCQE neutrino and antineutrino interactions with nuclei using only **two adjustable parameters**.



Cooking a duck



NO! Ducking a cook

We do not intend discussing the physical meaning of the proposed recipe; instead we wish to demonstrate its usefulness as an **empirical tool** which could be used in the data processing of the neutrino oscillation experiments with accelerator and atmospheric (anti)neutrino beams.

Outline

- **Introduction**
- **Total Cross Sections – Recent data**
- **FNAL MiniBooNE 2010–2013**
- **FNAL MINER ν A 2013**
- **T2K ND280 2016**
- **Parameters of the Smith–Moniz RFG Model**
- **Comparison with the early “golden” data**
- **Comparison with certain datasets unclaimed in the fits**
- **Implementation in GENIE**
- **Conclusions**
- **Backup slides (details of the fit, inputs, and all that)**

Introduction

One of the main sources of ambiguity in predicted neutrino event rates in the accelerator experiments at low and intermediate energies is caused by **nuclear effects** for the charged-current quasielastic (CCQE) $\nu/\bar{\nu}$ interactions with various detection targets.

Another closely-related problem arises from the experimental uncertainty of the **nucleon axial mass parameter, M_A** , in the dipole model of the nucleon axial form factor

$$F_A(Q^2) = F_A(0) \left(1 + \frac{Q^2}{M_A^2}\right)^{-2}.$$

The most familiar Relativistic Fermi Gas (RFG) model cannot describe the up-to-date CCQE data (NOMAD, MiniBooNE, MINER ν A, T2K, etc.) with a unique value of M_A .

In fact, there are a lot of different models based on the Fermi-gas approach. One of the most popular models is the model by **Smith and Moniz (SM)**.^a Below, the term “**RFG**” is used for the slightly-modified SM model,^b with an updated set of the input parameters.

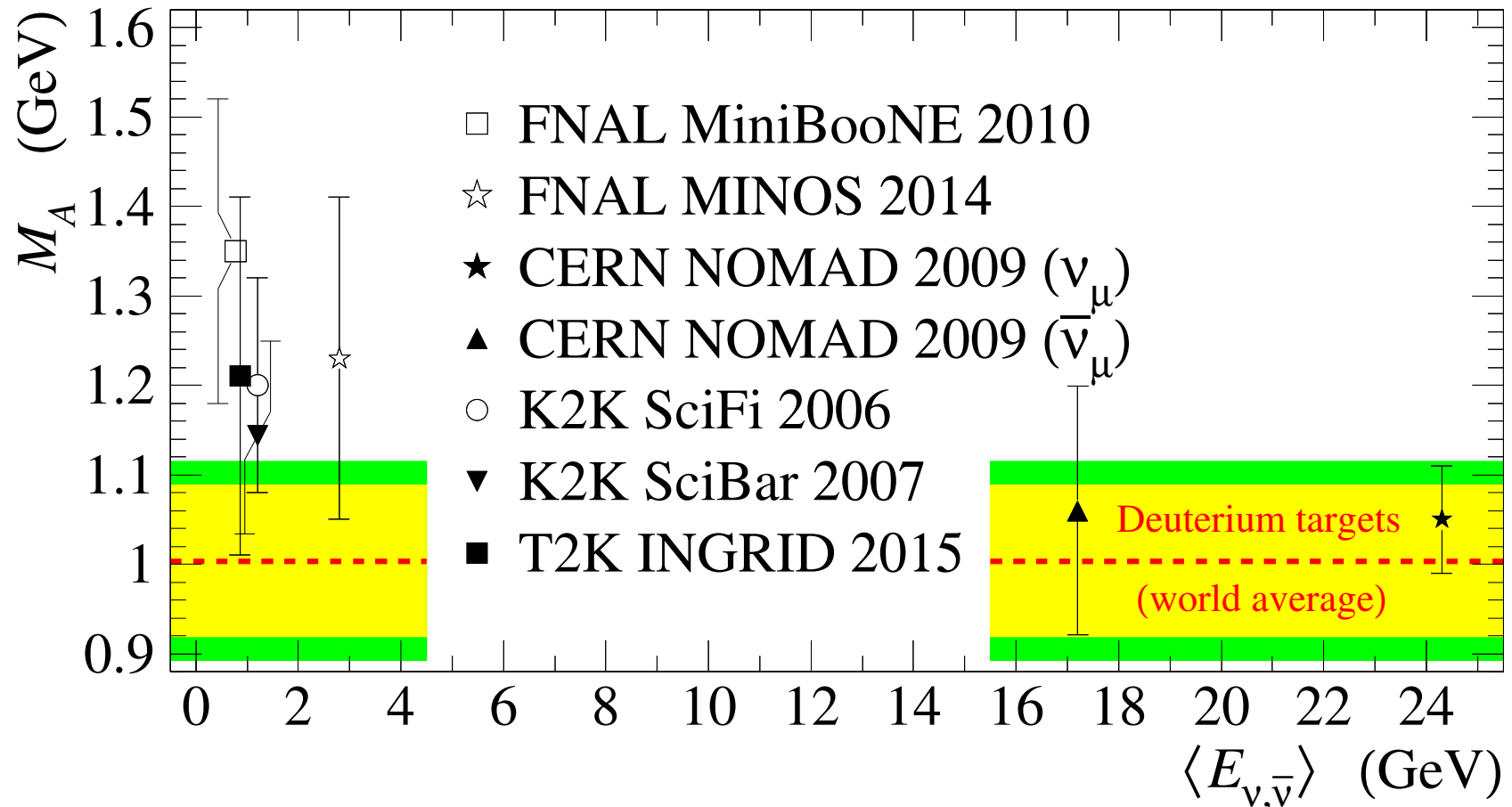
NOTE: The default RFG model in GENIE is the **Bodek-Ritchie (BR)** model rather than the **SM**.

^aR.A. Smith and E.J. Moniz, “*Neutrino reactions on nuclear targets,*” Nucl. Phys. B **43**, 605 (1972); erratum – *ibid.* **101**, 547 (1975).

^bK.S. Kuzmin, V.V. Lyubushkin and V.A. Naumov, “*Quasielastic axial-vector mass from experiments on neutrino-nucleus scattering,*” Eur. Phys. J. C **54**, 517 (2008) [arXiv:0712.4384 [hep-ph]].

Some nuclear models currently on the market.

- **RFG Extensions:**
 - **Local Fermi Gas (LFG)** or **Local Density Approximation (LDA)**
[Fermi momenta and separation energies are functions of the position in the nucleus]
 - **Spectral Function (SF)**
[correlations between removal energies and initial state momenta of the nucleons, Gaussian spectrum of each shell]
- **Scaling and Superscaling (SuSA) models.**
- **Relativistic Mean Field (RMF) models.**
- **Relativistic Green's Function (RGF) models.**
- **Transverse Enhancement Model (TEM).**
- **Many-body Currents:**
 - **Short-range correlations (SRC),**
 - **Meson Exchange Currents (MEC, 2p2h),** \Leftarrow (most popular and successful)
 - **Random Phase Approximation (RPA) and Quasiparticle RPA (QRPA).**
- **Hotchpotchs** (e.g., SuSA+MEC, MEC+RPA, etc.).



The nucleon axial mass vs. neutrino energy, obtained in several recent experiments. The dashed line and surrounding shaded double band represent the value of M_A and its 1σ and 2σ uncertainties extracted from the deuterium experiments (M_A^D hereafter).

This effect is now explained to an extent by the advanced nuclear models.

Besides, the much simpler RFG-based calculations can be somewhat fine-tuned by using a larger value of M_A in the lower energy range.^a This observation can be used for an **empirical** description of the experimental data within the RFG model. Namely, it is shown^b that disadvantages of the RFG model can be **effectively compensated** by introducing the **energy-dependent (“running”) axial mass**

$$M_A^{\text{run}} = M_0 \left(1 + \frac{E_0}{E_\nu} \right)$$

with the parameters values

$$M_0 = 1.006 \pm 0.025 (0.030) \text{ GeV} \quad \text{and} \quad E_0 = 334_{-54}^{+58 (70)} \text{ MeV}$$

$$\left(\frac{\chi^2}{\text{NDF}} = \frac{300.4}{435 - 19} = 0.72 \right)$$

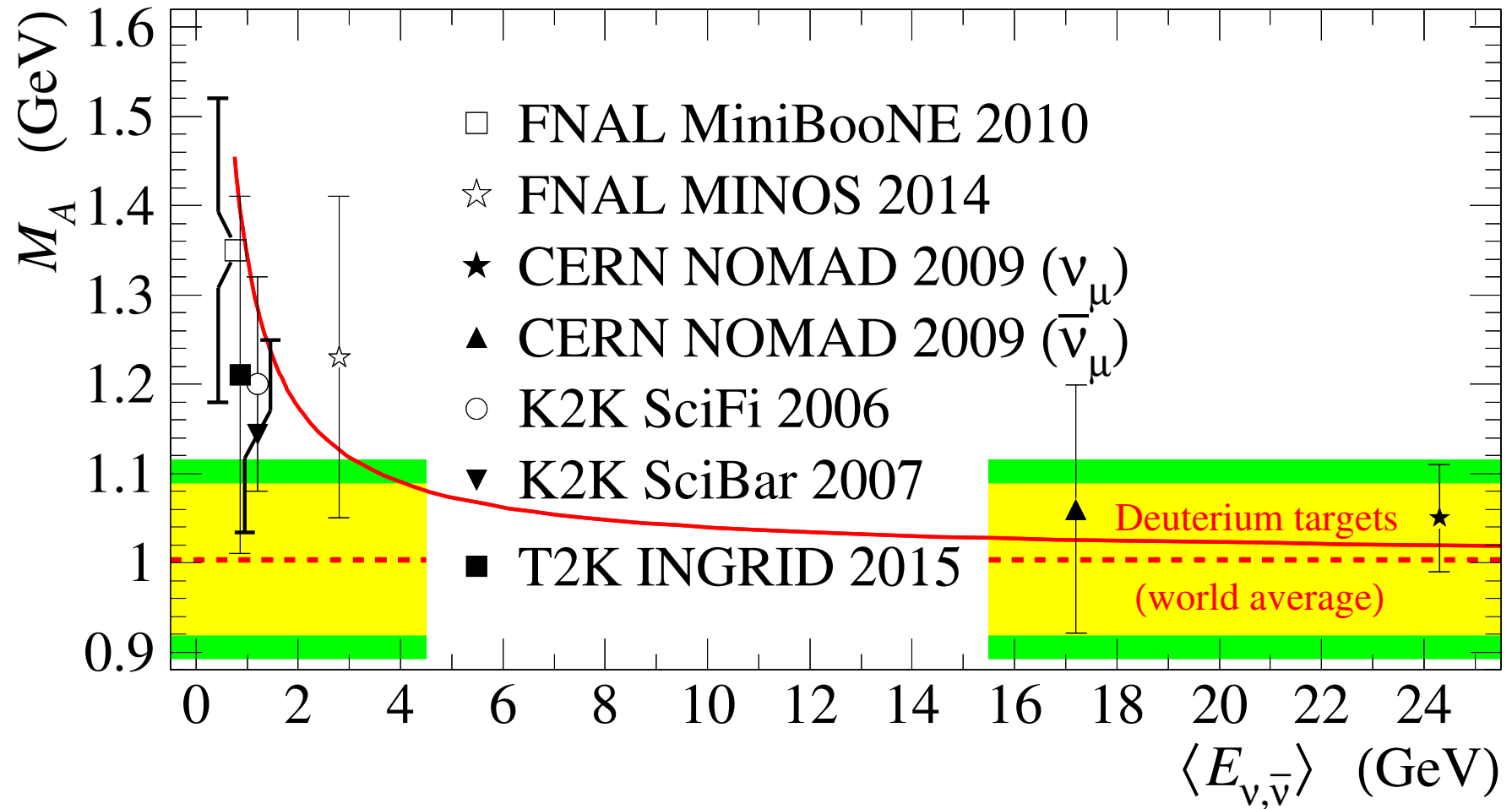
obtained from a global fit to all available data on neutrino-nucleus and antineutrino-nucleus CCQE scattering. This allows to phenomenologically account for the intricate nuclear effects beyond RFG, significant at low and medium (anti)neutrino energies, for the nuclei with $A \gtrsim 10$.

As a bonus, the parameter M_0 can be treated as the **“current” dipole axial mass of the nucleon**, that is the good old parameter M_A appearing in the weak hadronic current.

^aA lot of papers; see, e.g., A.M. Ankowski, O. Benhar, C. Mariani and E. Vagnoni, Phys. Rev. D **93**, 113004 (2016) [arXiv:1603.01072 [hep-ph]] and references therein.

^bK. S. Kuzmin and V. A. Naumov, in preparation; see also Refs. [70–72] in backup slide 103.

The red solid curve represents the behavior of M_A^{run} :

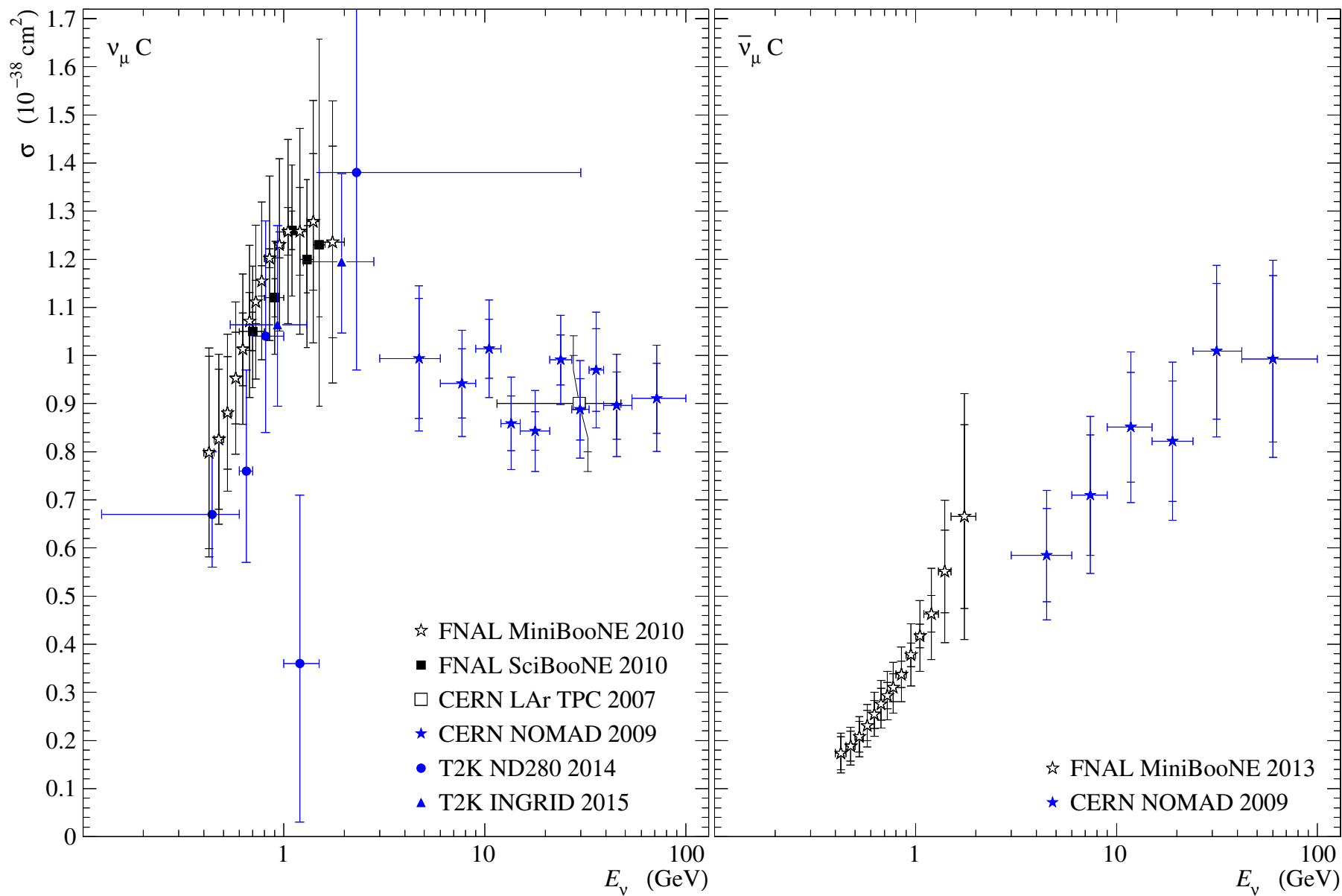


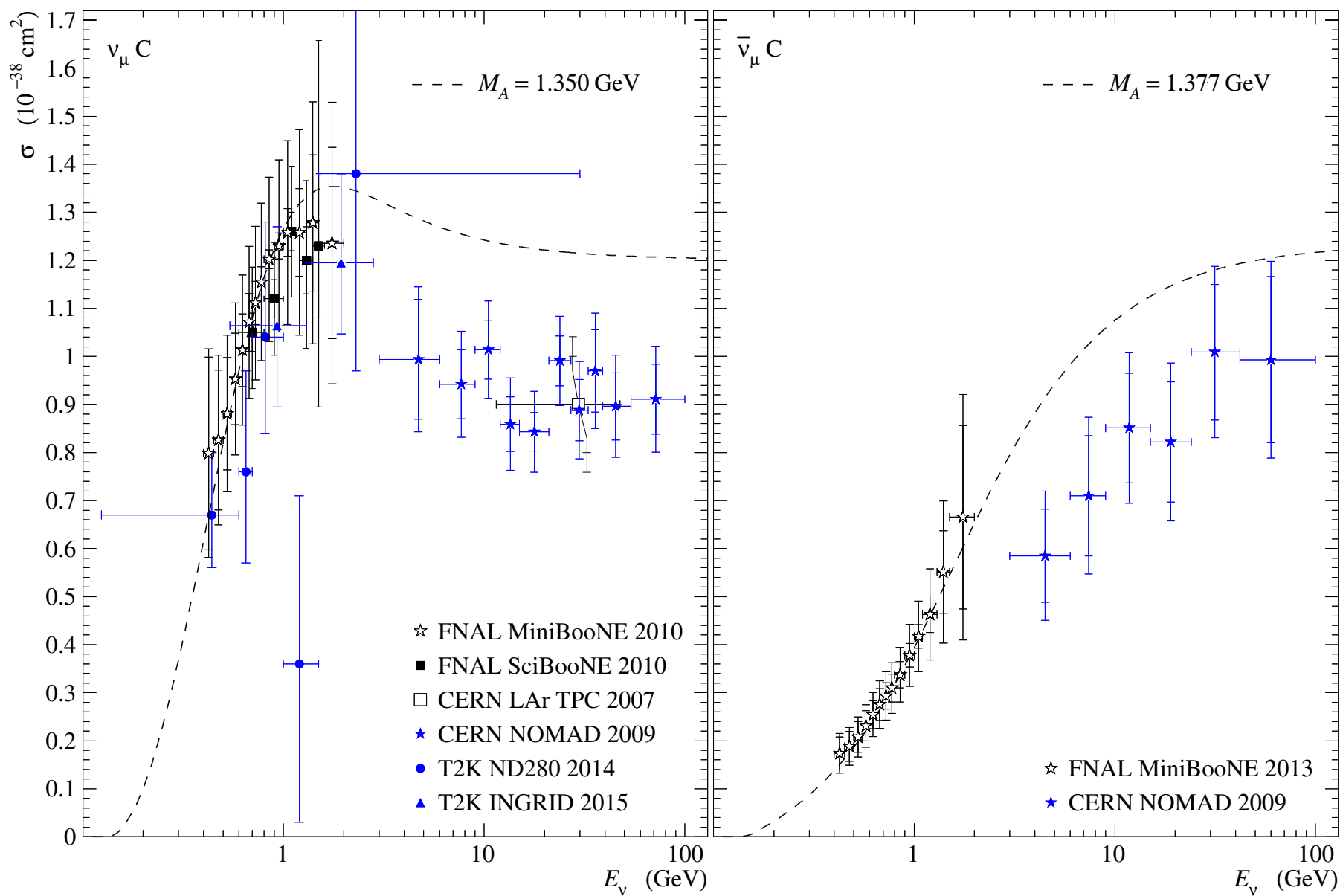
You may not be much impressed by that...

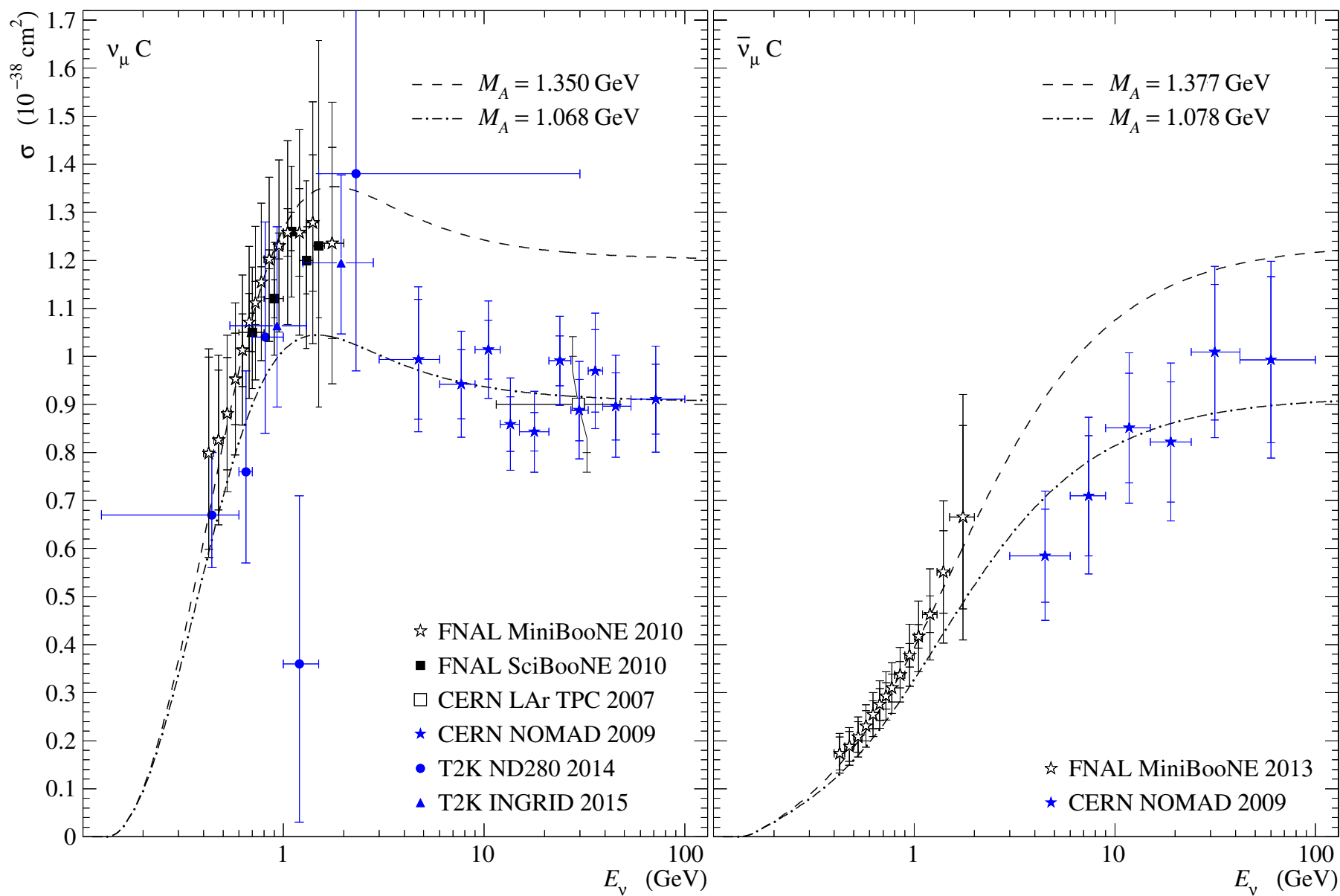
But let us now examine, how does the running axial mass describe the real data rather than the values of M_A forcibly extracted from these data.

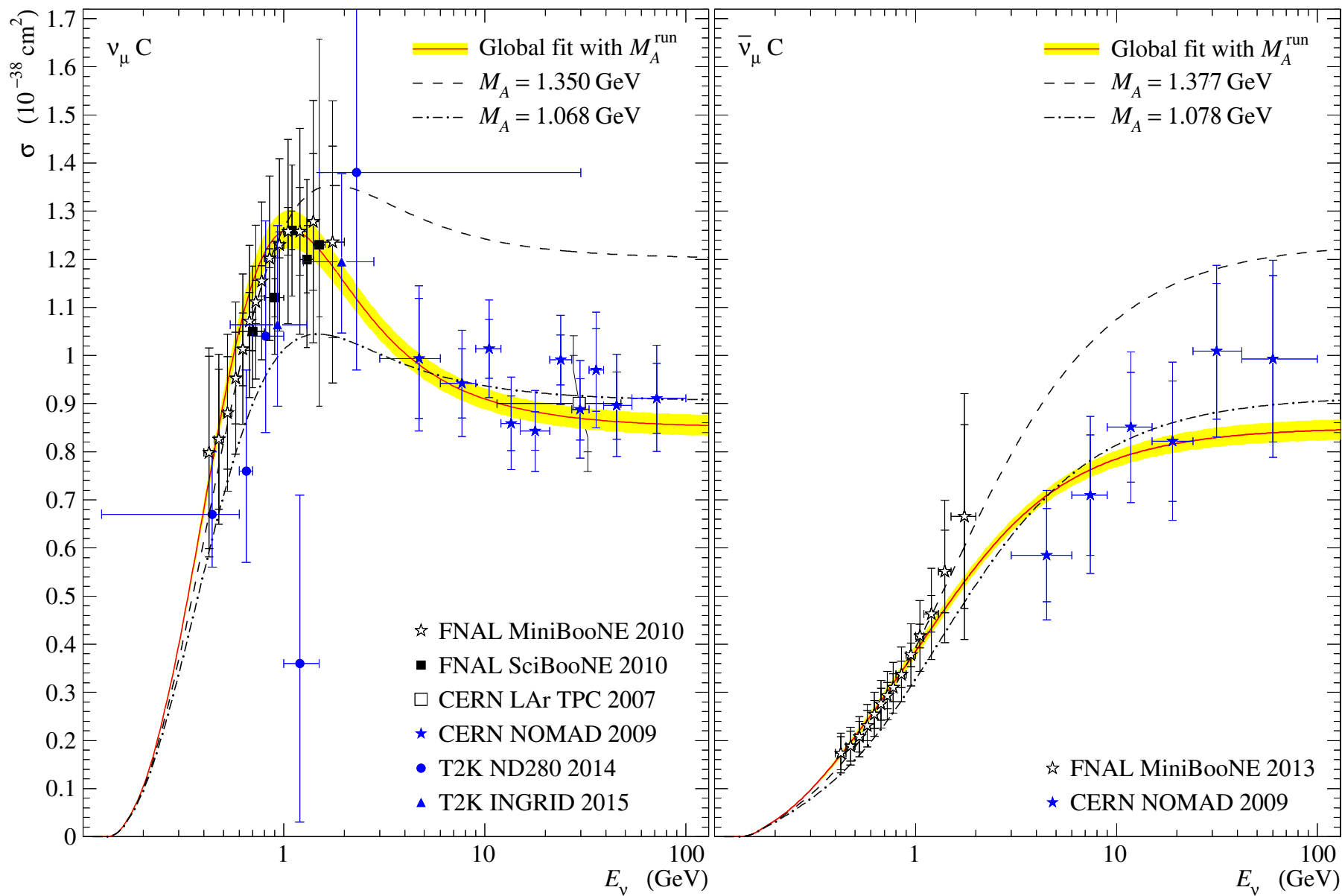
Total Cross Sections

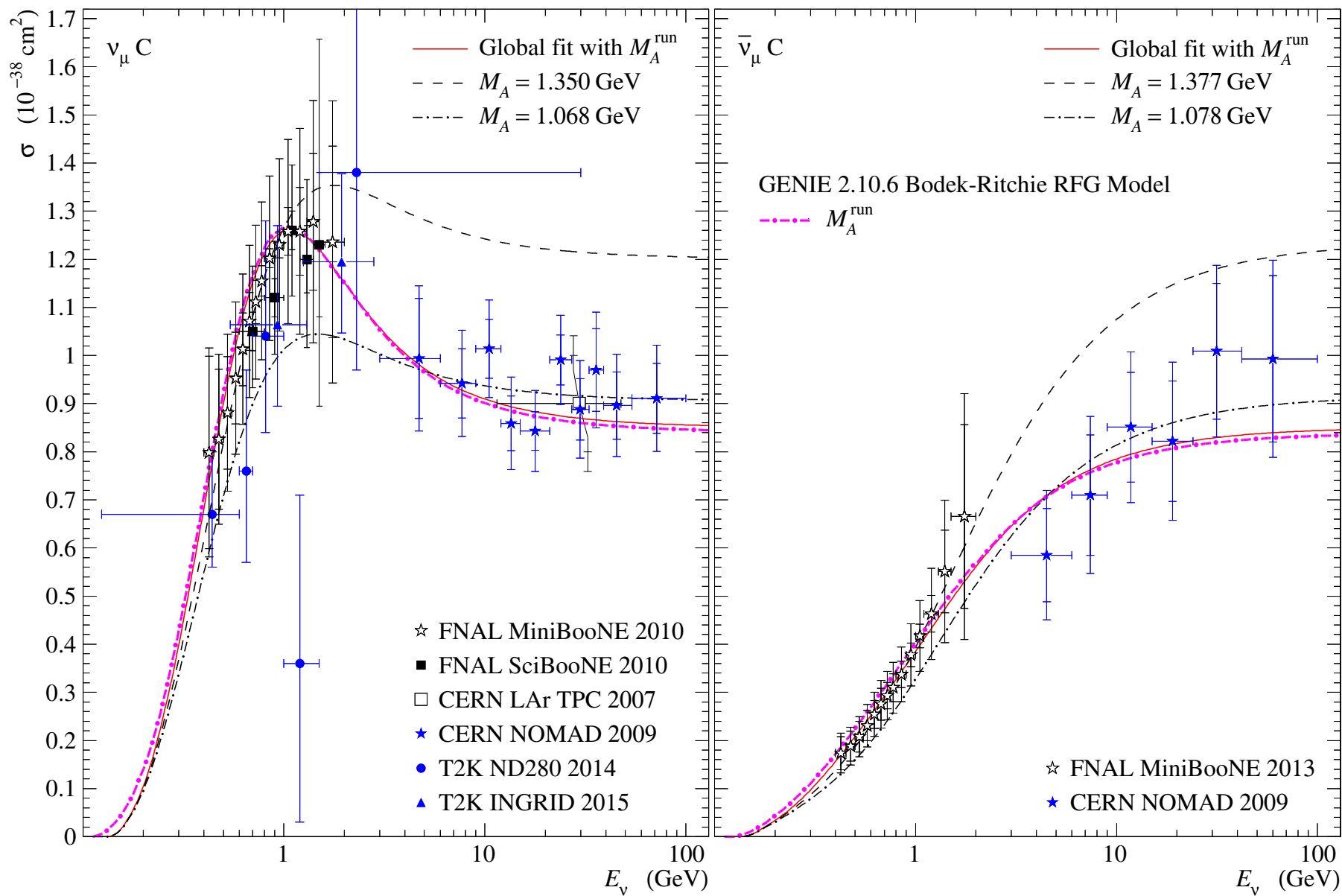
Recent data

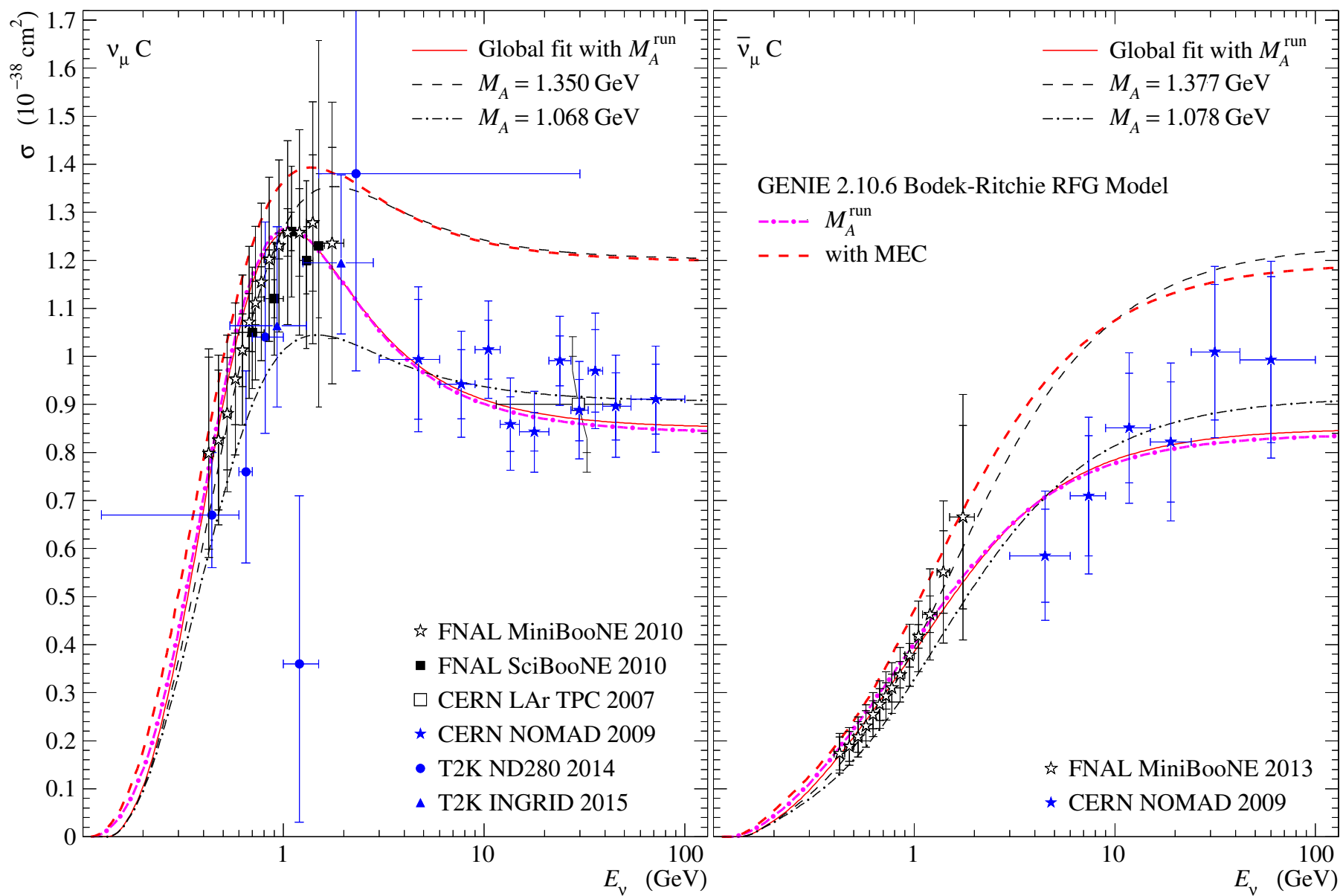


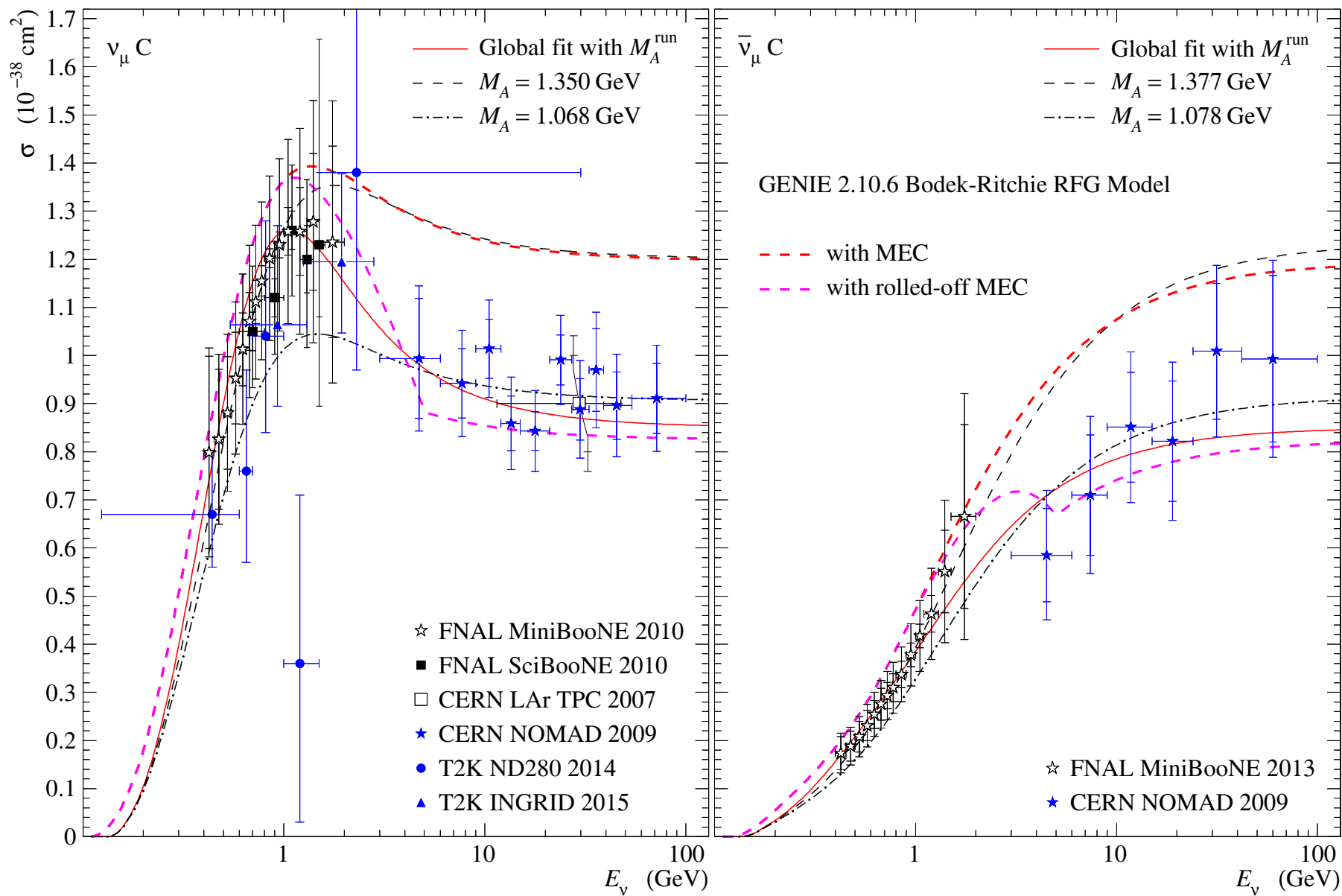




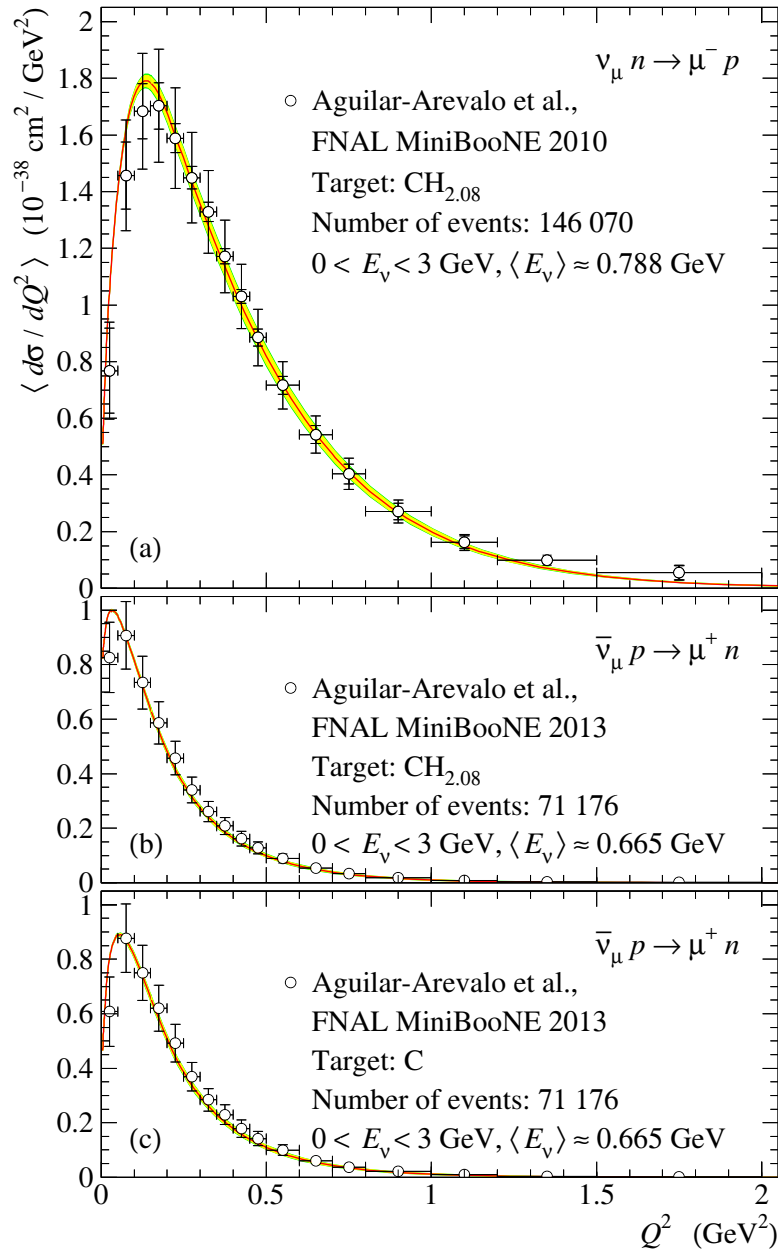




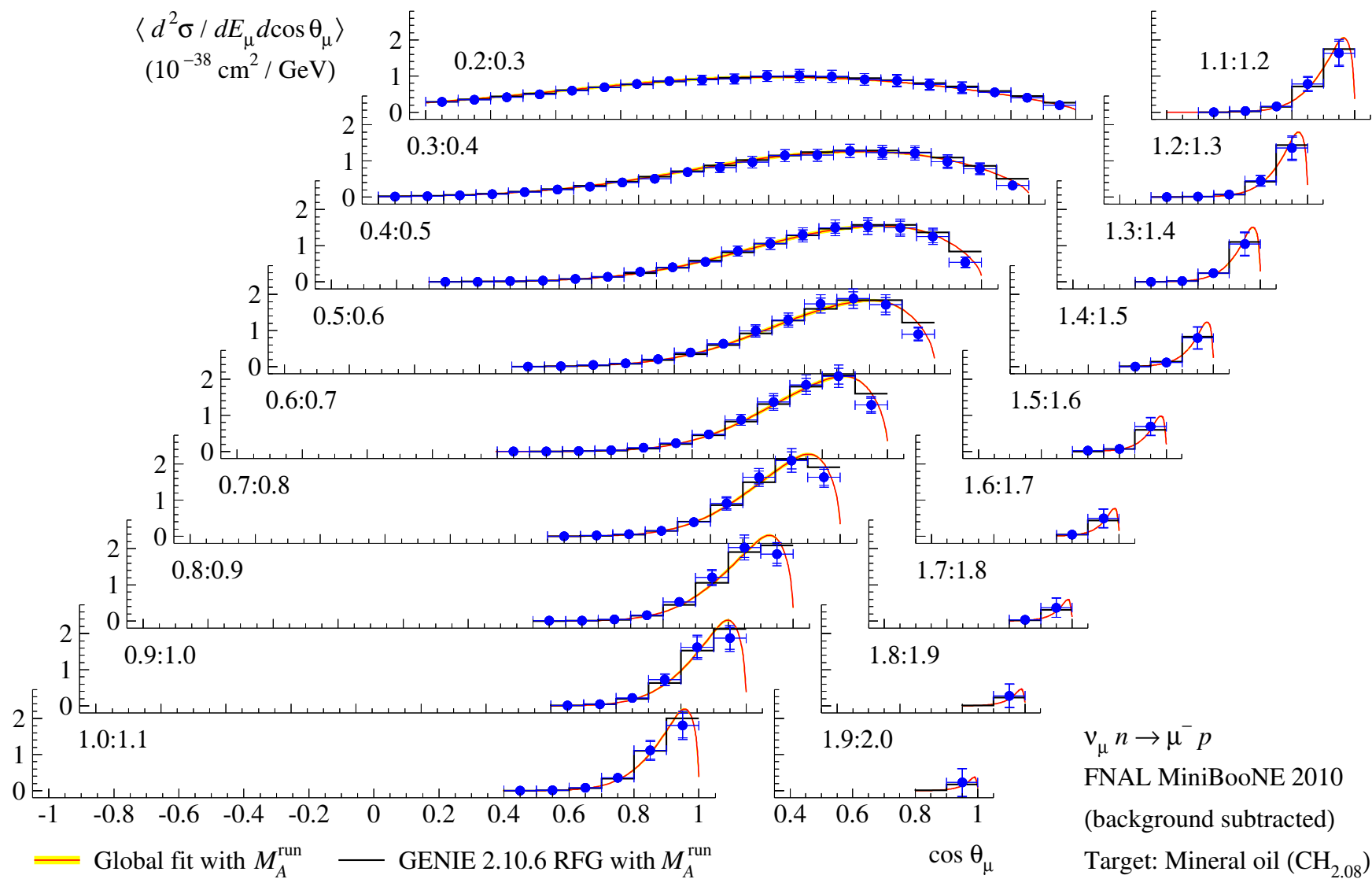


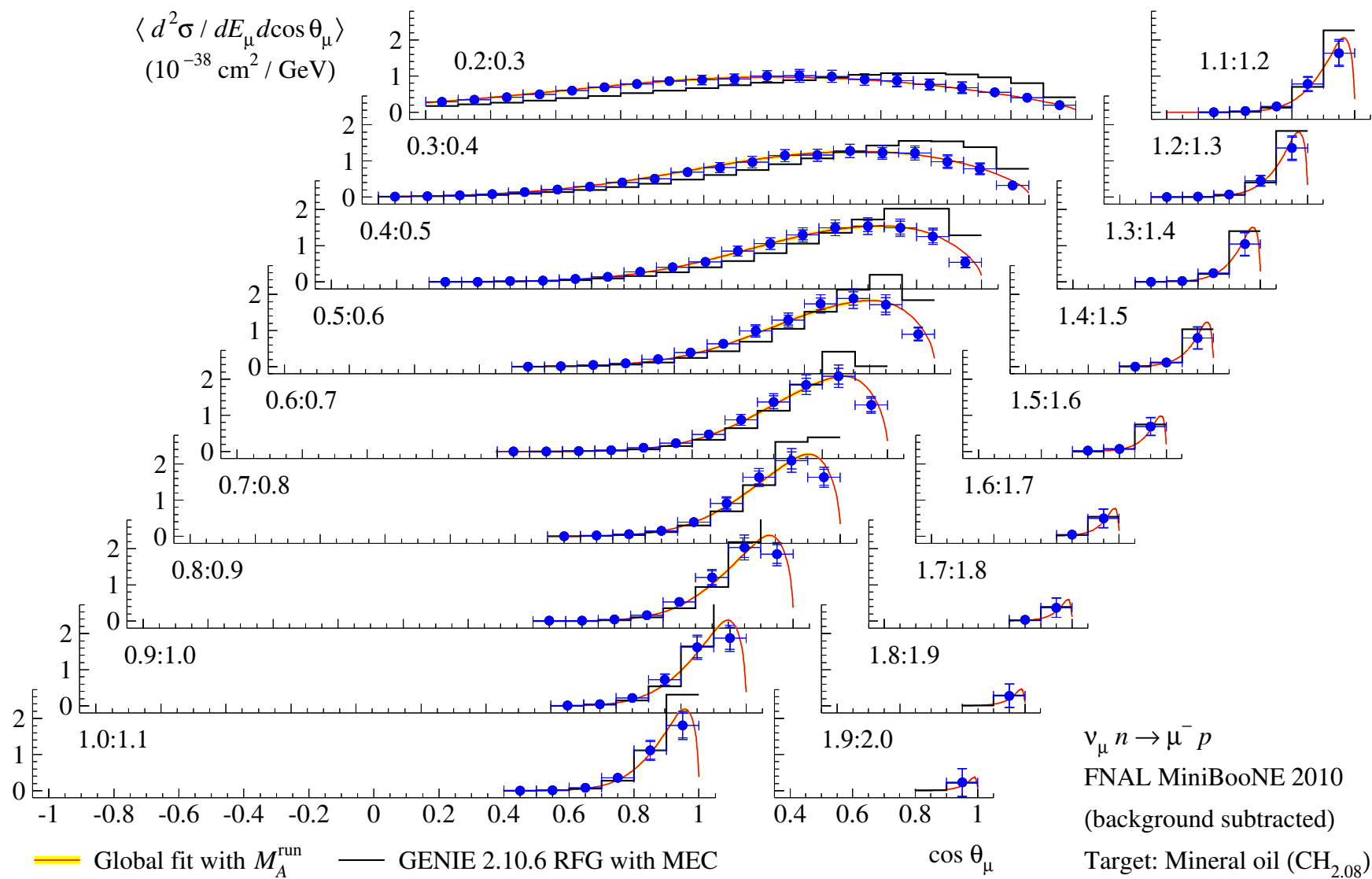


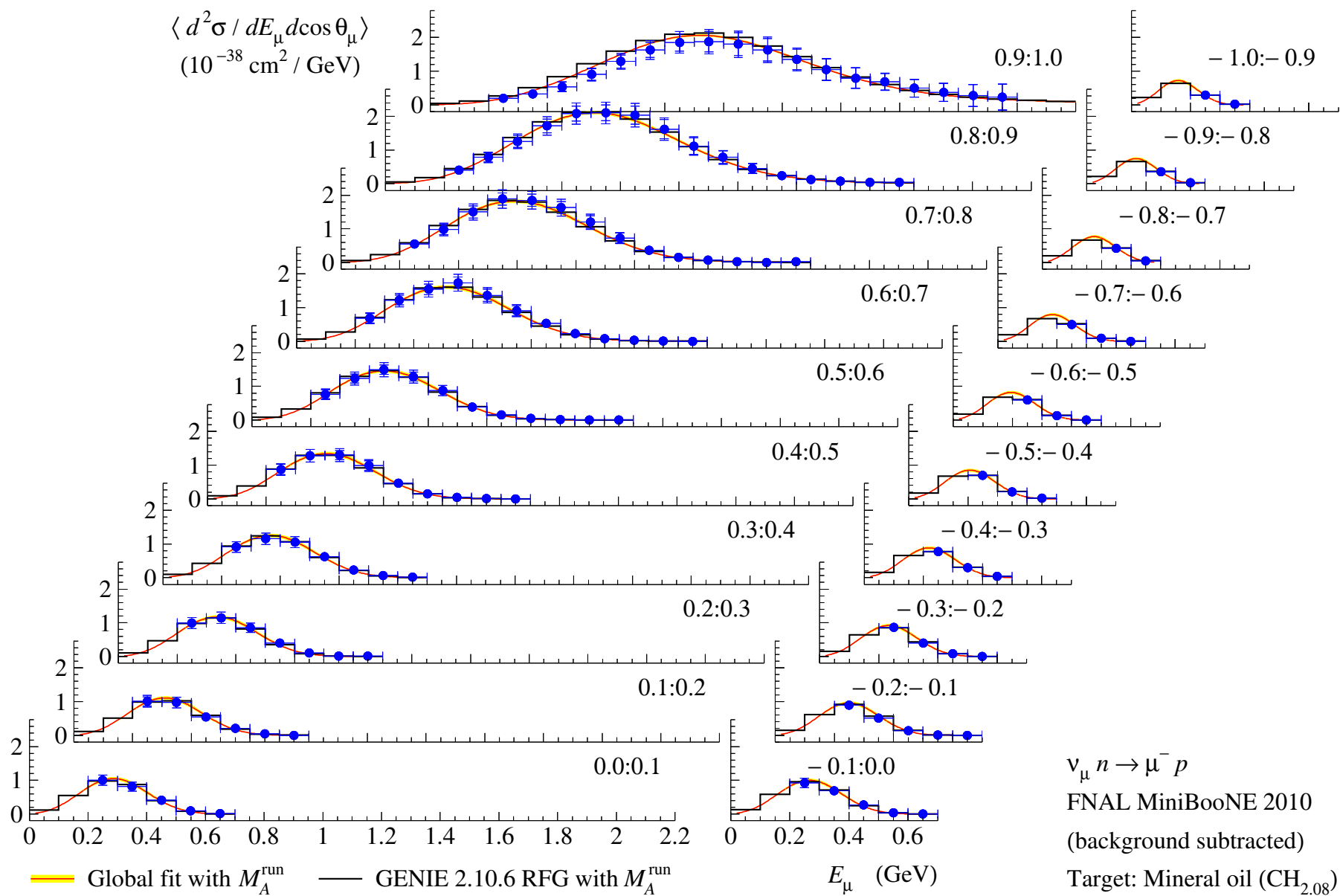
FNAL MiniBooNE 2010–2013

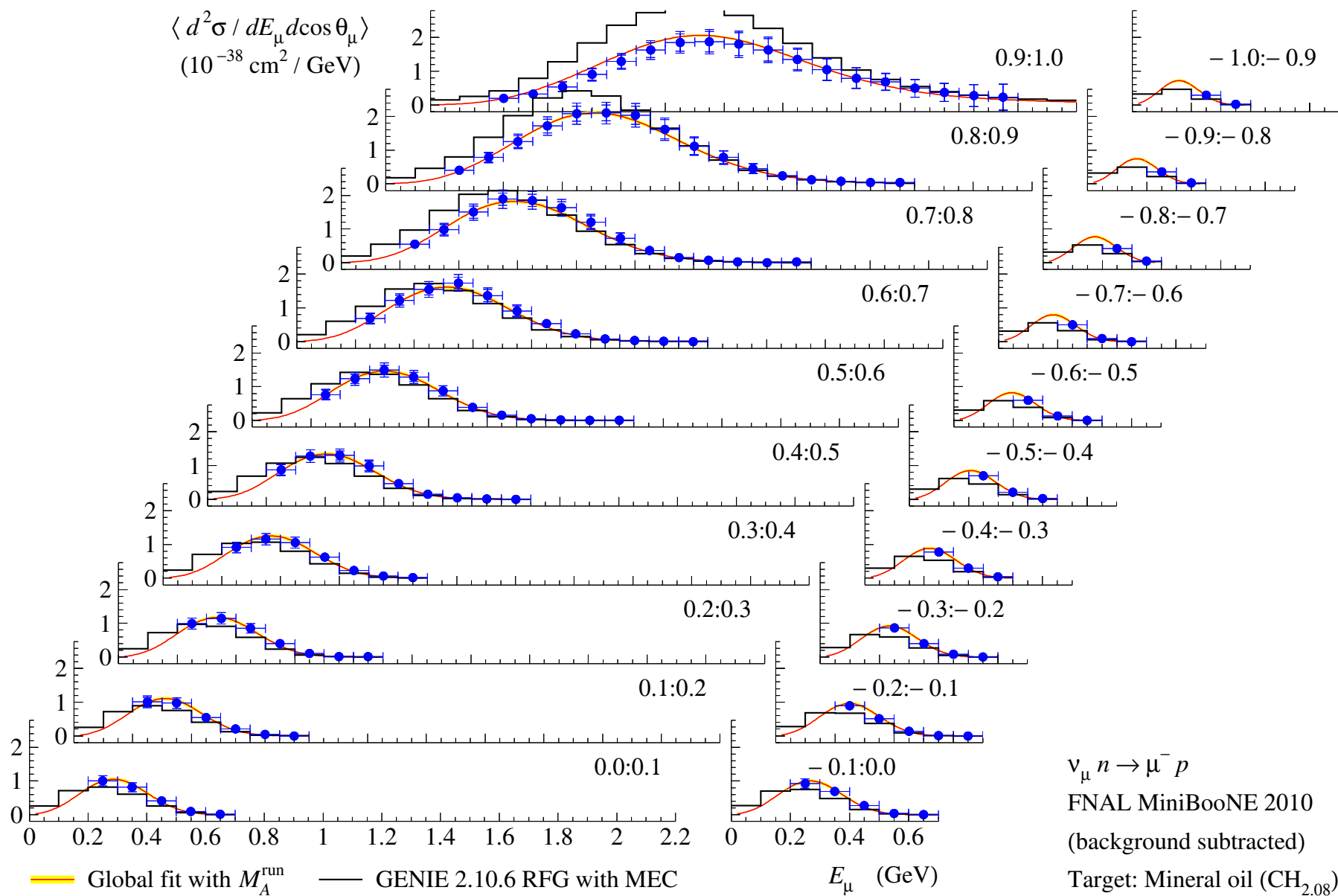


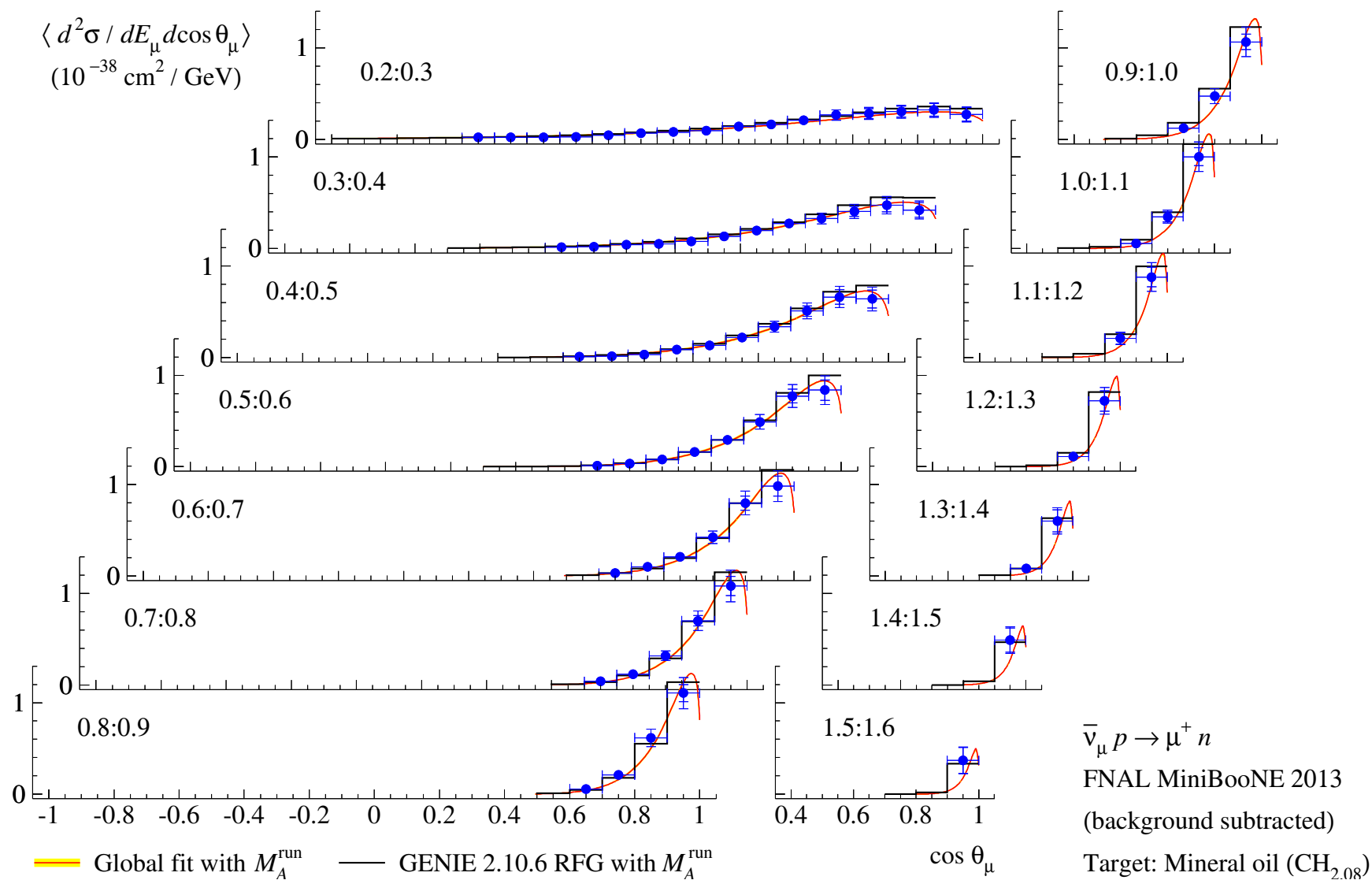
← Recalculated by the MiniBooNE Co. from the “raw” data on the CH_{2.08} target. The agreement is a little bit worse and we know why...

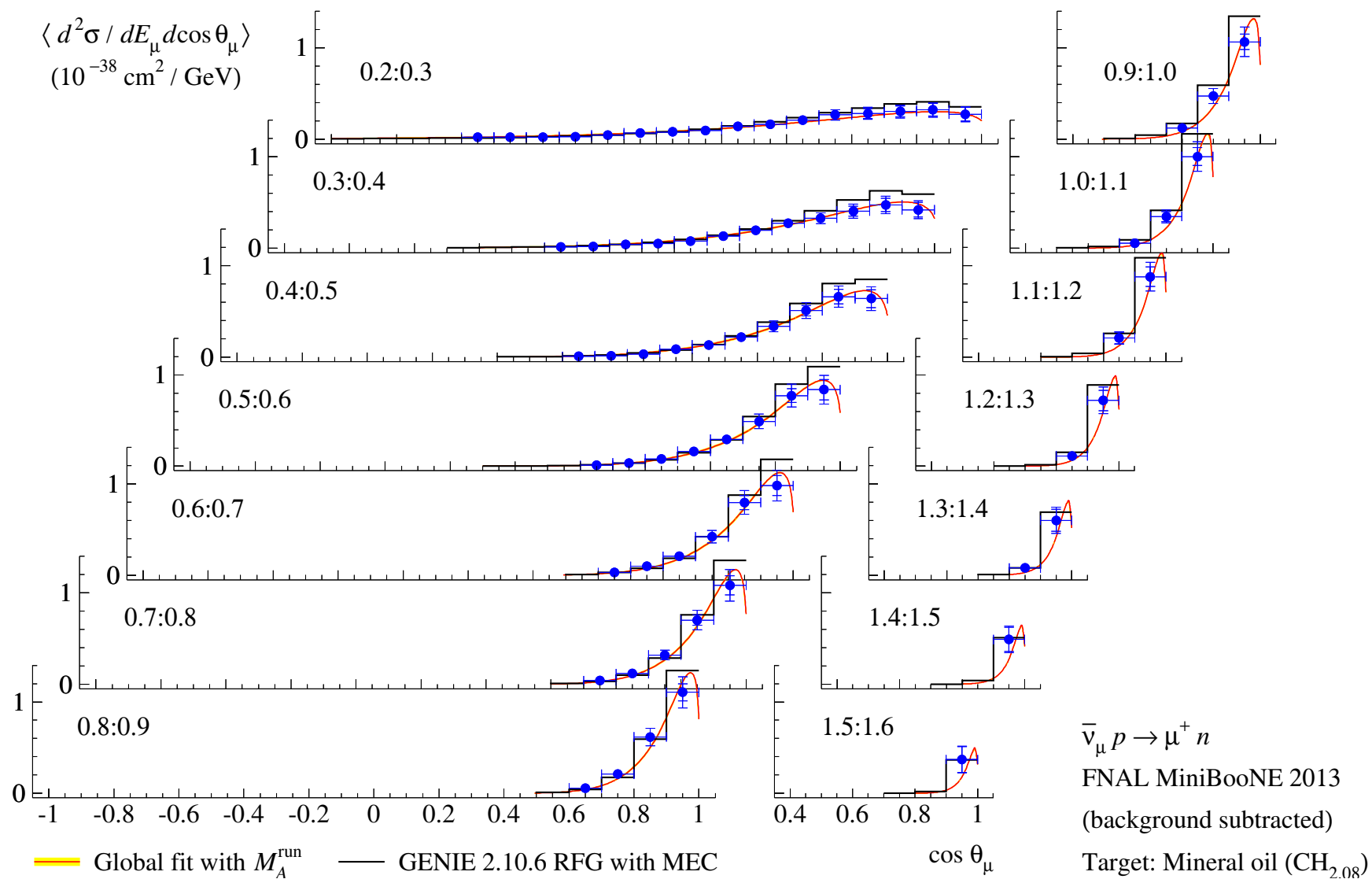


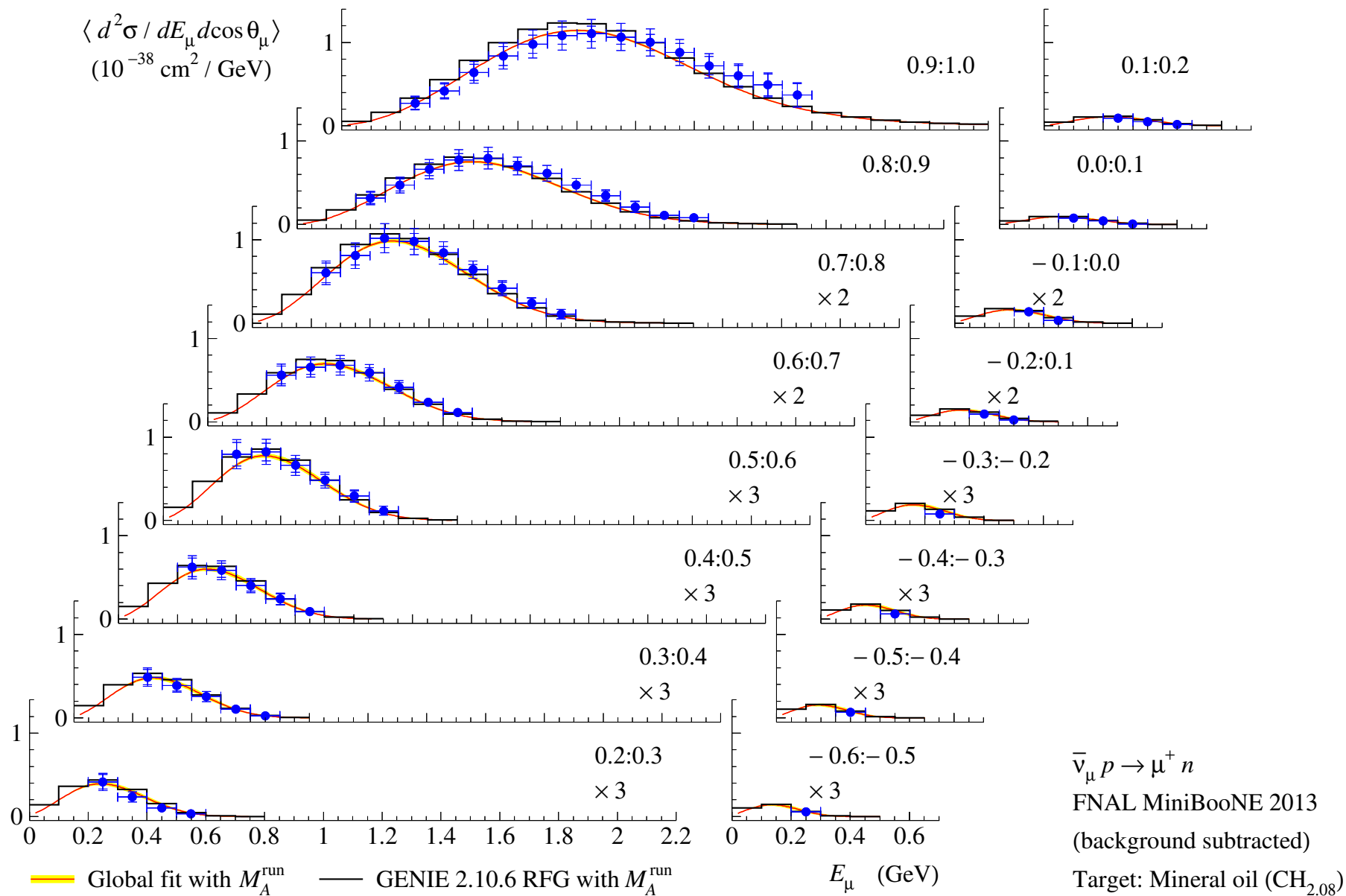


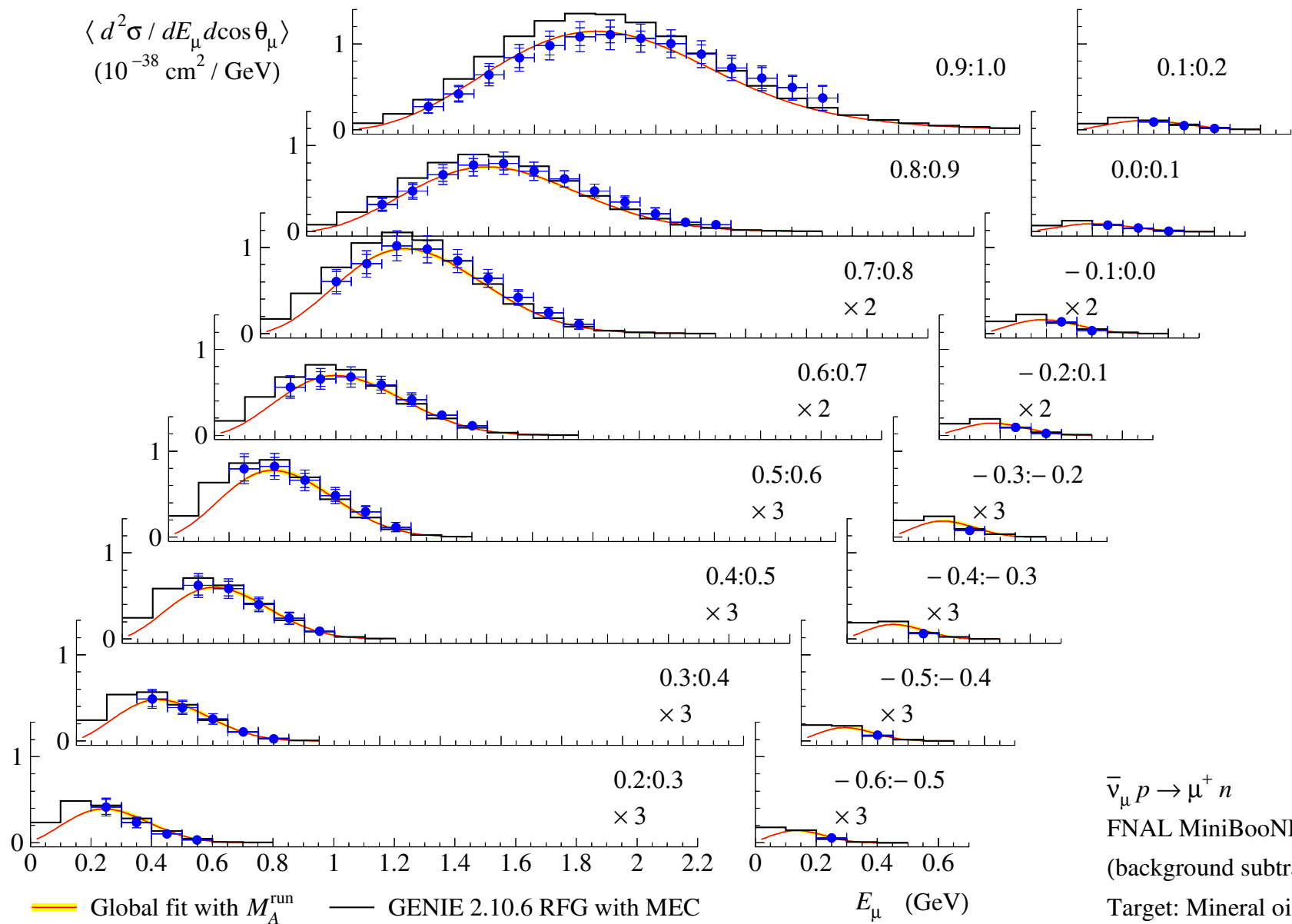






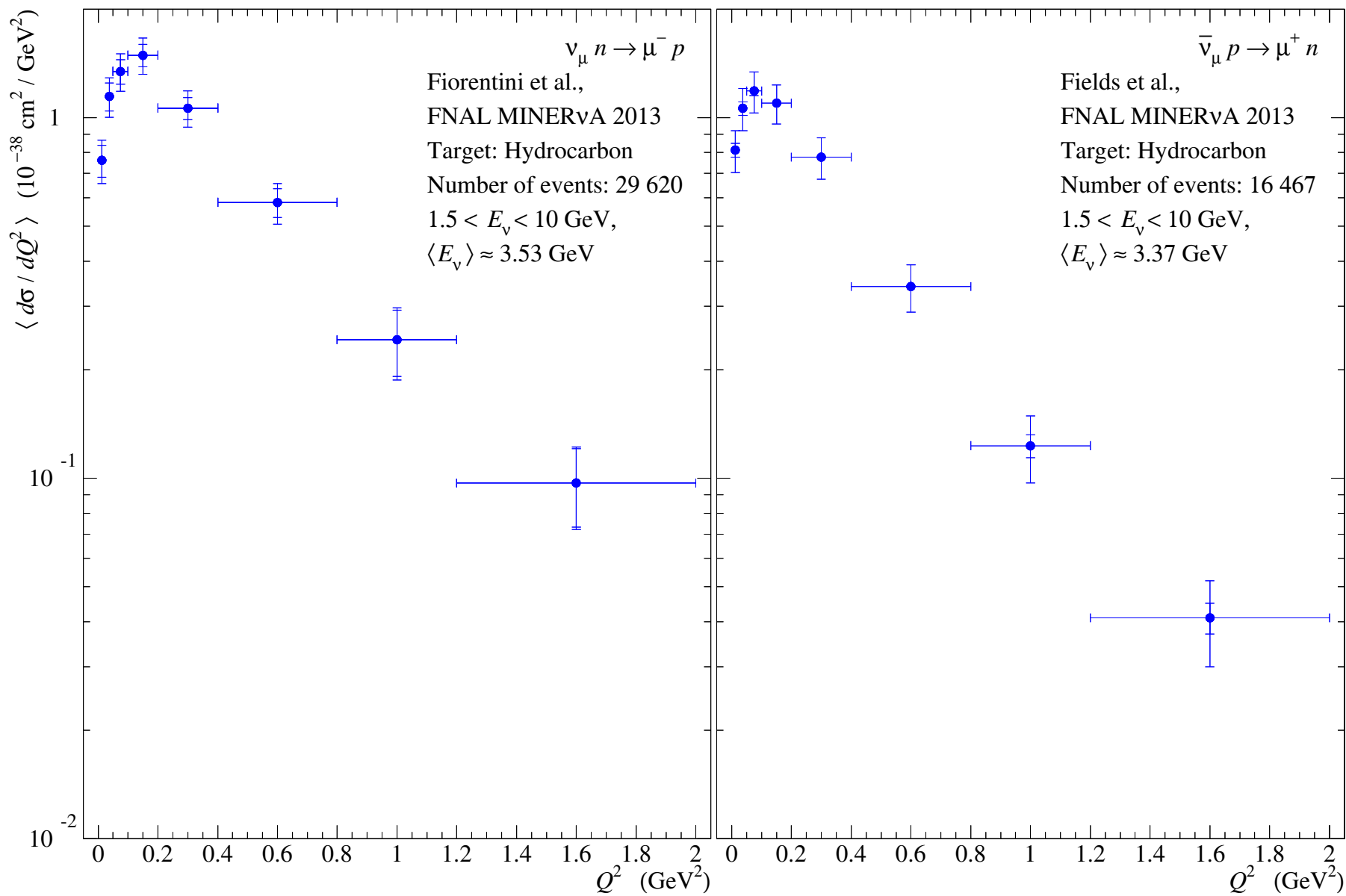


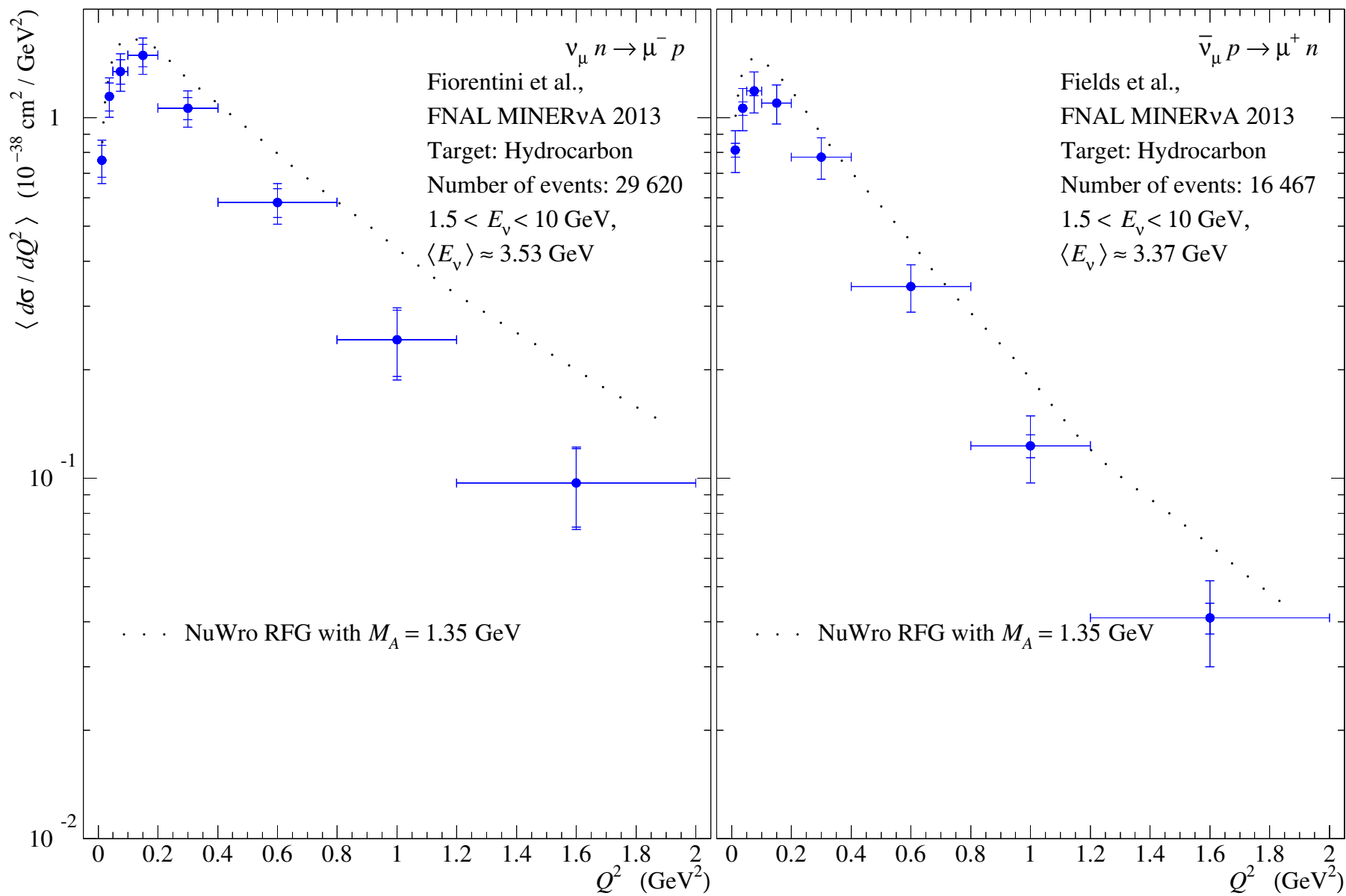


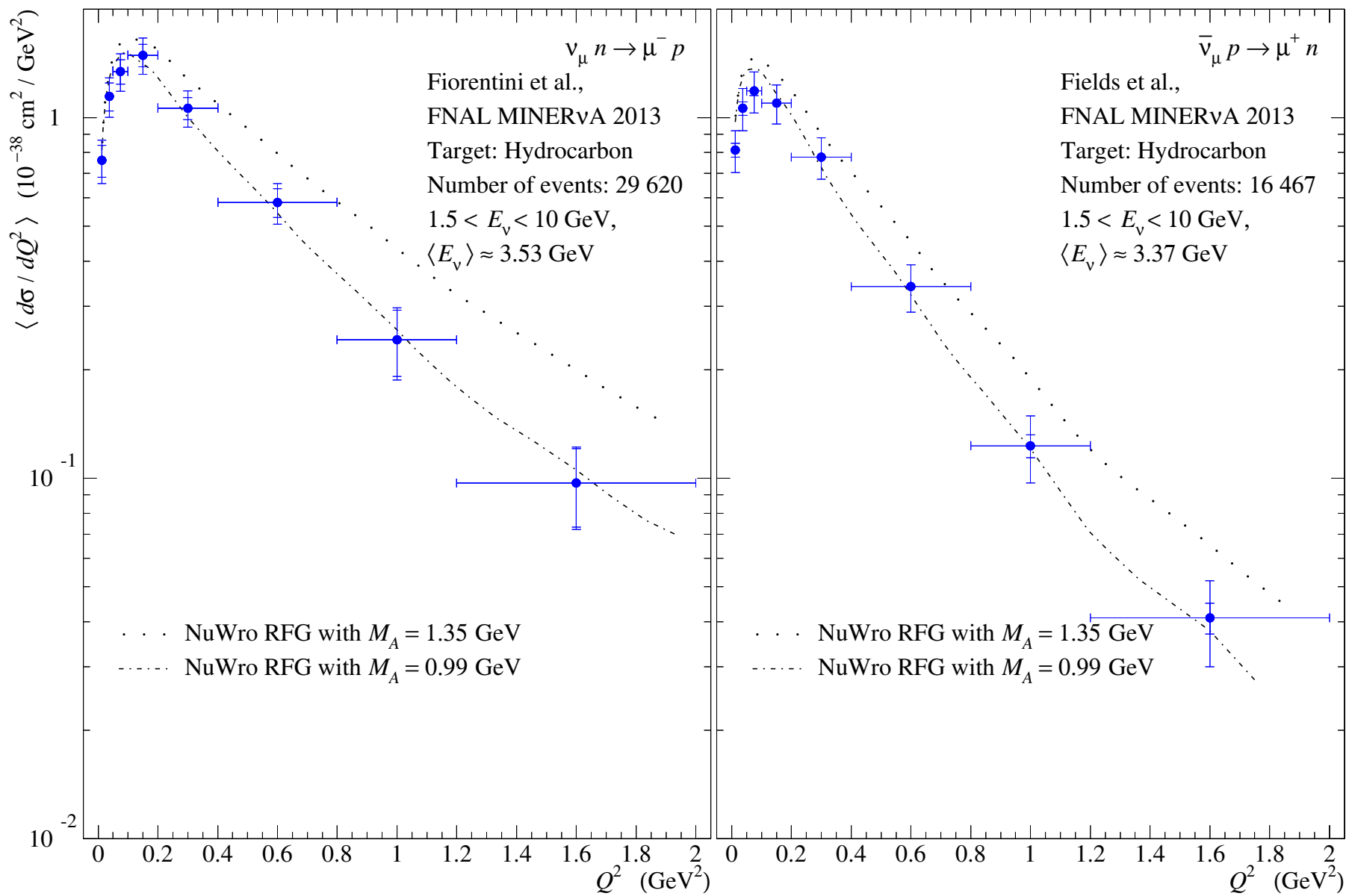


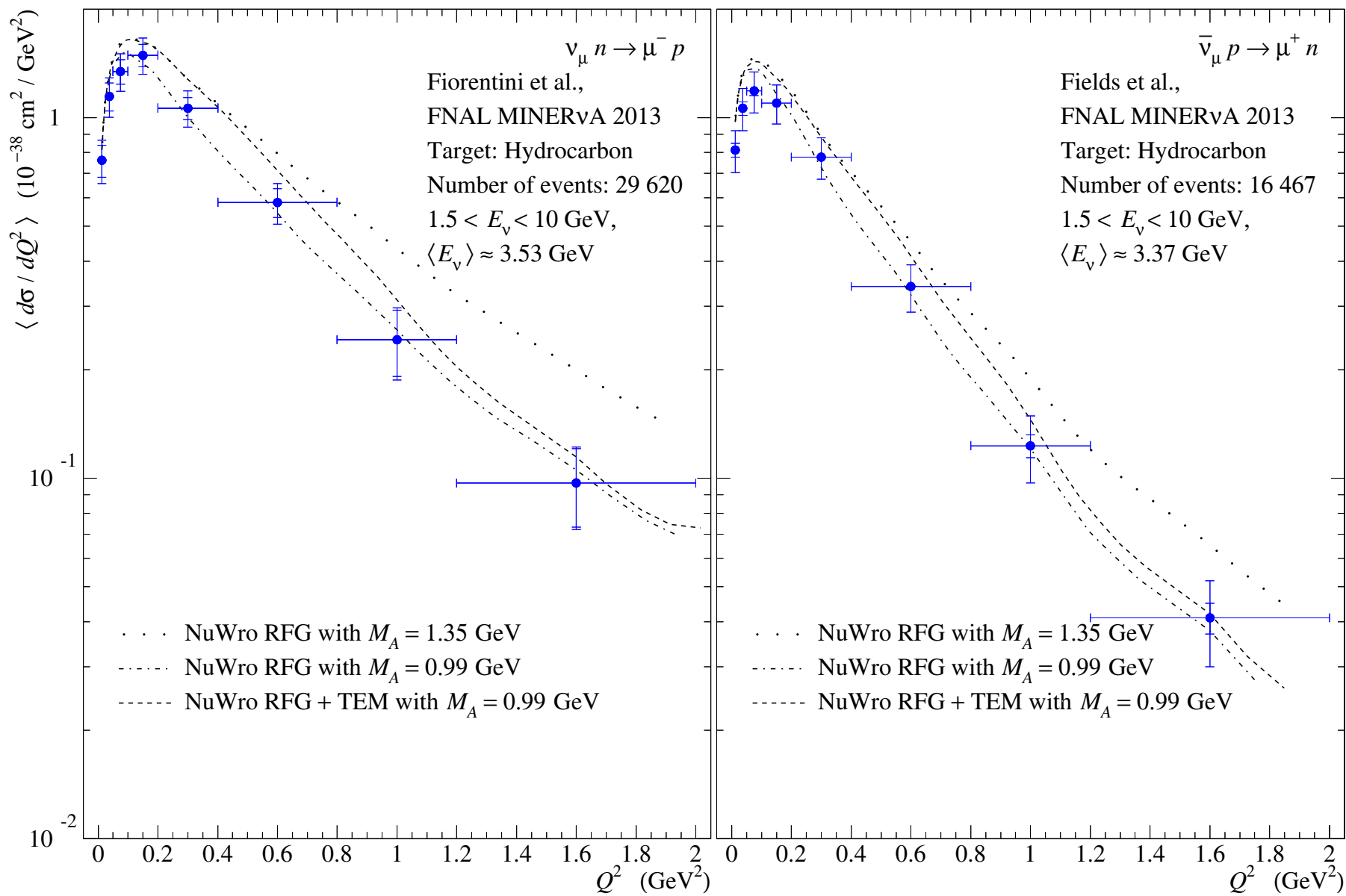
$\bar{\nu}_\mu p \rightarrow \mu^+ n$
 FNAL MiniBooNE 2013
 (background subtracted)
 Target: Mineral oil (CH_{2.08})

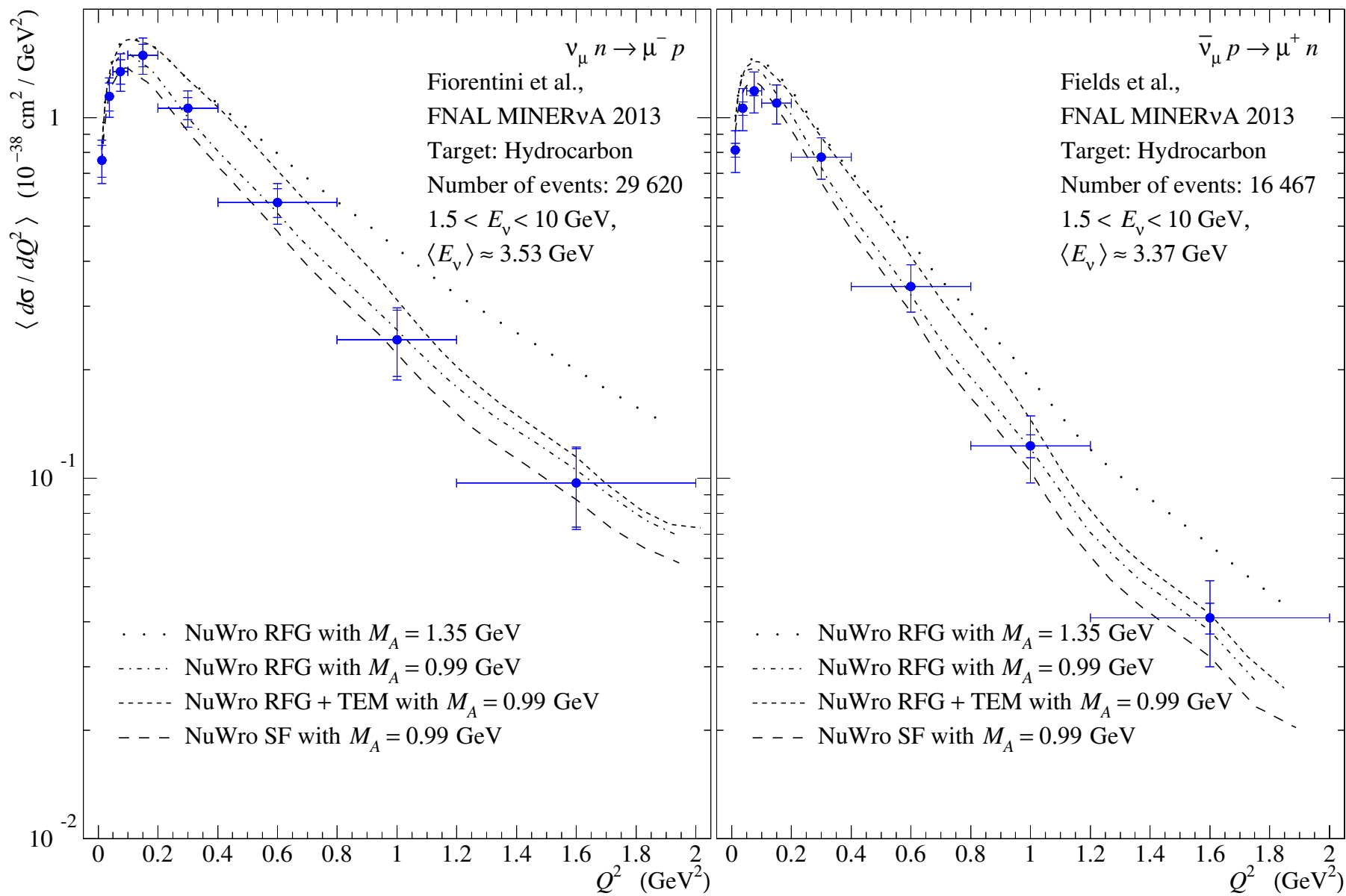
FNAL MINER ν A 2013

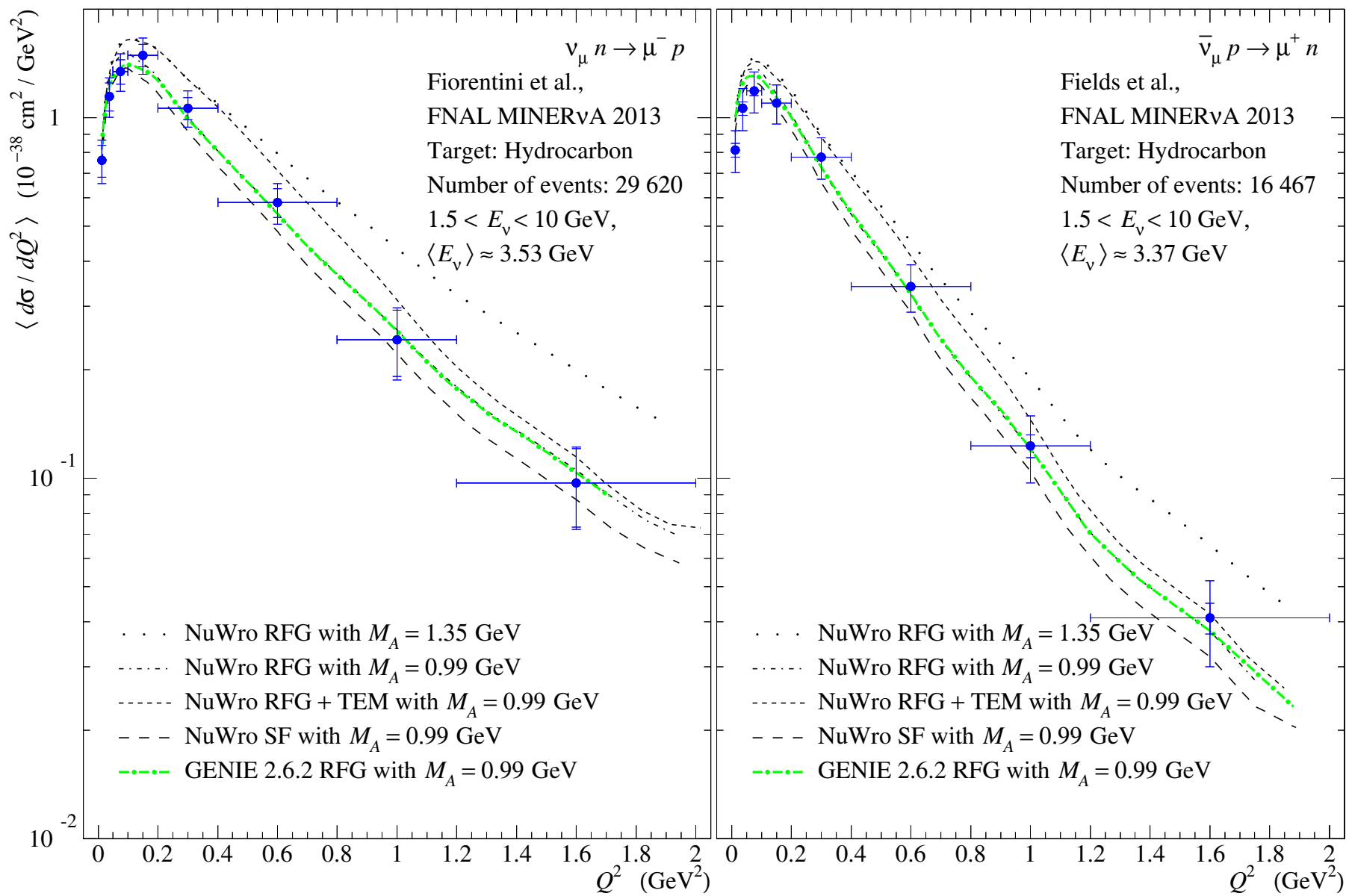


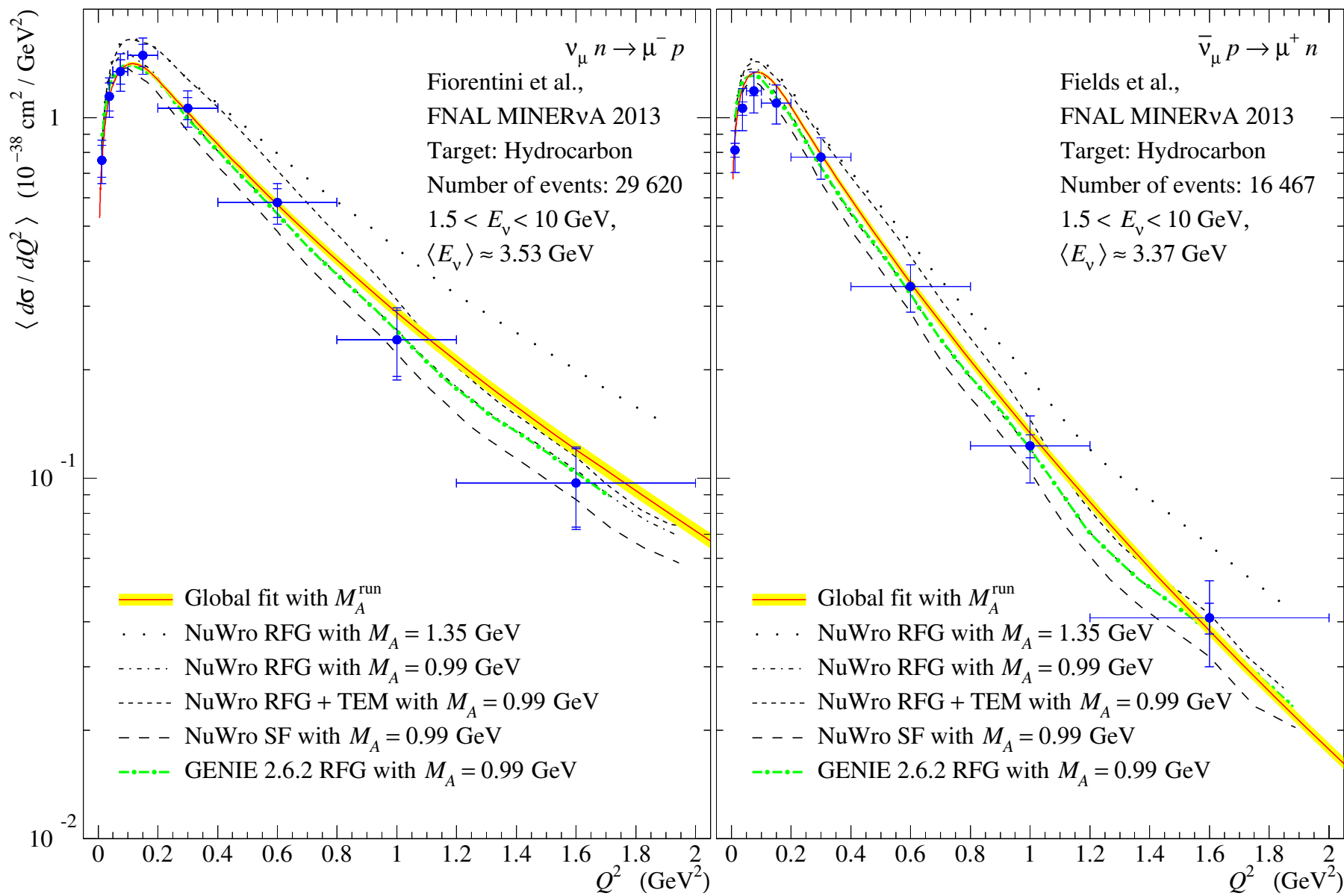


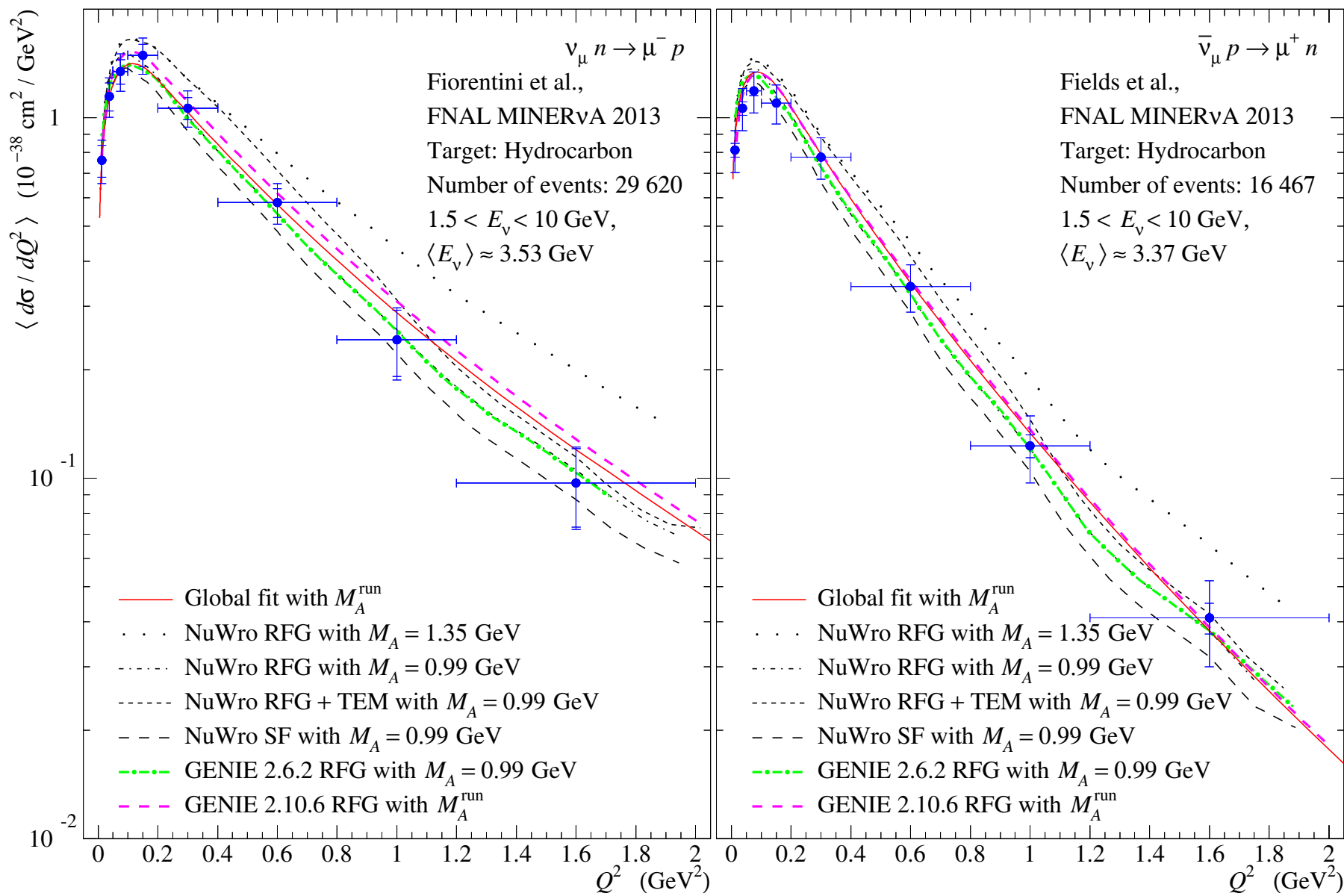






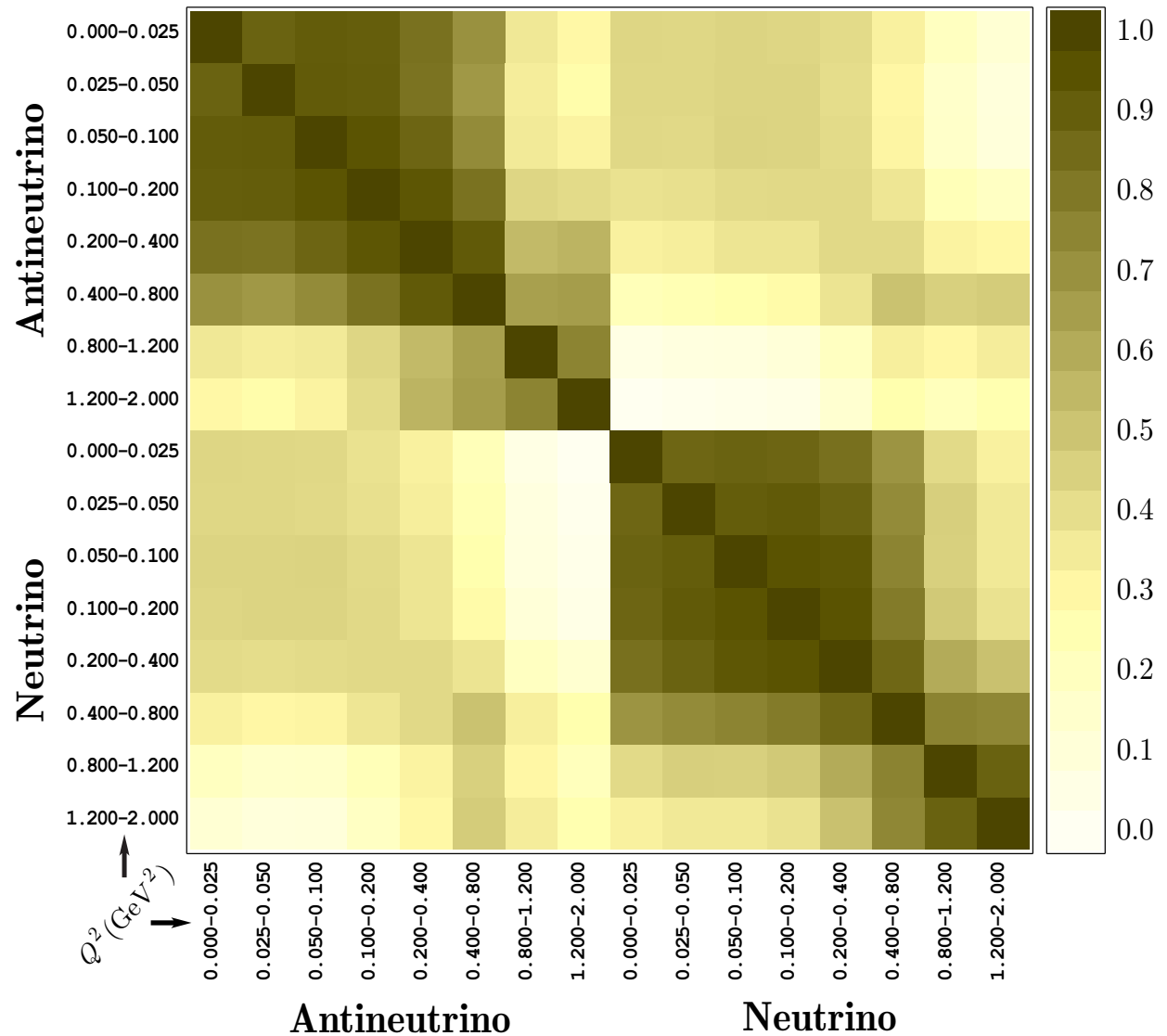






As it is seen from the correlation matrix, the MINER ν A data are highly correlated. Therefore the *by-eye* comparison between the data and the model predictions is not very conclusive.

The values of χ^2/N (where N is the number of datapoints) listed in next slide allow us to conclude that our model provides the best description of the MINER ν A results among the models shown in slides 30–36.



Model	Author's estimation (by bin medians)	Our estimation (by bin medians)	Our estimation (by bin averages)
ν_μ FNAL MINER ν A 2013 [27], $N = 8$			
NuWro RFG with $M_A = 1.35$	3.7	29.26/8 = 3.66	31.13/8 = 3.89
NuWro RFG with $M_A = 0.99 + \text{TEM}$	2.4	18.40/8 = 2.30	20.93/8 = 2.62
NuWro RFG with $M_A = 0.99$	3.5	28.19/8 = 3.52	23.24/8 = 2.91
NuWro SF with $M_A = 0.99$	2.8	22.66/8 = 2.83	18.69/8 = 2.34
GENIE 2.6.2 RFG with $M_A = 0.99$	—	16.04/8 = 2.00	15.27/8 = 1.91
Global fit with M_A^{run}	—	7.19/8 = 0.90	8.04/8 = 1.00
GENIE 2.10.6 with M_A^{run}	—	11.16/8 = 1.39	10.77/8 = 1.35
$\bar{\nu}_\mu$ FNAL MINER ν A 2013 [28], $N = 8$			
NuWro RFG with $M_A = 1.35$	2.90	23.50/8 = 2.94	23.20/8 = 2.90
NuWro RFG with $M_A = 0.99 + \text{TEM}$	1.06	8.35/8 = 1.04	9.50/8 = 1.19
NuWro RFG with $M_A = 0.99$	2.64	21.39/8 = 2.67	17.80/8 = 2.23
NuWro SF with $M_A = 0.99$	2.14	17.37/8 = 2.17	14.59/8 = 1.82
GENIE 2.6.2 RFG with $M_A = 0.99$	—	19.96/8 = 2.50	18.23/8 = 2.28
Global fit with M_A^{run}	—	7.29/8 = 0.91	5.51/8 = 0.69
GENIE 2.10.6 with M_A^{run}	—	19.31/8 = 2.41	15.92/8 = 1.99
$\nu_\mu \oplus \bar{\nu}_\mu$ FNAL MINER ν A 2013 [27, 28], $N = 16$			
NuWro RFG with $M_A = 1.35$	—	59.15/16 = 3.70	59.34/16 = 3.71
NuWro RFG with $M_A = 0.99 + \text{TEM}$	—	28.33/16 = 1.77	30.74/16 = 1.92
NuWro RFG with $M_A = 0.99$	—	48.11/16 = 3.01	40.59/16 = 2.54
NuWro SF with $M_A = 0.99$	—	38.12/16 = 2.38	32.39/16 = 2.02
GENIE 2.6.2 RFG with $M_A = 0.99$	—	34.87/16 = 2.18	33.04/16 = 2.07
Global fit with M_A^{run}	—	19.93/16 = 1.25	17.90/16 = 1.10
GENIE 2.10.6 with M_A^{run}	—	34.77/16 = 2.17	30.02/16 = 1.88

T2K ND280 2016

A caveat

We have not yet included the new (2016) T2K ND280 data [69] into the global fit due to the following reasons:

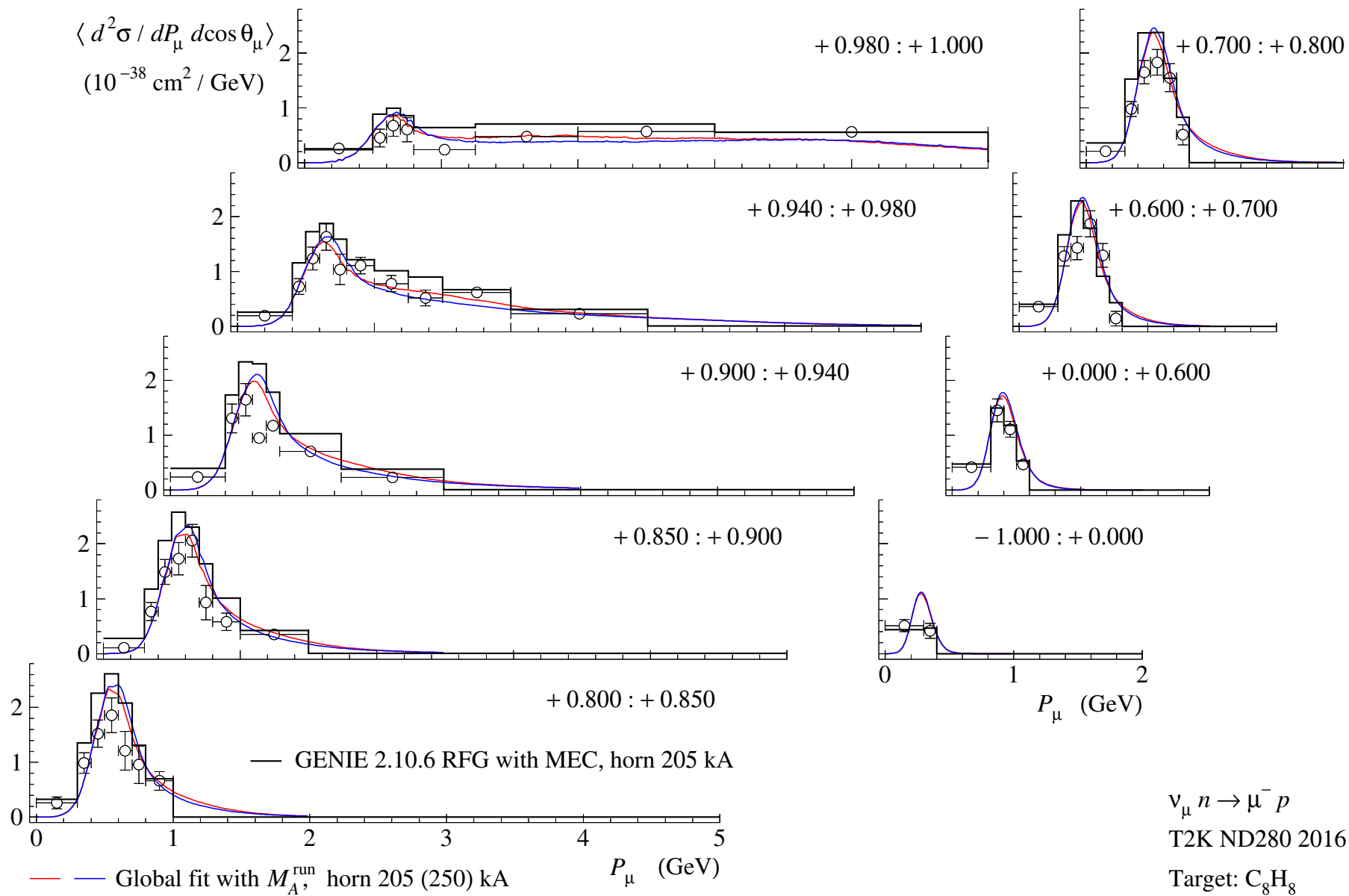
- We don't know the actual ν_μ spectrum since in several runs of the experiment, the three magnetic horns were excited by different current pulses.
- We don't know which of two data analyses (or both with certain weights) should be used in the fit.
- There is some small additional uncertainty related to complicated elemental composition of the detector target (fine-grained detector FGD1).^a The measurement has been effectively considered as if on the FGD1 scintillator (C₈H₈). But our experience suggests that such simplification is not quite harmless...

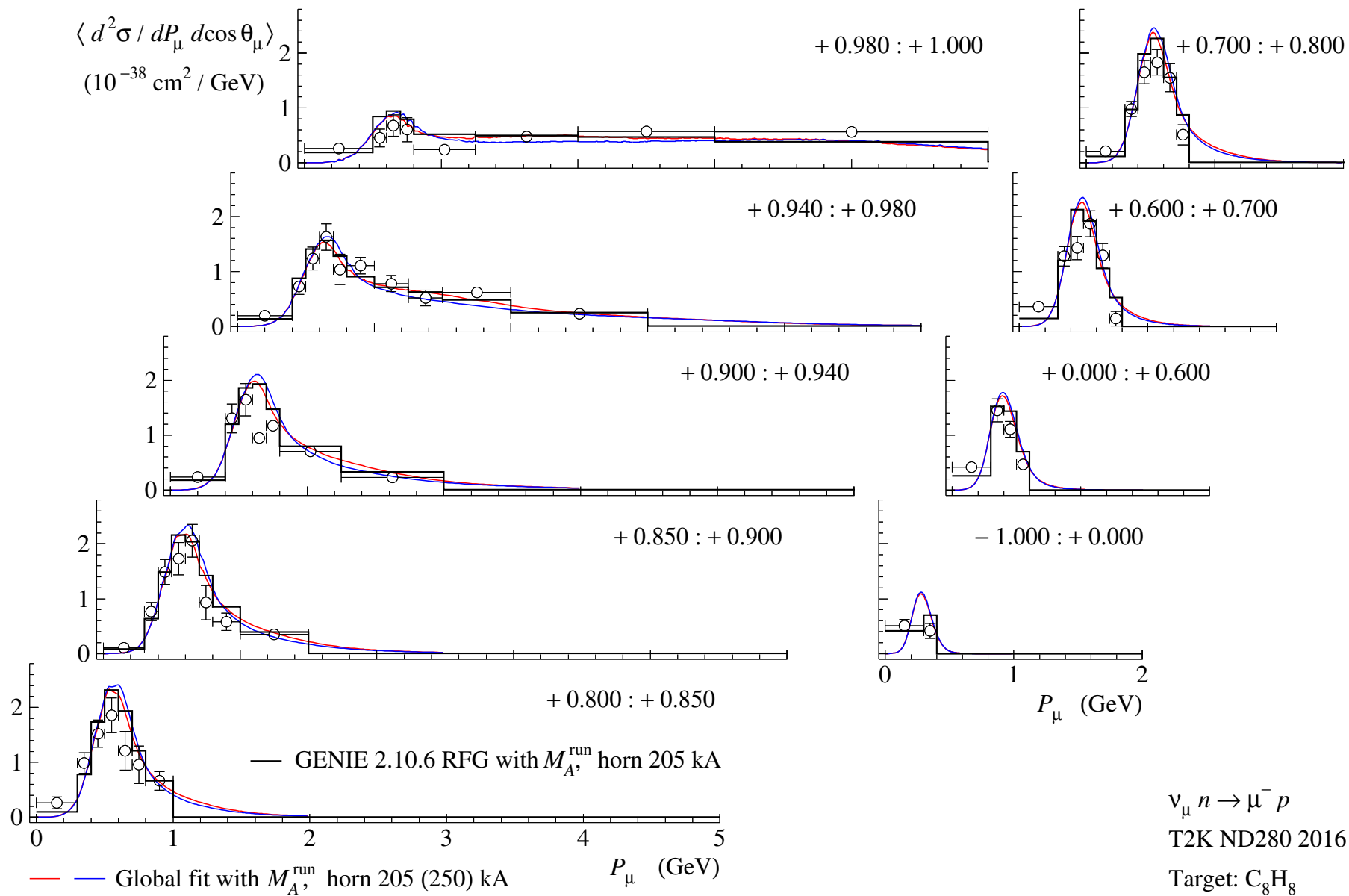
Here we only compare our calculations with the data from [Analyses 1 & 2](#) [69] by using the two ν_μ spectra corresponding to the horn currents of 250 and 205 kA.

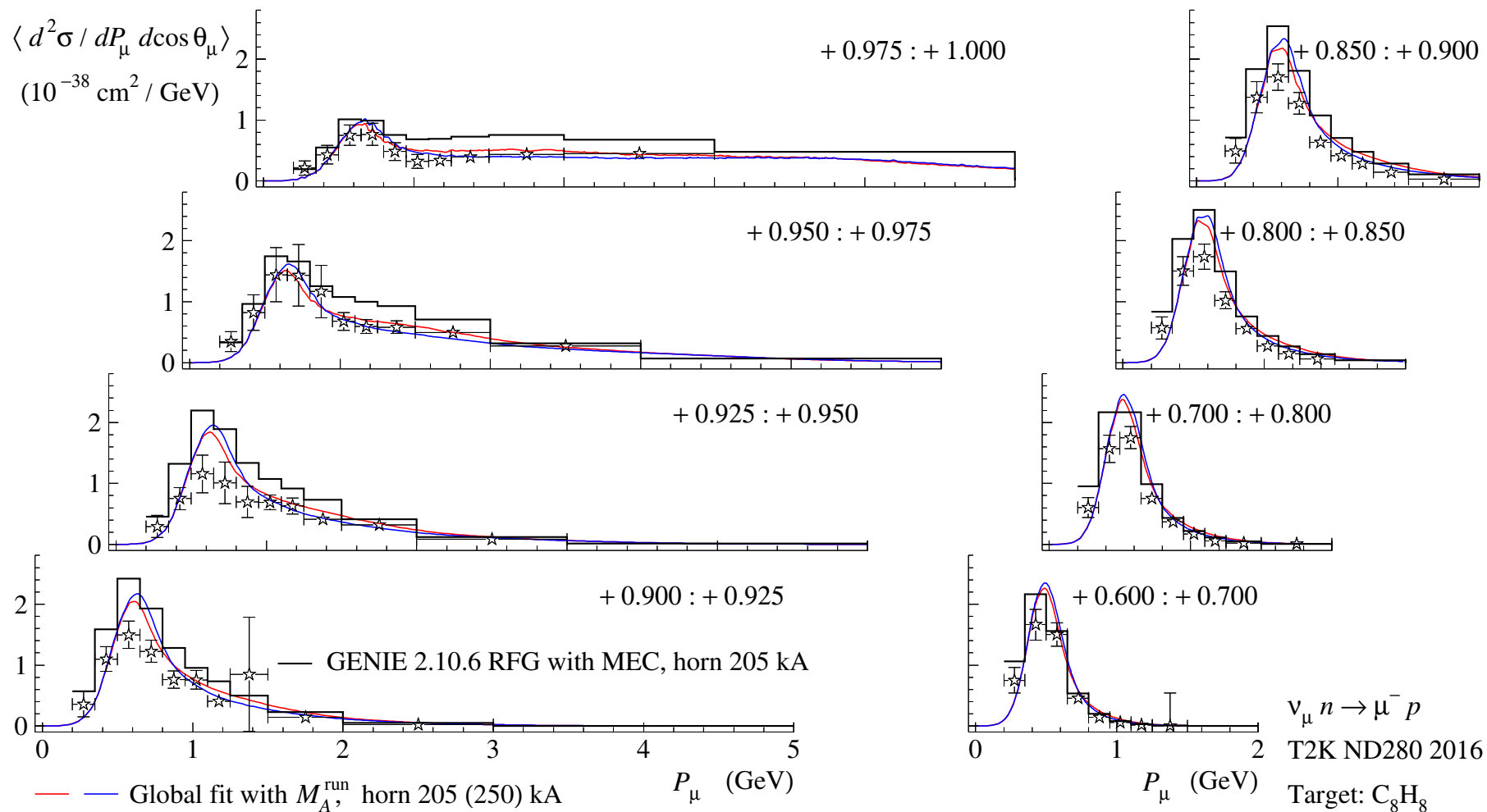
We find a reasonable (within the uncertainties) agreement between the ND280 results and those predicted by our model.

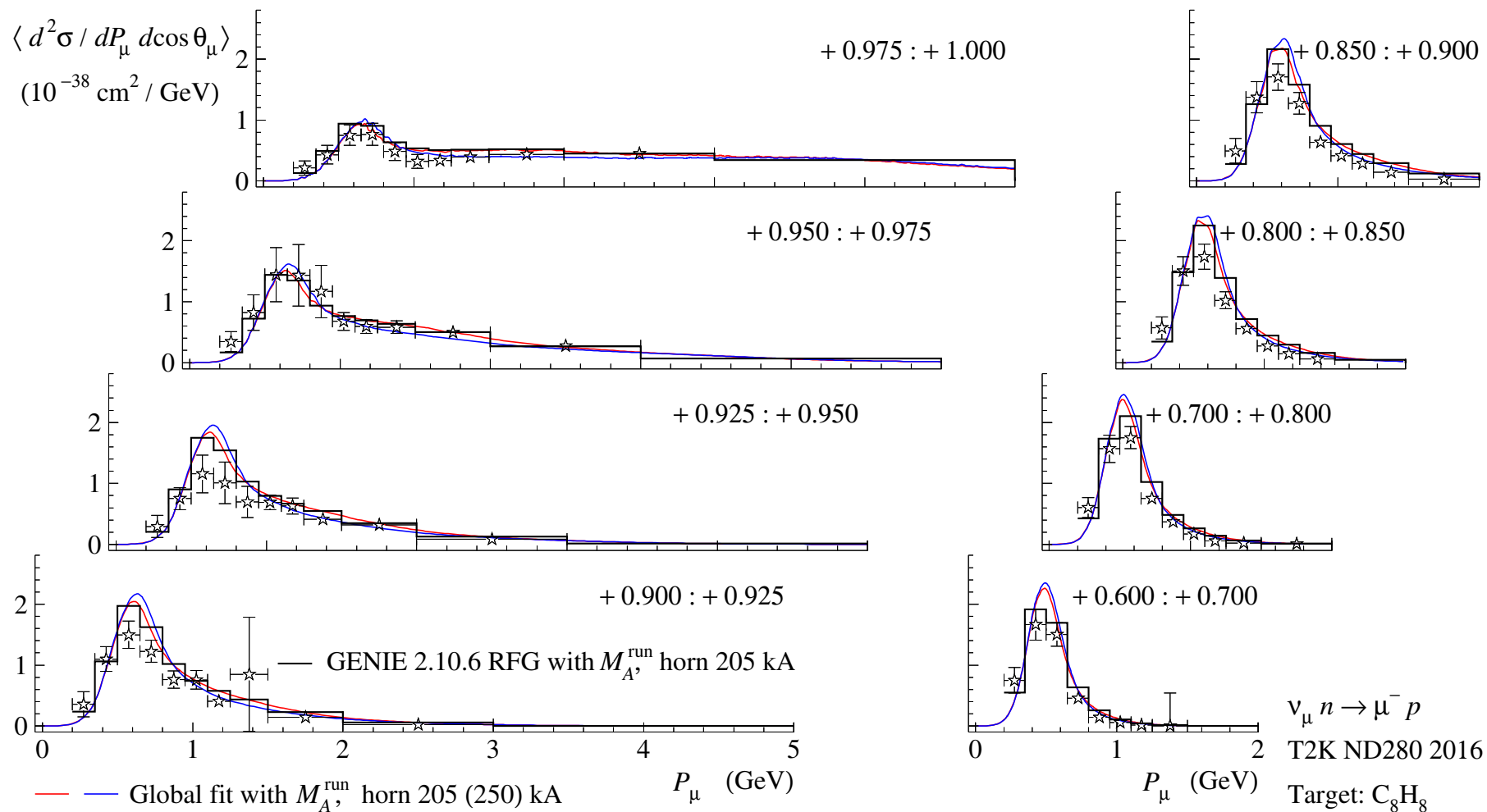
Therefore, it can be preliminary concluded that adding the T2K ND280 2016 data into the global fit would not drastically change the result.

^aThe FGD1 composition: carbon (86.1%), hydrogen (7.35%), oxygen (3.70%), and small quantities of other elements such as titanium, silicon, and nitrogen (2.85%) [69].









Parameters of the SM RFG Model

Interpolation formulas

The Fermi momenta for isoscalar nuclei and binding (separation) energies are calculated by using the following interpolation formulas (valid for $A \geq 6$):

$$p_F = 270[1 - 4.2/A + (6.0/A)^2 - (5.3/A)^3]$$

and

$$E_b = 50.4 [1 - 2.26/\xi + (1.73/\xi)^2 - (1.21/\xi)^3], \quad \xi = Z/A^{1/3},$$

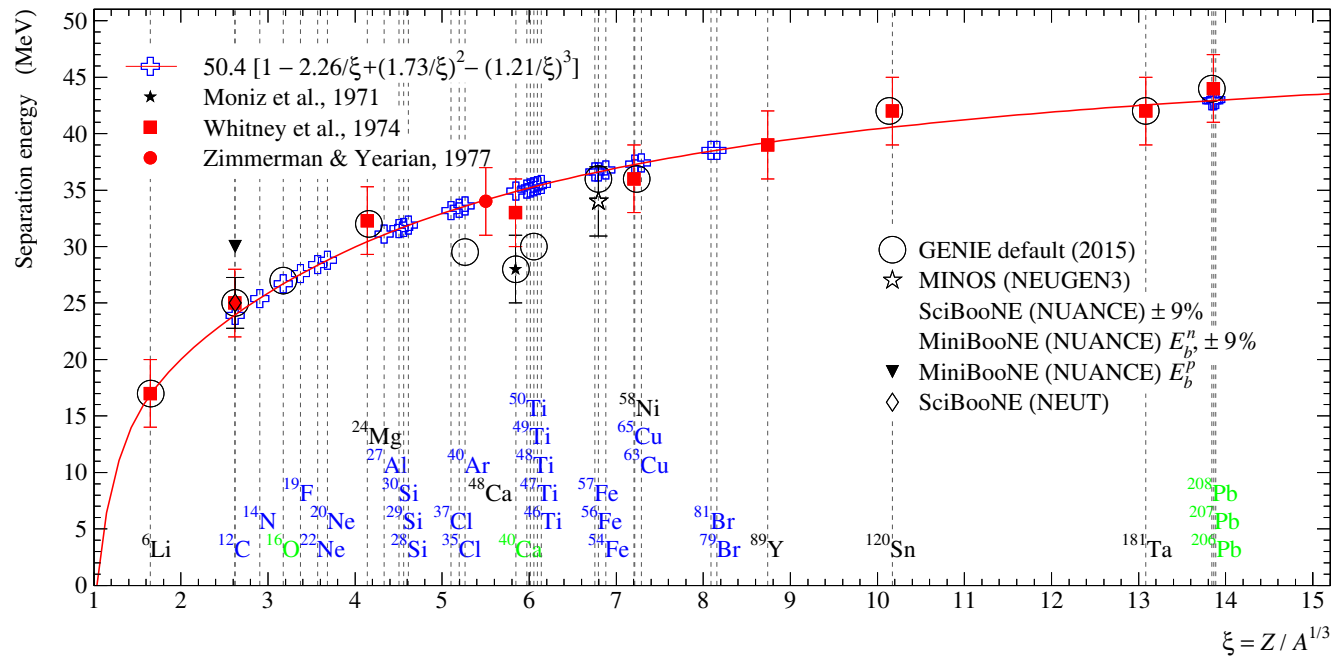
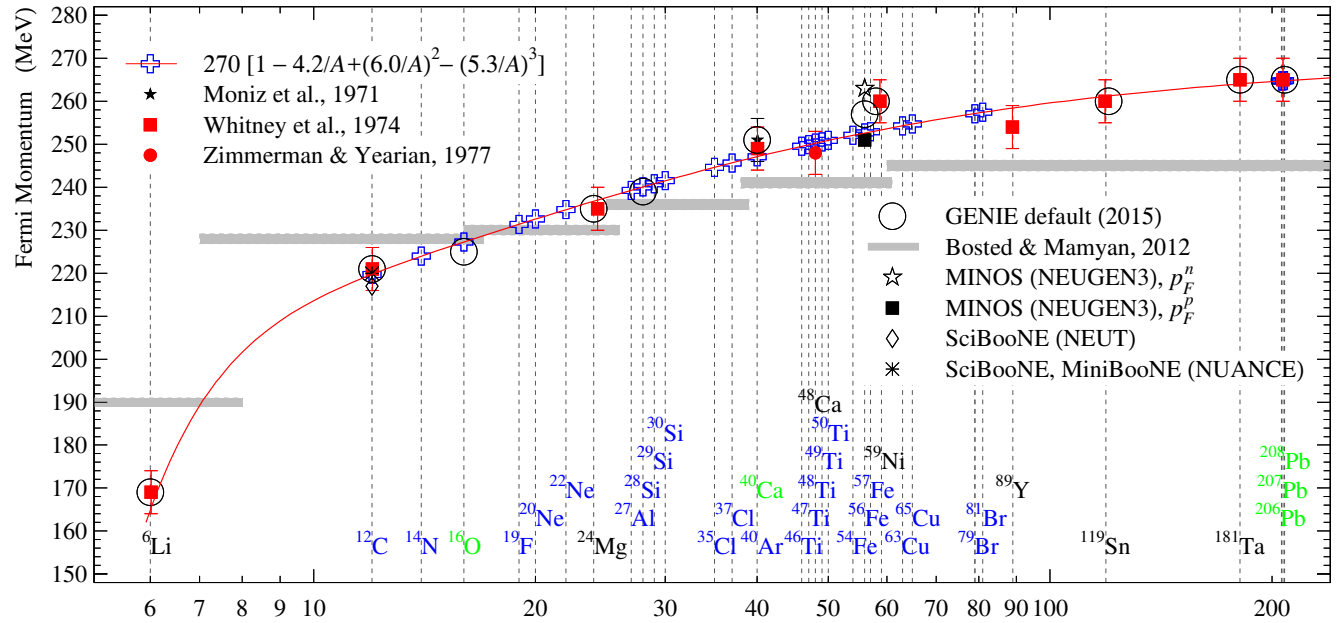
obtained from available (unfortunately, rather old) data on electron-nucleus scattering.^a

The proton and neutron Fermi momenta (p_F^p and p_F^n , respectively) are then calculated in the conventional way:^b

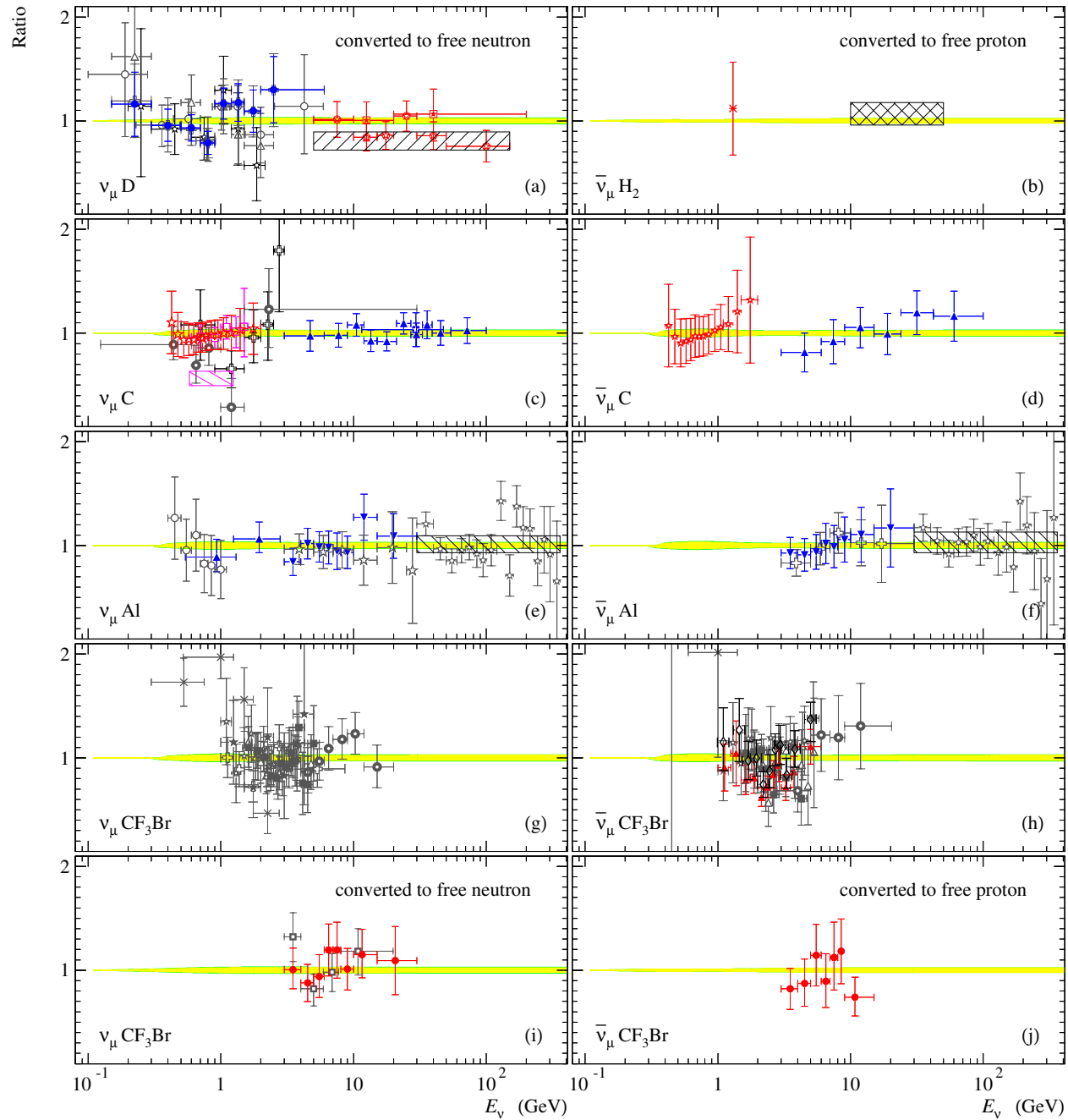
$$p_F^p = (2Z/A)^{1/3} p_F \quad \text{and} \quad p_F^n = (2N/A)^{1/3} p_F \quad (N = A - Z).$$

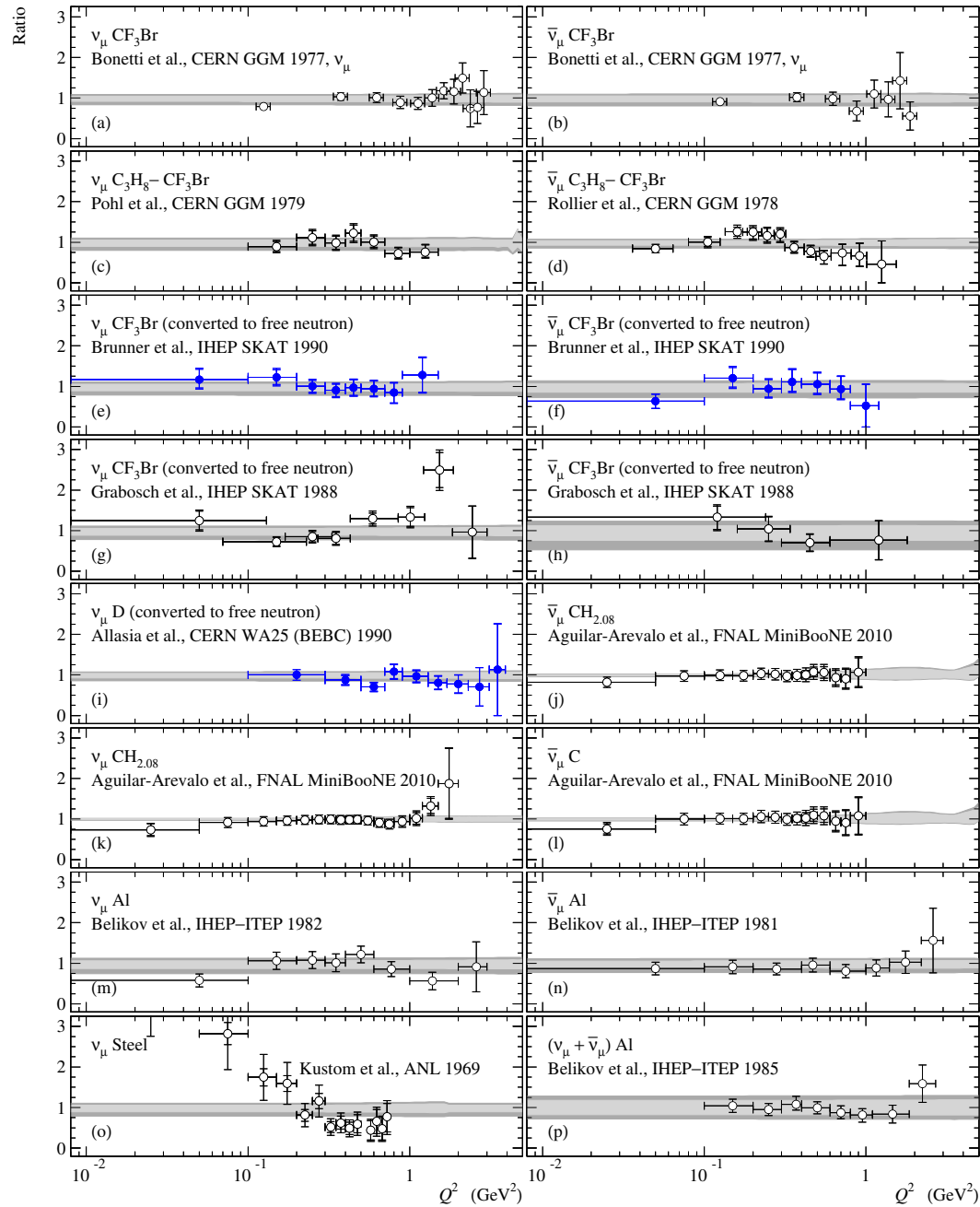
^a E.J. Moniz, I. Sick, R.R. Whitney, J.R. Ficenece, R.D. Kephart, and W.P. Trower, "Nuclear Fermi momenta from quasielastic electron scattering," Phys. Rev. Lett. **26**, 445 (1971); R.R. Whitney, I. Sick, J.R. Ficenece, R.D. Kephart and W.P. Trower, "Quasielastic electron Scattering," Phys. Rev. C **9**, 2230 (1974); P.D. Zimmerman and M.R. Yearian, "Fermi momenta and separation energies obtained from the quasi-elastic scattering of electrons from ^{48}Ca and ^{40}Ca ," Z. Phys. A **278**, 291 (1976).

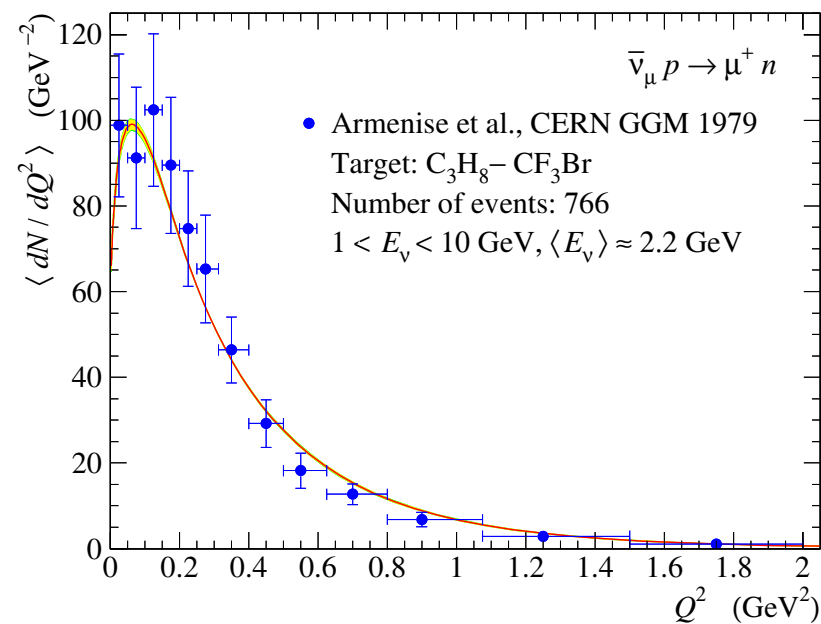
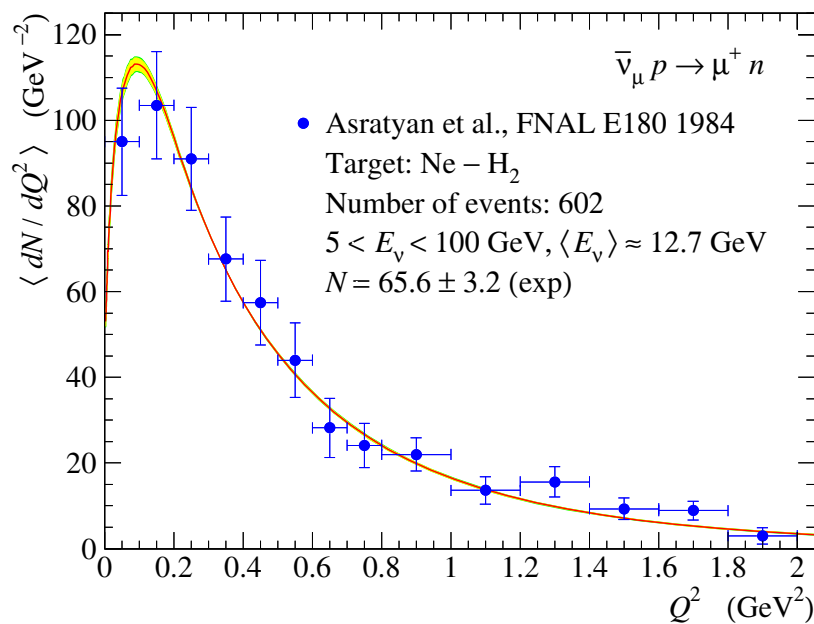
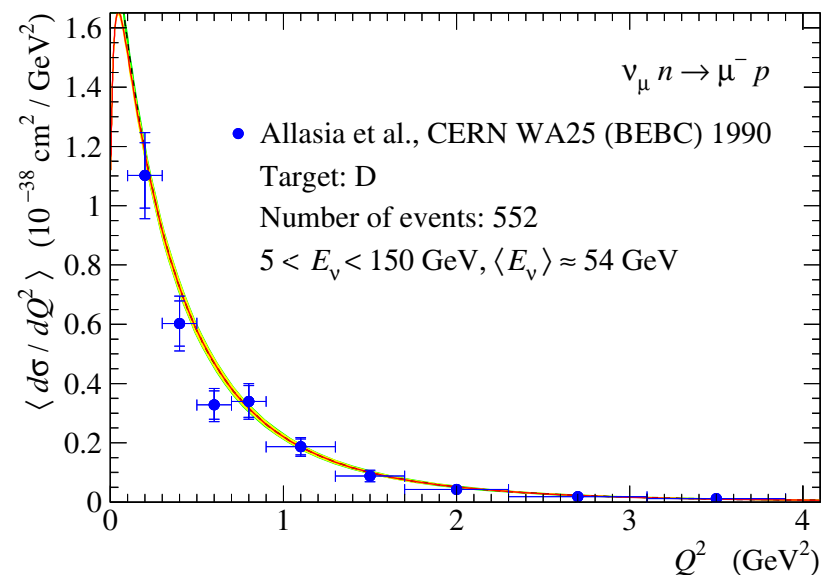
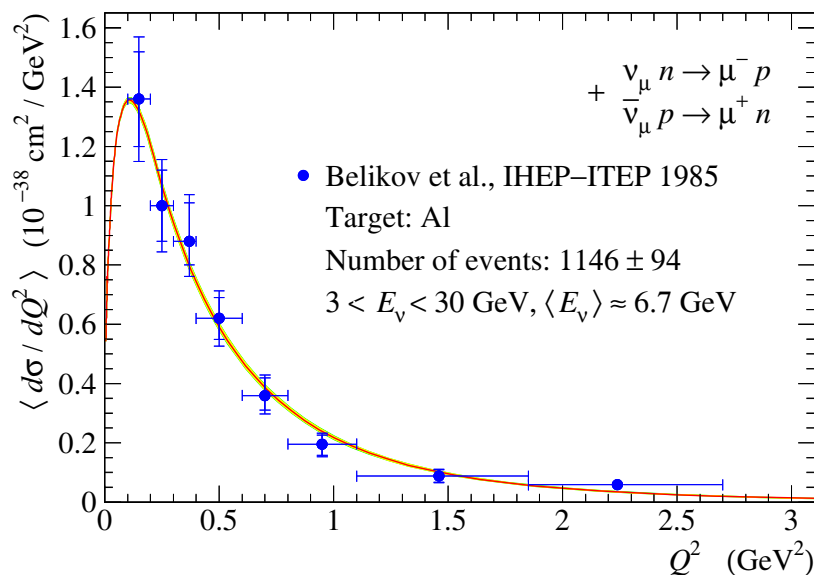
^bThese relations are based on the simplest assumption that the density of nuclear matter is approximately constant irrespective of the proton-to-neutron ratio Z/N .

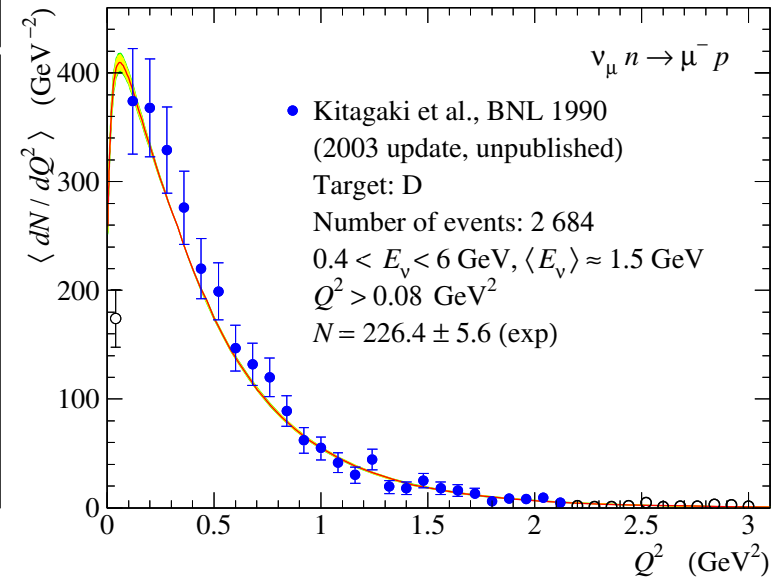
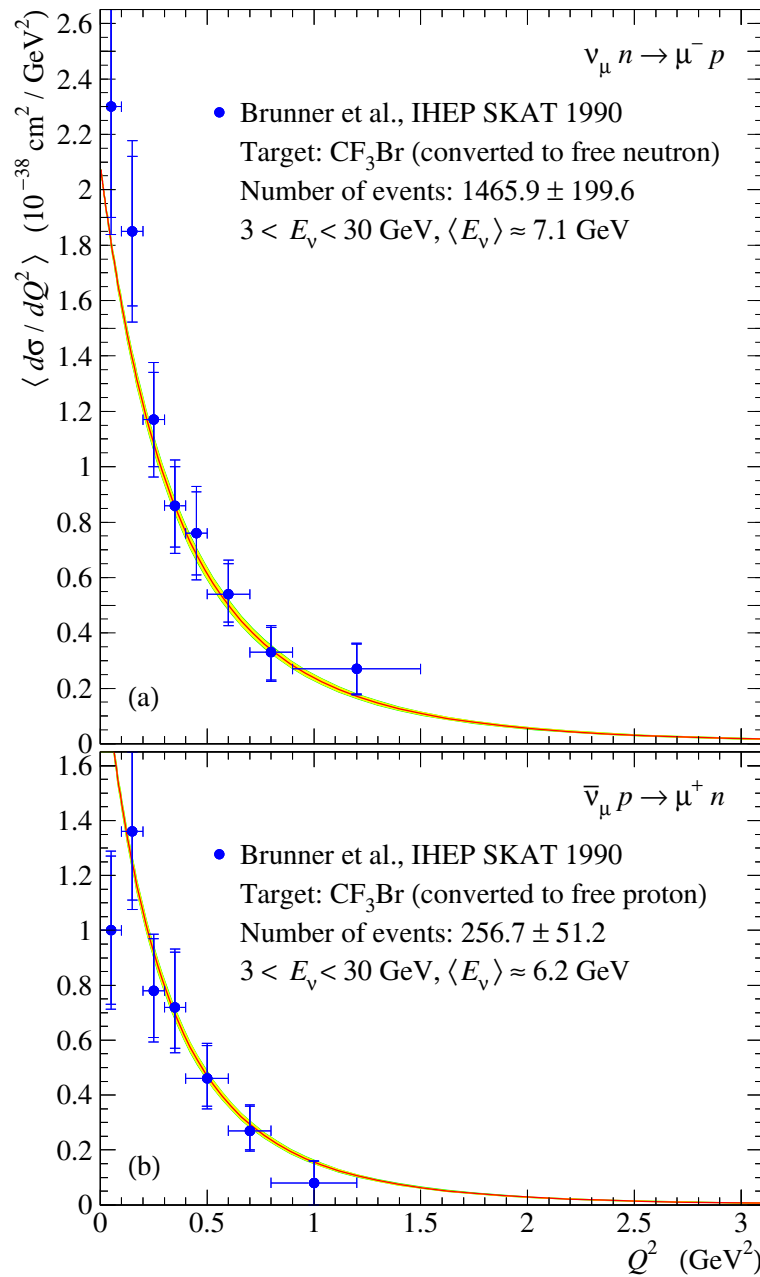


Comparison with the early “golden” data

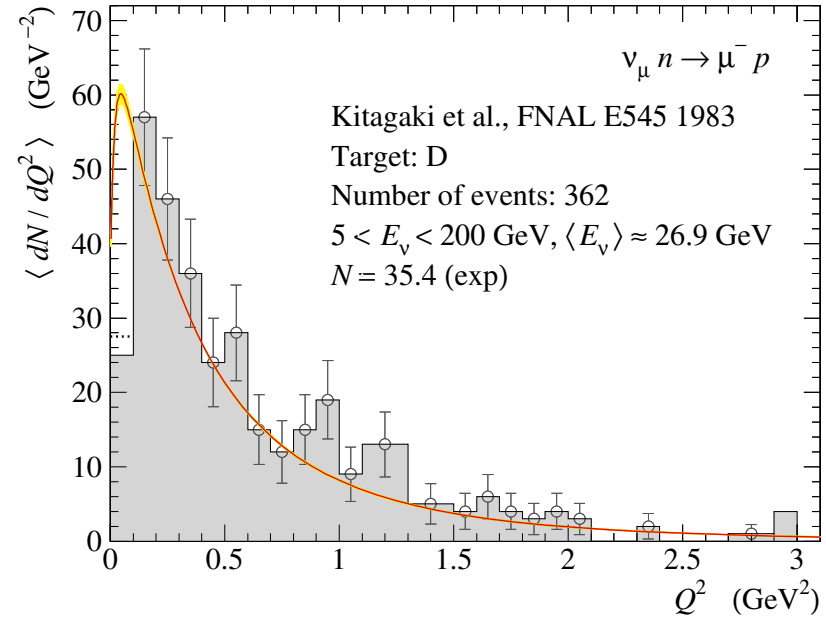
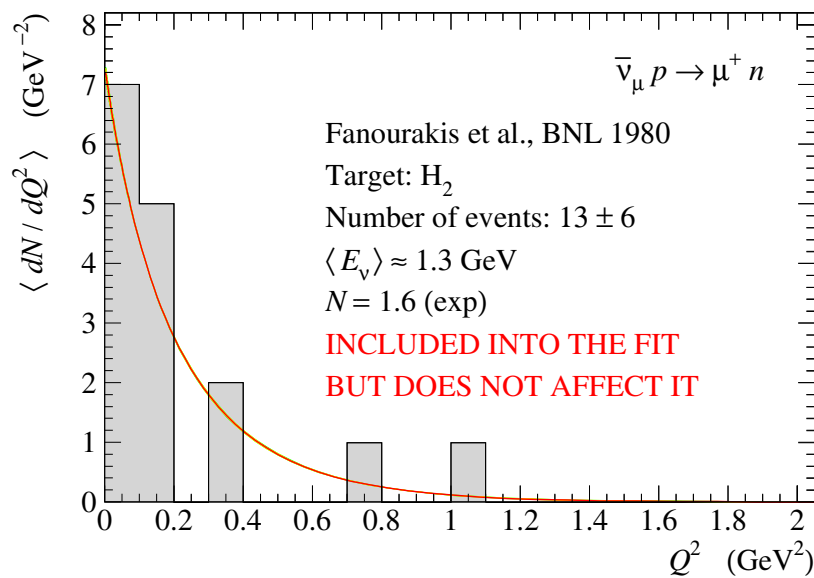
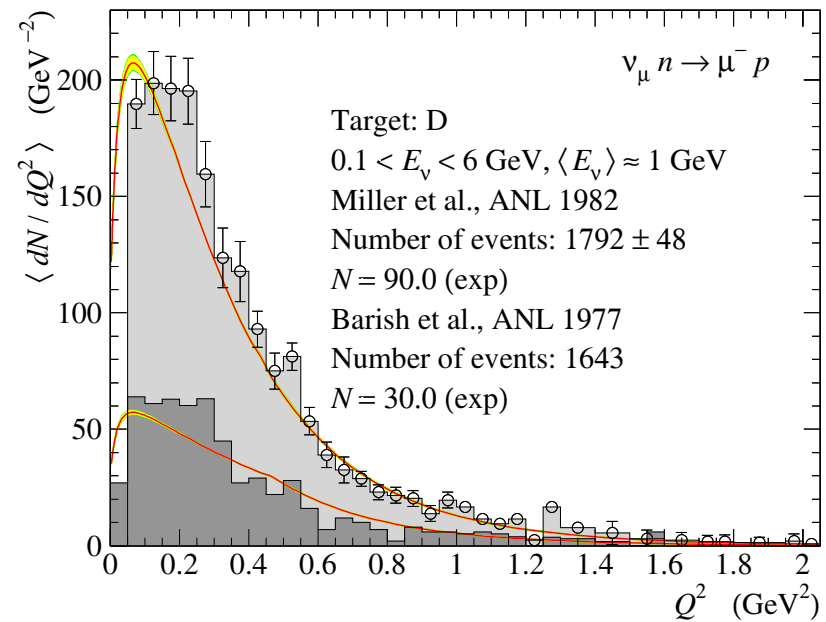
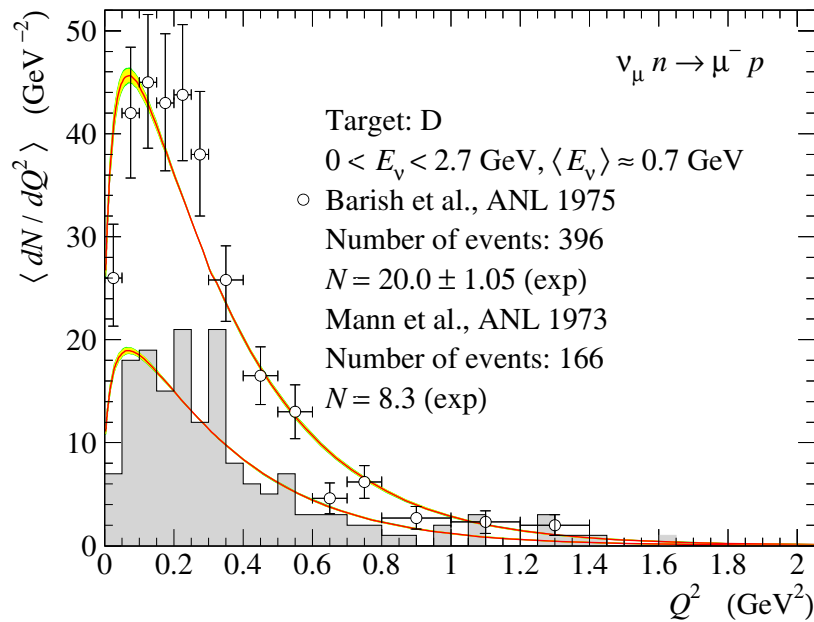


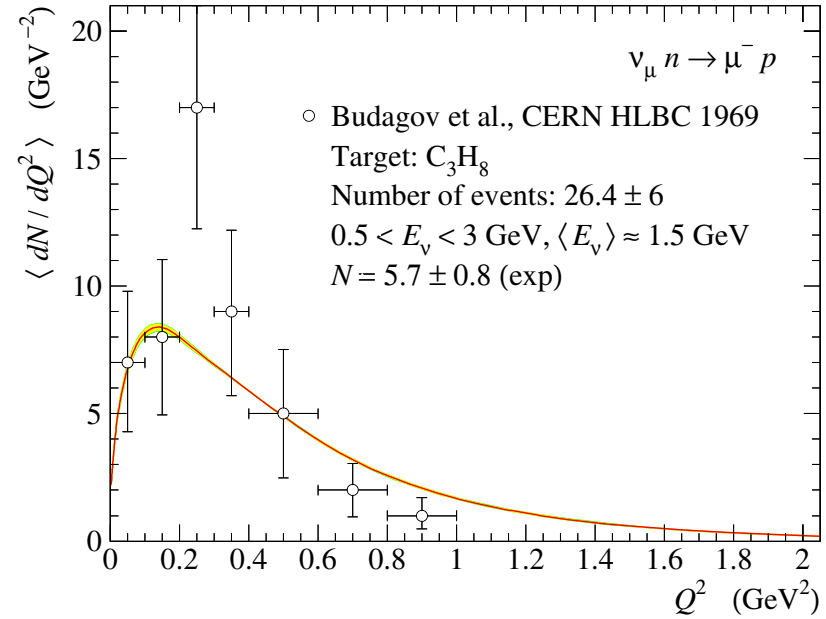
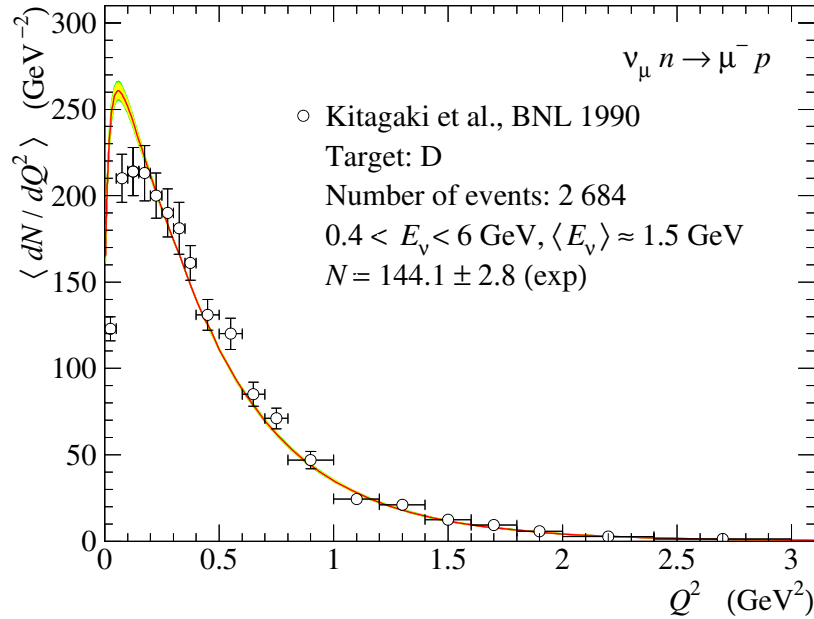
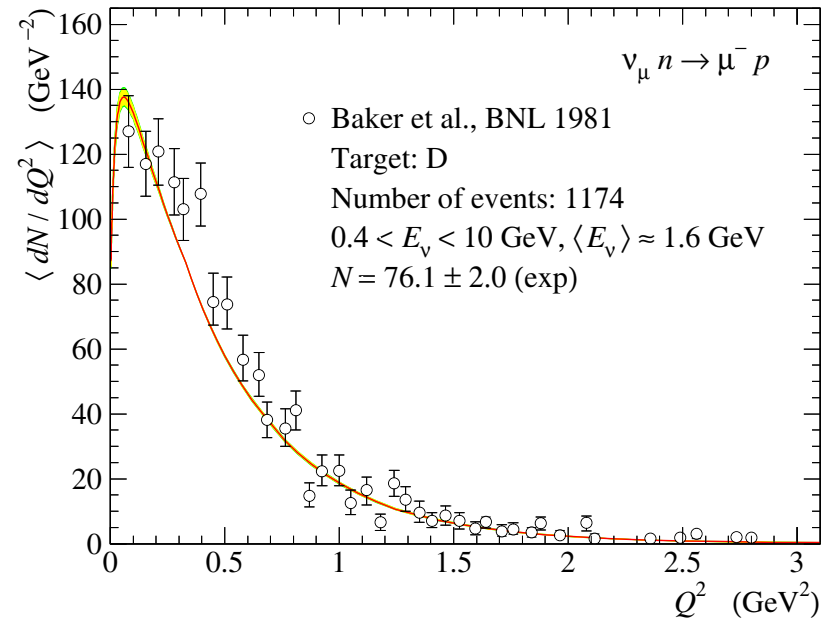
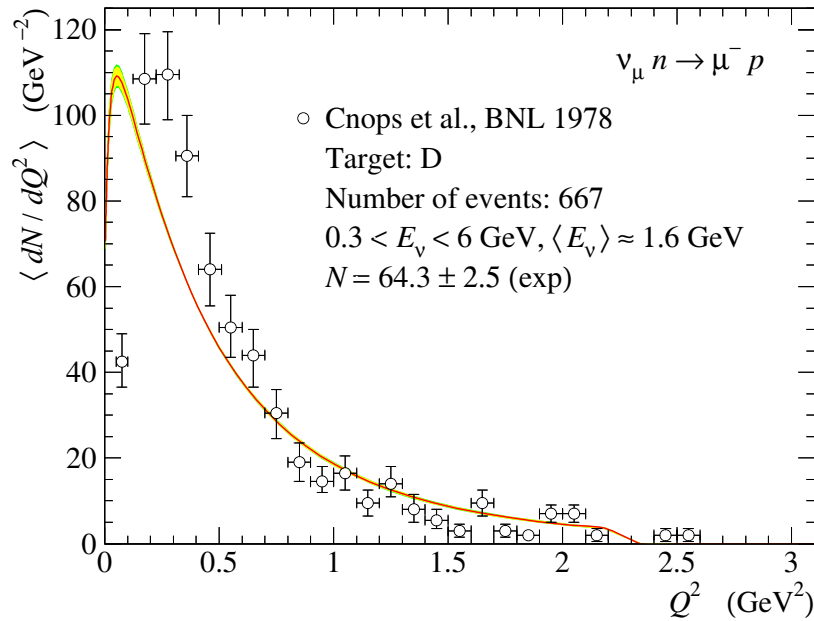


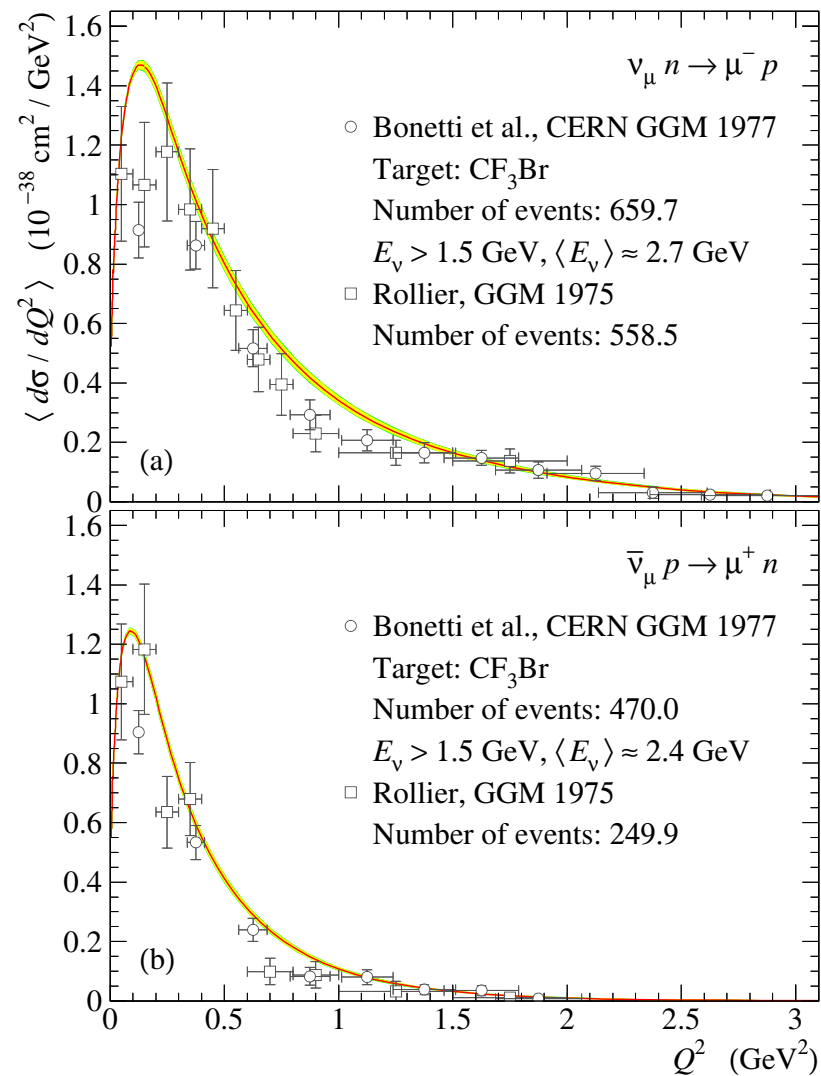
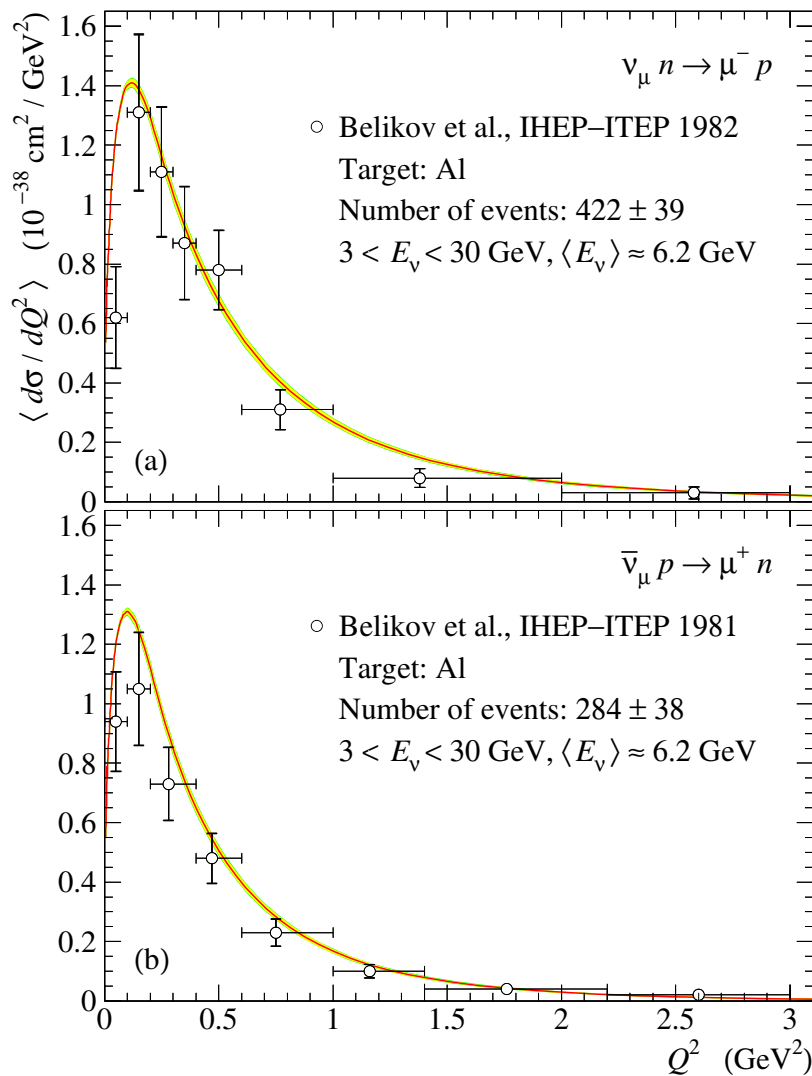


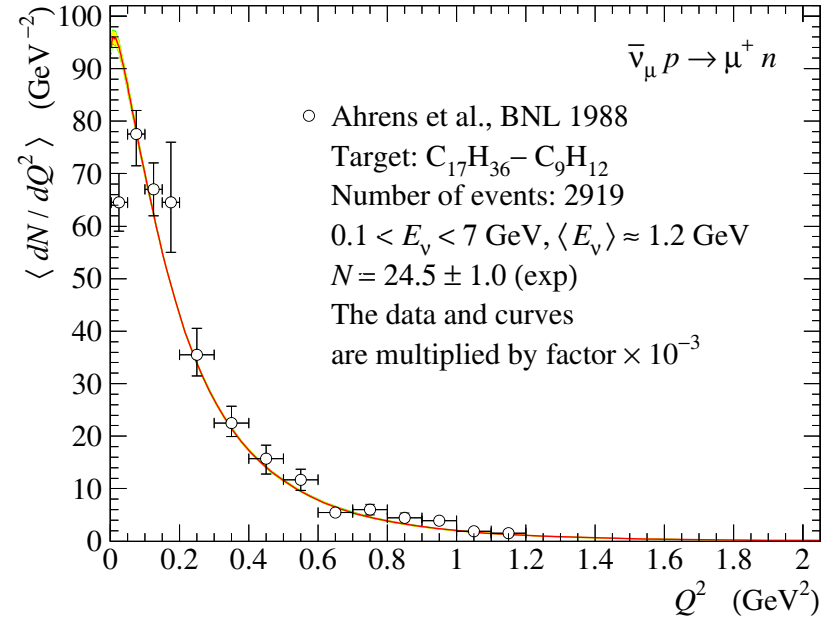
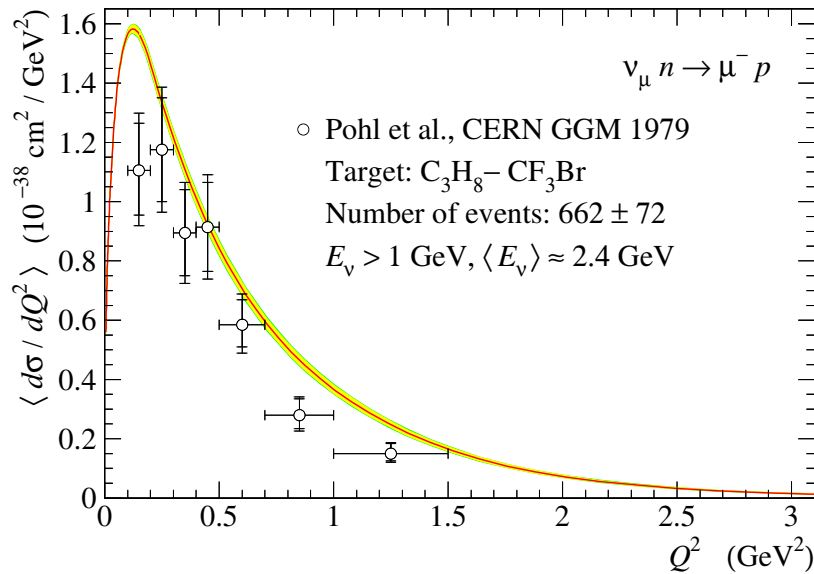
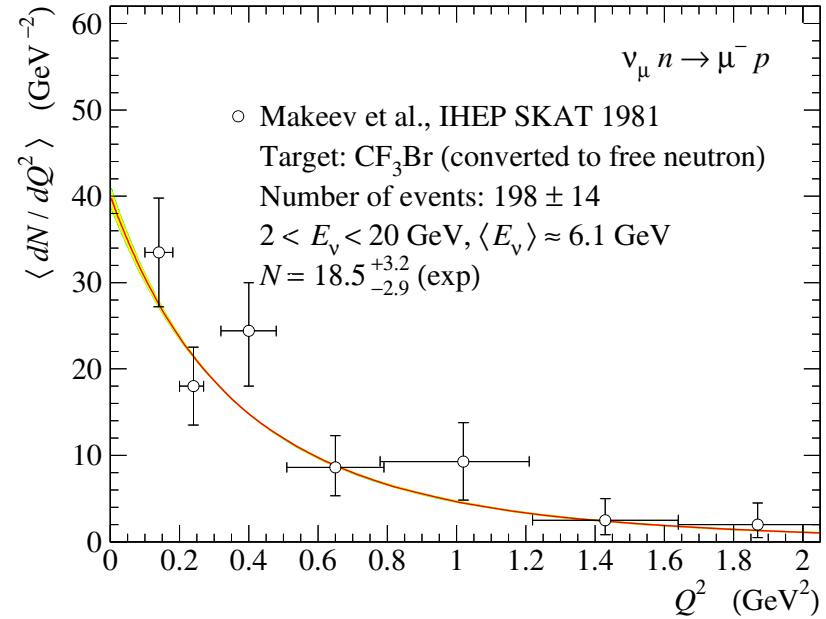
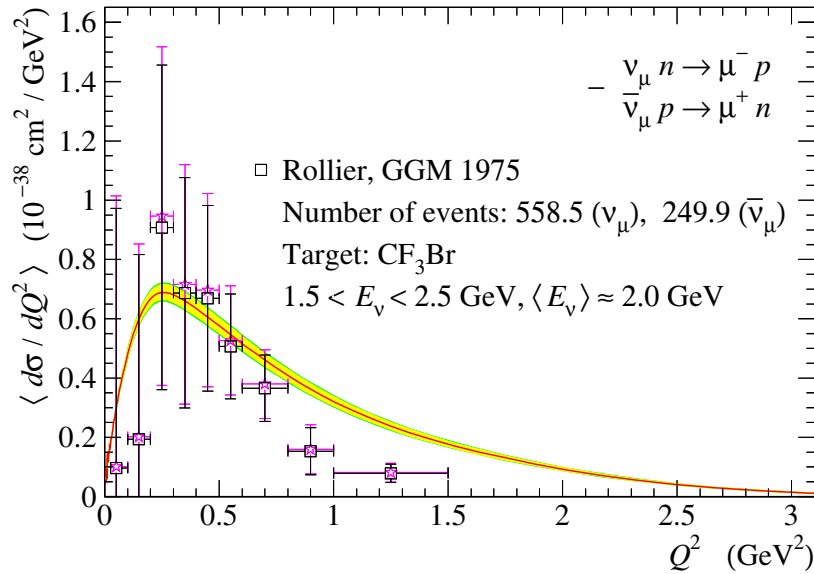


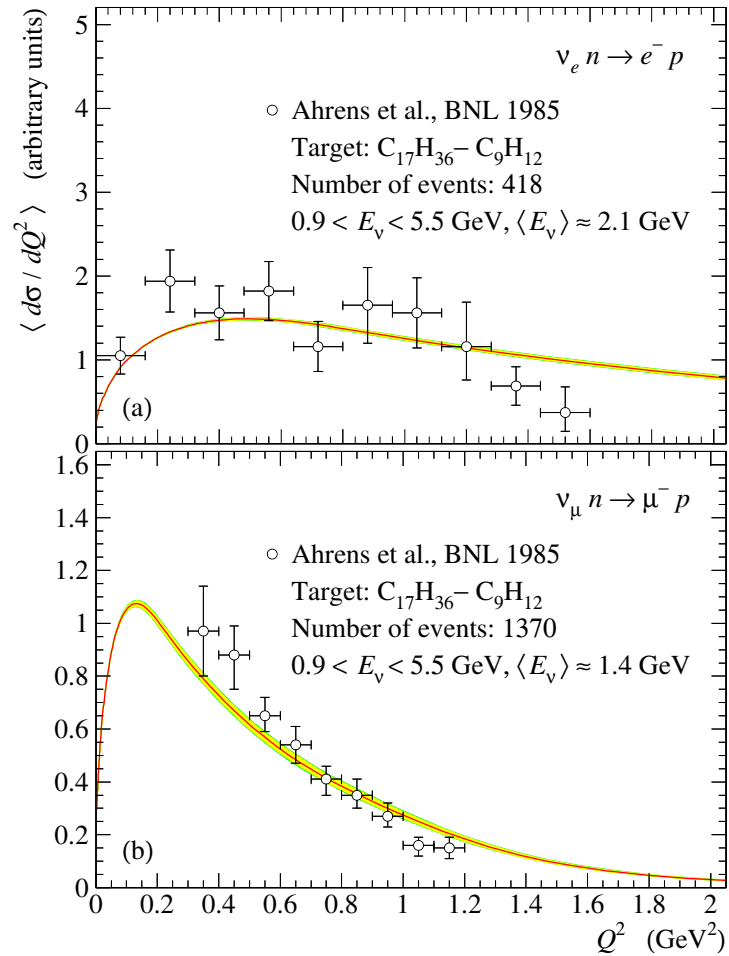
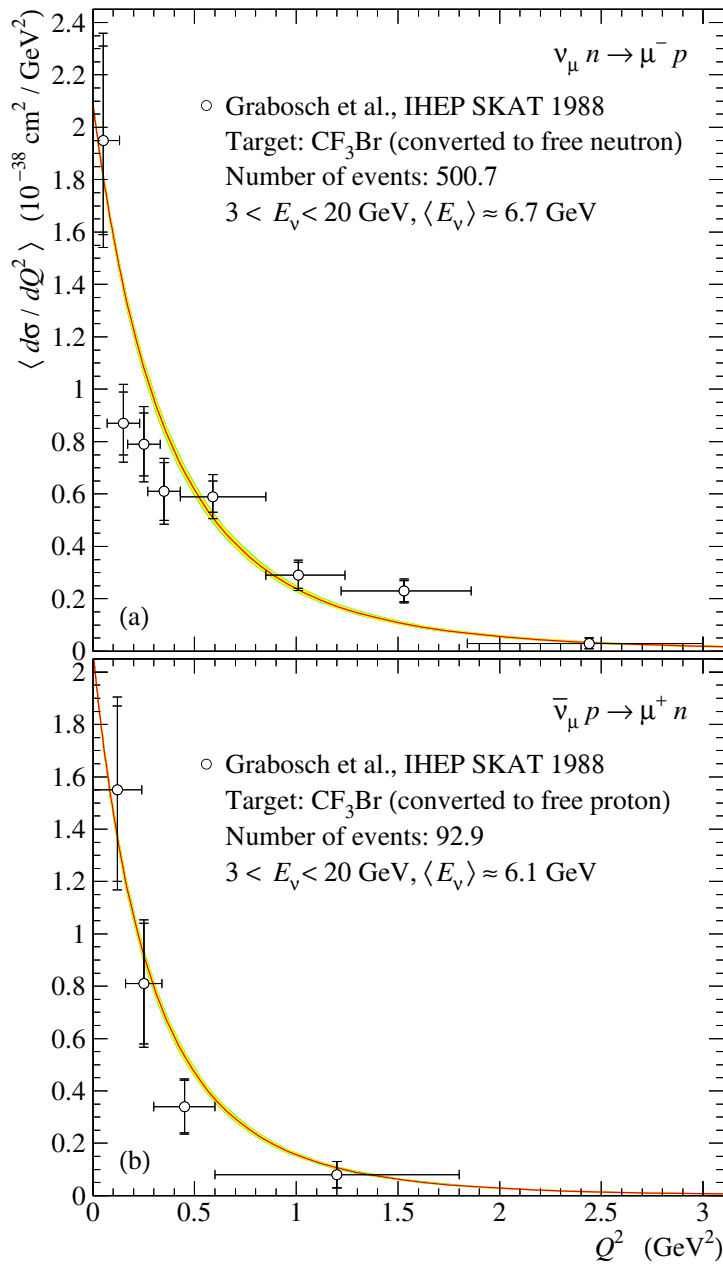
Comparison with certain datasets unclaimed in the global fit

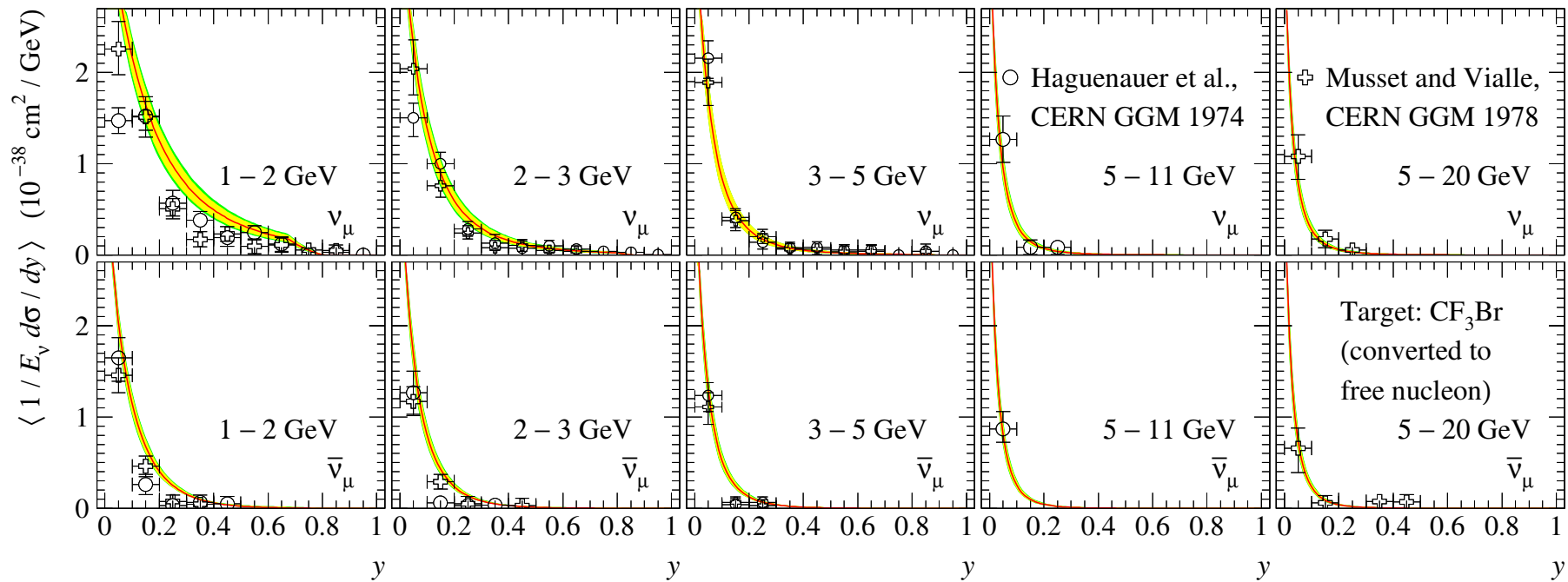












Flux-weighted differential cross sections for $\nu_\mu n \rightarrow \mu^- p$ (top) and $\bar{\nu}_\mu p \rightarrow \mu^+ n$ (bottom). The cross sections were measured in the Gargamelle bubble chamber filled with heavy liquid freon and exposed to the CERN-PS ν_μ and $\bar{\nu}_\mu$ beams.

The shaded regions around the solid curves represent 1σ and 2σ deviations from the best-fitted values of M_A^{run} obtained in the global fit. Only the events with $E_{\nu, \bar{\nu}} > 1.5$ GeV were accepted.

The energy range for each experiment is shown in the legends.

Obsolete GGM 1975 data are also shown for completeness.

Implementation in GENIE


The running axial mass model is implemented into release 2.11.0 of the GENIE Neutrino Event MC generator and is called `genie::KuzminNaumov2016AxialFormFactorModel`.

It works with the default CCQE cross sections model `genie::LwlynSmithQELCCPXSec` and there is no need to make any changes in the 'cross section model' part of the GENIE configuration file `$GENIE/config/UserPhysicsOptions.xml`:

```
<!--
~~~~~
Specify which cross section model is to be used by each GENIE event generation thread.
The parameter name is build as: "XSecModel@[name of thread]"
-->
<!-- New Nieves QE model -->
<!--
<param type="alg" name="XSecModel@genie::EventGenerator/QEL-CC">          genie::NievesQELCCPXSec/ZExp          </param>
-->
<param type="alg" name="XSecModel@genie::EventGenerator/QEL-CC">          genie::LwlynSmithQELCCPXSec/Default    </param>
<param type="alg" name="XSecModel@genie::EventGenerator/QEL-NC">          genie::AhrensNCELXPXSec/Default       </param>
<param type="alg" name="XSecModel@genie::EventGenerator/QEL-EM">          genie::RosenbluthPXSec/Default        </param>
```

To start working with the running axial mass, you need to set the corresponding parameter to `genie::KuzminNaumov2016AxialFormFactorModel` in the configuration file `$GENIE/config/UserPhysicsOptions.xml`:

```
<!--
~~~~~
Axial form factors used for QEL CC cross section calculation.
Options are:
- genie::DipoleAxialFormFactorModel
- genie::ZExpAxialFormFactorModel, Bhattacharya, Paz, and Hill, Phys.Rev. D84 (2011) 073006
- genie::KuzminNaumov2016AxialFormFactorModel, K. Kuzmin and V. Naumov, in press (2016).
<param type="alg" name="AxialFormFactorModel"> genie::ZExpAxialFormFactorModel/Default </param>
-->
<param type="alg" name="AxialFormFactorModel"> genie::DipoleAxialFormFactorModel/Default </param>
```



```
<!--
~~~~~
Axial form factors used for QEL CC cross section calculation.
Options are:
- genie::DipoleAxialFormFactorModel
- genie::ZExpAxialFormFactorModel, Bhattacharya, Paz, and Hill, Phys.Rev. D84 (2011) 073006
- genie::KuzminNaumov2016AxialFormFactorModel, K. Kuzmin and V. Naumov, in press (2016).
<param type="alg" name="AxialFormFactorModel"> genie::ZExpAxialFormFactorModel/Default </param>
-->
<param type="alg" name="AxialFormFactorModel"> genie::KuzminNaumov2016AxialFormFactorModel/Default </param>
```

The values of M_A and $F_A(0)$ in the configuration file [\\$GENIE/config/KuzminNaumov2016AxialFormFactorModel.xml](#) should be set to our best-fit values (instead of the GENIE default ones).

```

<alg_conf>


<!--
Configuration sets for the Kuzmin-Naumov running axial form factors model.

Algorithm Configurable Parameters:
.....
Name          Type    Optional  Comment          Default
.....
Ma            double  Yes      Axial Mass       GPL value: QEL-Ma
FA0          double  Yes      FA(q2 = 0)       GPL value: QEL-FA0
E0           double  Yes      E0                GPL value: CCQE-E0
-->
-----
<param_set name="Default">
</param_set>

</alg_conf>
-----
<param_set name="Default">
  <param type="double" name="Ma"> 1.006 </param>
  <param type="double" name="FA0"> -1.2695 </param>
</param_set>

</alg_conf>

```



There is not need to change the GENIE default value of the parameter E_0 .

A few more comments:

- The best fit parameters M_0 and E_0 were obtained within the SM RFG model but GENIE (in all releases) uses the BR RFG model.
- The set of RFG input parameters (p_F and E_b) in GENIE 2.11.0 is in general different from that used in our analysis.
- There is still uncorrected bug in GENIE 2.11.0 which affects the calculation accuracy for the elastic and quasielastic cross sections for **non-isoscalar** nuclei.
- The electromagnetic form factor models used in GENIE 2.11.0 and in our analysis are slightly different.
- Several general physics constants (e.g. masses of nuclei) used in our analysis are slightly different from those in GENIE 2.11.0.

Most important

Important for some targets

Generally important

Almost negligible

Negligible

We plan:

- Incorporation of the SM RFG into the GENIE (at least its local version).
- Adjustment of the M_A^{run} parameters for the BR RFG model.

Conclusions

- The Smith-Moniz RFG model supplemented by the energy-dependent (running) axial mass, M_A^{run} , defined by only **two universal parameters** M_0 and E_0 , describes well the earlier and modern CCQE data on various nuclear targets.
- The best-fit values of M_0 and E_0 **are sensitive to the details of the RFG model** (including the input Fermi momenta and separation energies) and to the model of the nucleon electromagnetic form factors. However the fit can almost automatically be repeated with other versions of RFG (e.g., Bodek–Ritchie), or its extensions (SF, LFG, etc.), or with more advanced models and improved inputs.
- A more sophisticated parametrization of M_A^{run} **is unreasonable** for the present-day level of accuracy of the CCQE (and CCQE-like) data but may be needed in the future.
- Individual parametrizations for different nuclei or nuclear groups **are not warranted**, but mainly because the currently available dataset for the inorganic heavy nuclear targets is not accurate enough and is not fully self-consistent.
- There's no statistically significant difference between the M_A^{run} parameters extracted separately from the ν and $\bar{\nu}$ data, but there is **a weak hint to a possible difference**. Any case, the available $\bar{\nu}$ dataset is not yet sufficient for a more definite statement.

Finally, we suggest to use the running axial mass option in the NO ν A analyses.

Thanks for attention





“Golden” dataset for the global fits

Accountancy & taxonomy

Experiments with **deuterium** and **hydrogen** targets:

ANL 1977 [5] (σ_ν , 8 data points),
 ANL 1982 [7] ($\langle dN_\nu/dQ^2 \rangle$, 39 data points),
 BNL 1980 [10] ($\sigma_{\bar{\nu}}$, 5 data point),
 BNL 1990 [14, 15] ($\langle dN_\nu/dQ^2 \rangle$, 37 data points),
 FNAL 1983 [16] ($\langle dN_\nu/dQ^2 \rangle$, 20 data points), and
 CERN BEBC 1990 [44] ($\langle d\sigma_\nu/dQ^2 \rangle$, 8 data points).

Experiment with **Ne-H₂** mixture

FNAL 1984 [17] ($dN_{\bar{\nu}}/dQ^2$, 14 data points).

Experiment with **aluminium** target

IHEP-ITEP 1985 [51] (σ_ν , $\sigma_{\bar{\nu}}$, $\langle d\sigma_{\nu+\bar{\nu}}/dQ^2 \rangle$, 8 data points in each set).

Experiments with **carbonaceous** targets

FNAL MiniBooNE 2010 [24] ($\langle d^2\sigma_\nu/dE_\mu d\cos\theta_\mu \rangle$, 137 data points),
 FNAL MiniBooNE 2013 [25] ($\langle d^2\sigma_{\bar{\nu}}/dE_\mu d\cos\theta_\mu \rangle$, 75 data points),
 CERN NOMAD 2009 [47, 48] (σ_ν and $\sigma_{\bar{\nu}}$, 10 and 6 data points, respectively), and
 FNAL MINER ν A 2013 [27, 28] ($\langle d\sigma_\nu/dQ^2 \rangle$, $\langle d\sigma_{\bar{\nu}}/dQ^2 \rangle$, 8 data points in each set).

Experiments with **carbon-containing** mixtures

CERN GGM 1979 [43, 45] ($\langle dN_{\bar{\nu}}/dQ^2 \rangle$, 13 data points),
 CERN LAr-TPC 2007 [46] (σ_ν , 1 data point),
 IHEP SKAT 1990 [56] ($\langle d\sigma_\nu/dQ^2 \rangle$ and $\langle d\sigma_{\bar{\nu}}/dQ^2 \rangle$, 8 and 7 data points, respectively).

Experiment with **iron** target T2K INGRID 2015 [63] (σ_ν , 2 data points).

- Thus the fitted dataset consists of **430** data points with
 - 286** data points for the ν_μ cross sections (66.5% of the full dataset),
 - 136** data points for the $\bar{\nu}_\mu$ cross sections (31.6%), and
 - 8** data points for the summarized cross sections of $\nu_\mu + \bar{\nu}_\mu$ (1.9%).
- The experimental data are presented as follows:
 - 212** data points for the flux-averaged double differential cross sections $\langle d^2\sigma/dE_\mu d\cos\theta_\mu \rangle$ (49.3% of the full dataset, FNAL MiniBooNE),
 - 47** data points for the flux-averaged differential cross sections $\langle d\sigma/dQ^2 \rangle$ (10.9%),
 - 128** data points for the flux-averaged Q^2 distributions $\langle dN/dQ^2 \rangle$ (29.8%), and
 - 43** data points for the total cross sections (10.0%).
- The dataset for extracting the current axial mass M_A (deuterium and hydrogen targets) contains **85** data points (27.2% of the full dataset): ANL 1977 [5], ANL 1982 [7], BNL 1980 [10], BNL 1990 [14, 15], FNAL 1983 [16], CERN 1990 [44].

Criteria for exclusion of data from the global fit:

- Obsolete data (superseded or reconsidered due to increased statistics, revised normalization, etc. in the posterior reports of the same experimental groups).
- Data from the experiments with inactive targets (suggested by Arie Bodek).
- Data with $\chi^2/\text{NDF} > 5$ and $|N - 1| > 2\sigma_N$ (where N is the flux normalization).

Convention: below, the **solid** symbols in the figures represent the data included into the global fit while **open** symbols represent the data excluded from the fit.

The set of experimental data used in the global fit.

Experiment	Data type	N	χ^2/NP
Deuterium & hydrogen data and data for nuclear targets recalculated to free nucleons			
Barish <i>et al.</i> , ANL 1977 [5]	σ_ν^*	$0.893 \pm 0.034 (0.068)$	$15.97/8 = 2.00$
Miller <i>et al.</i> , ANL 1982 [7]	$\langle dN_\nu/dQ^2 \rangle^*$	99.7×0.979	$73.90/38 = 1.95$
Fanourakis <i>et al.</i> , BNL 1980 [10]	$\langle dN_{\bar{\nu}}/dQ^2 \rangle^*$	2.4×0.901	$1.37/4 = 0.34$
	$\sigma_{\bar{\nu}}$	—	$0.05/1 = 0.05$
Kitagaki <i>et al.</i> , BNL 1990 (2003 update) [14]	$\langle dN_\nu/dQ^2 \rangle^*$	245.4×0.991	$21.49/37 = 0.58$
Kitagaki <i>et al.</i> , FNAL 1983 [16]	$\langle dN_\nu/dQ^2 \rangle^*$	41.5×0.945	$8.53/20 = 0.43$
	σ_ν	$1.020 \pm 0.077 (0.152)$	$0.18/2 = 0.09$
Allasia <i>et al.</i> , CERN BEBC 1990 [44]	$\langle d\sigma_\nu/dQ^2 \rangle^*$	$0.935 \pm 0.035 (0.070)$	$4.77/8 = 0.68$
	σ_ν	$0.873 \pm 0.032 (0.064)$	$15.11/6 = 3.02$
Brunner <i>et al.</i> , IHEP SKAT 1990 [55,56]	$\langle d\sigma_\nu/dQ^2 \rangle^*$	$1.077 \pm 0.059 (0.117)$	$3.89/8 = 0.49$
	σ_ν	$1.056 \pm 0.058 (0.115)$	$3.14/8 = 0.39$
	$\langle d\sigma_{\bar{\nu}}/dQ^2 \rangle^*$	$0.902 \pm 0.064 (0.126)$	$7.31/7 = 1.04$
	$\sigma_{\bar{\nu}}$	$0.823 \pm 0.056 (0.111)$	$8.10/7 = 1.15$
Heavy targets data			
Asratyan <i>et al.</i> , FNAL 1984 [17]	$\langle dN_{\bar{\nu}}/dQ^2 \rangle^*$	68.7×0.993	$7.93/14 = 0.57$
	$\sigma_{\bar{\nu}}$	—	$0.06/1 = 0.06$
Aguilar-Arevalo <i>et al.</i> , FNAL MiniBooNE 2010 [24]	$\langle d^2\sigma_\nu/dE_\mu d\cos\theta_\mu \rangle^*$	$1.000 \pm 0.008 (0.015)$	$35.76/137 = 0.26$
Aguilar-Arevalo <i>et al.</i> , FNAL MiniBooNE 2013 [25]	$\langle d^2\sigma_{\bar{\nu}}/dE_\mu d\cos\theta_\mu \rangle^*$	$1.017 \pm 0.012 (0.023)$	$46.86/75 = 0.63$
Fiorentini <i>et al.</i> , FNAL MINER ν A 2013 [27]	$\langle d\sigma_\nu/dQ^2 \rangle^*$	—	$8.04/8 = 1.01$
Fields <i>et al.</i> , FNAL MINER ν A 2013 [28]	$\langle d\sigma_{\bar{\nu}}/dQ^2 \rangle^*$	—	$5.51/8 = 0.67$
Armenise <i>et al.</i> , CERN GGM 1979 [43,45]	$\sigma_{\bar{\nu}}$	$0.781 \pm 0.031 (0.062)$	$20.57/11 = 1.87$
Martinez de la Ossa Romero <i>et al.</i> , CERN LAr-TPC 2007 [46]	σ_ν^*	—	$0.09/1 = 0.09$
Lyubushkin <i>et al.</i> , CERN NOMAD 2009 [47,48]	σ_ν^*	$1.036 \pm 0.026 (0.052)$	$5.91/10 = 0.59$
	$\sigma_{\bar{\nu}}^*$	$1.016 \pm 0.058 (0.114)$	$3.09/6 = 0.52$
Belikov <i>et al.</i> , IHEP-ITEP 1985 [51]	$\langle d\sigma_{\nu+\bar{\nu}}/dQ^2 \rangle^*$	$0.975 \pm 0.114 (0.184)$	$5.68/8 = 0.71$
		$0.988 \pm 0.131 (0.212)$	
	σ_ν^*	$0.873 \pm 0.036 (0.071)$	$7.02/8 = 0.88$
	$\sigma_{\bar{\nu}}^*$	$0.897 \pm 0.045 (0.089)$	$2.66/8 = 0.33$
Abe <i>et al.</i> , T2K ND280 2014 [61]	σ_ν^*	—	$9.57/5 = 2.39$
Abe <i>et al.</i> , T2K INGRID 2015 [63]	σ_ν^*	$0.977 \pm 0.086 (0.170)$	$0.55/2 = 0.28$

* The data included into the global fits.

The fitting method

χ^2 schematically

$$\chi^2 = \sum_{i \text{ (uncorr)}} \sum_{j \in G_i} \frac{[N_i T_{ij}(\boldsymbol{\lambda}) - E_{ij}]^2}{\sigma_{ij}^2} + \sum_{i \text{ (uncorr)}} \frac{(N_i - 1)^2}{\sigma_i^2} + \sum_{i \text{ (corr)}} [\mathbf{T}_i(\boldsymbol{\lambda}) - \mathbf{E}_i] \mathbf{W}_i^{-1} [\mathbf{T}_i(\boldsymbol{\lambda}) - \mathbf{E}_i]^T .$$

Here

- index i enumerates the experiments (or data groups) G_i ,
- index $j \in G_i$ enumerates the bin-averaged experimental data E_{ij} from the group G_i with the errors σ_{ij} which do not include the flux normalization uncertainty, σ_i . The data sets include the total CCQE cross sections, flux-averaged differential cross sections ($d\sigma_{\nu,\bar{\nu}}/dQ^2$, $d^2\sigma_{\nu,\bar{\nu}}/dE_\mu d\cos\theta_\mu$, etc.), and unnormalized Q^2 distributions ($dN_{\nu,\bar{\nu}}/dQ^2$).
- $T_{ij}(\boldsymbol{\lambda})$ represent the model predictions dependent on the set of fitting parameters $\boldsymbol{\lambda}$ (in our particular case, $\boldsymbol{\lambda} = (M_0, E_0)$ for heavy nuclear targets and $\boldsymbol{\lambda} = M_0$ for hydrogen and deuterium targets).
- \mathbf{W}_i is the correlation matrix for the i th group.

Nuclear corrections for the CCQE cross sections on deuterium are, as a rule, already taken into account by the authors of the experiment and are represented as the cross sections or Q^2 distribution for a free nucleon target.

The formal analytic expressions for the normalization factors N_i can be found by solving the system of equations

$$\partial\chi^2/\partial N_i = 0.$$

The solution is of the form:

$$N_i = \frac{1 + \sigma_i^2 \sum_{j \in G_i} \sigma_{ij}^{-2} T_{ij}(\boldsymbol{\lambda}) E_{ij}}{1 + \sigma_i^2 \sum_{j \in G_i} \sigma_{ij}^{-2} [T_{ij}(\boldsymbol{\lambda})]^2}.$$

The penalty terms $(N_i - 1)^2 / \sigma_i^2$ contain the flux uncertainties (σ_i) common to the data group G_i .

The χ^2 for the final fit to all data also includes another penalty term

$$\left(\frac{M_0 - M_A^D}{\Delta M_A^D} \right)^2,$$

which provides a “soft anchoring” of the parameter M_0 to the current axial mass $M_A^D \pm \Delta M_A^D$ obtained from the fitting the robust deuterium data only.

Including the “mixed” data into the χ^2 sum

The expression for χ^2 shown in the slide 73 becomes a bit more complicated when the data is a combination of the values obtained in the experiments with the neutrino and antineutrino beams.

Here we consider the case when we have to fit the *uncorrelated* data like E_1 , E_2 and $E_3 = E'_1 + E'_2$, where the pairs (E_1, E'_1) and (E_2, E'_2) have the common normalization uncertainty. Let's construct the sum for minimization for this case:

$$\begin{aligned} \chi_{\text{mix}}^2 = & \sum_{j \in G_1} \frac{[N_1 T_{1j}(\boldsymbol{\lambda}) - E_{1j}]^2}{\sigma_{1j}^2} + \sum_{j \in G_2} \frac{[N_2 T_{2j}(\boldsymbol{\lambda}) - E_{1j}]^2}{\sigma_{2j}^2} \\ & + \sum_{j \in G_3} \frac{[N_1 T_{1'j}(\boldsymbol{\lambda}) + N_2 T_{2'j}(\boldsymbol{\lambda}) - E_{3j}]^2}{\sigma_{3j}^2} \\ & + \left(\frac{N_1 - 1}{\sigma_1} \right)^2 + \left(\frac{N_2 - 1}{\sigma_2} \right)^2 \end{aligned}$$

(the notation is obvious). From the minimization conditions

$$\frac{\partial \chi_{\text{mix}}^2}{\partial N_1} = \frac{\partial \chi_{\text{mix}}^2}{\partial N_2} = 0$$

we obtain the expressions for the normalization factors:

$$N_1 = \frac{1}{d} (C_1 A_{22} - C_2 A_{12}), \quad N_2 = \frac{1}{d} (C_2 A_{11} - C_1 A_{12}),$$

where

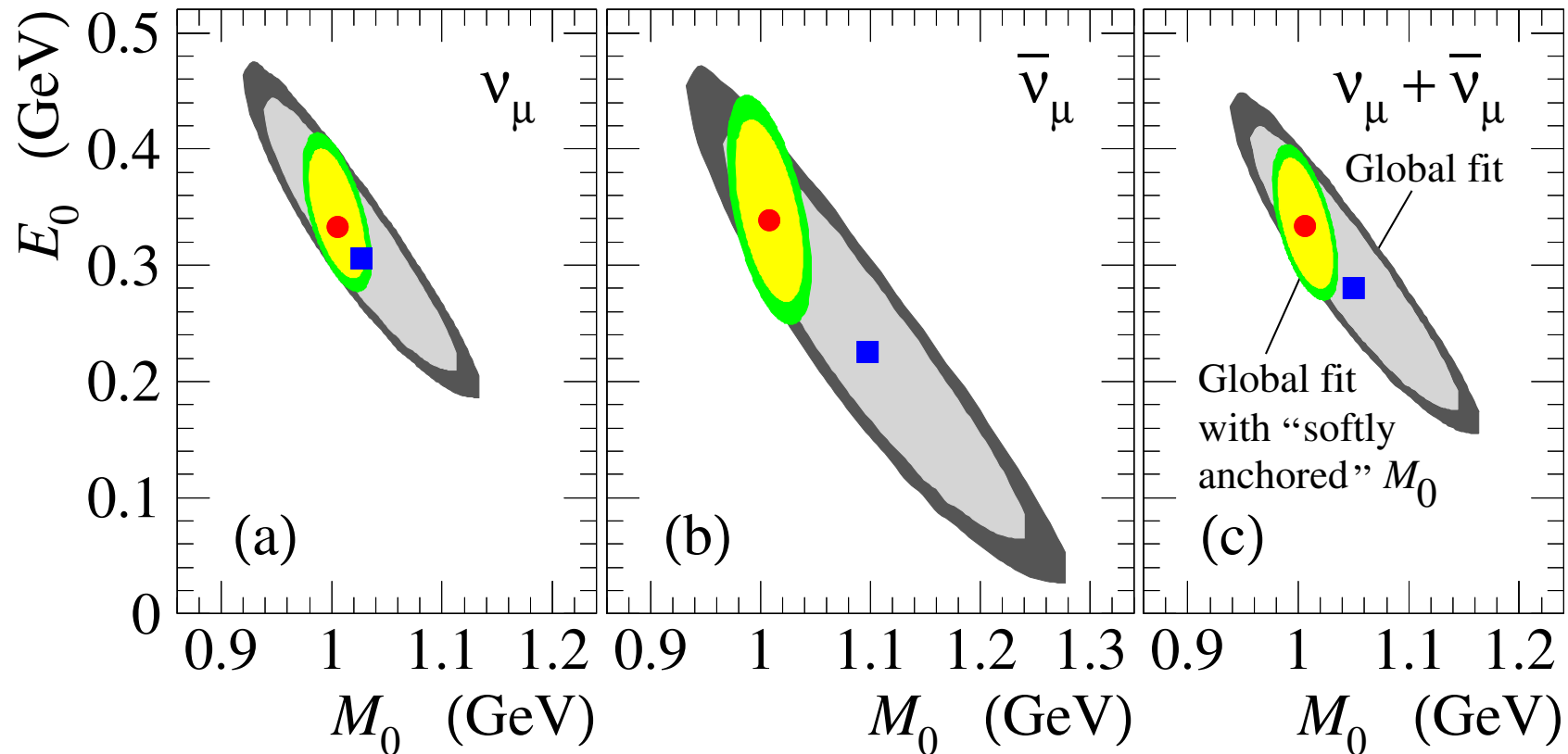
$$d = A_{11}A_{22} - A_{12}^2,$$

$$A_{11} = \sum_{j \in G_1} \frac{[T_{1j}(\lambda)]^2}{\sigma_{1j}^2} + \sum_{j \in G_3} \frac{[T_{1'j}(\lambda)]^2}{\sigma_{3j}^2} + \frac{1}{\sigma_1^2},$$

$$A_{22} = \sum_{j \in G_2} \frac{[T_{2j}(\lambda)]^2}{\sigma_{2j}^2} + \sum_{j \in G_3} \frac{[T_{2'j}(\lambda)]^2}{\sigma_{3j}^2} + \frac{1}{\sigma_2^2},$$

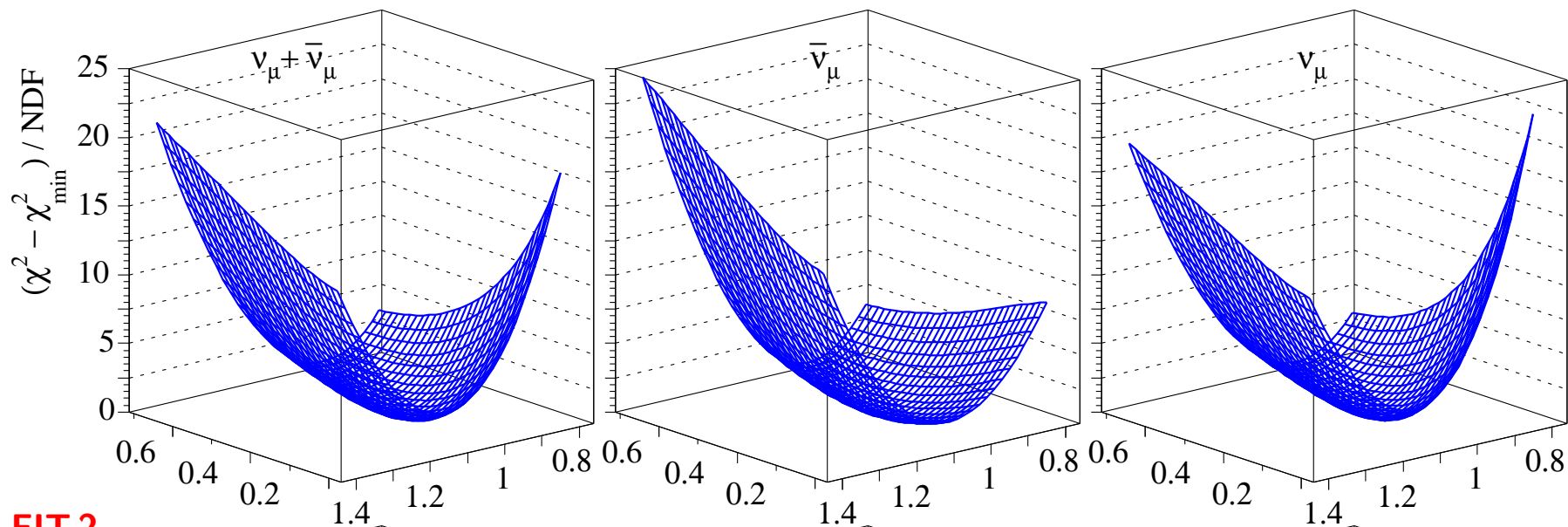
$$A_{12} = \sum_{j \in G_3} \frac{T_{1'j}(\lambda)T_{2'j}(\lambda)}{\sigma_{3j}^2},$$

$$C_i = \sum_{j \in G_2} \frac{T_{ij}(\lambda)E_{ij}(\lambda)}{\sigma_{ij}^2} + \sum_{j \in G_3} \frac{T_{i'j}(\lambda)E_{3j}(\lambda)}{\sigma_{3j}^2} + \frac{1}{\sigma_2^2}.$$

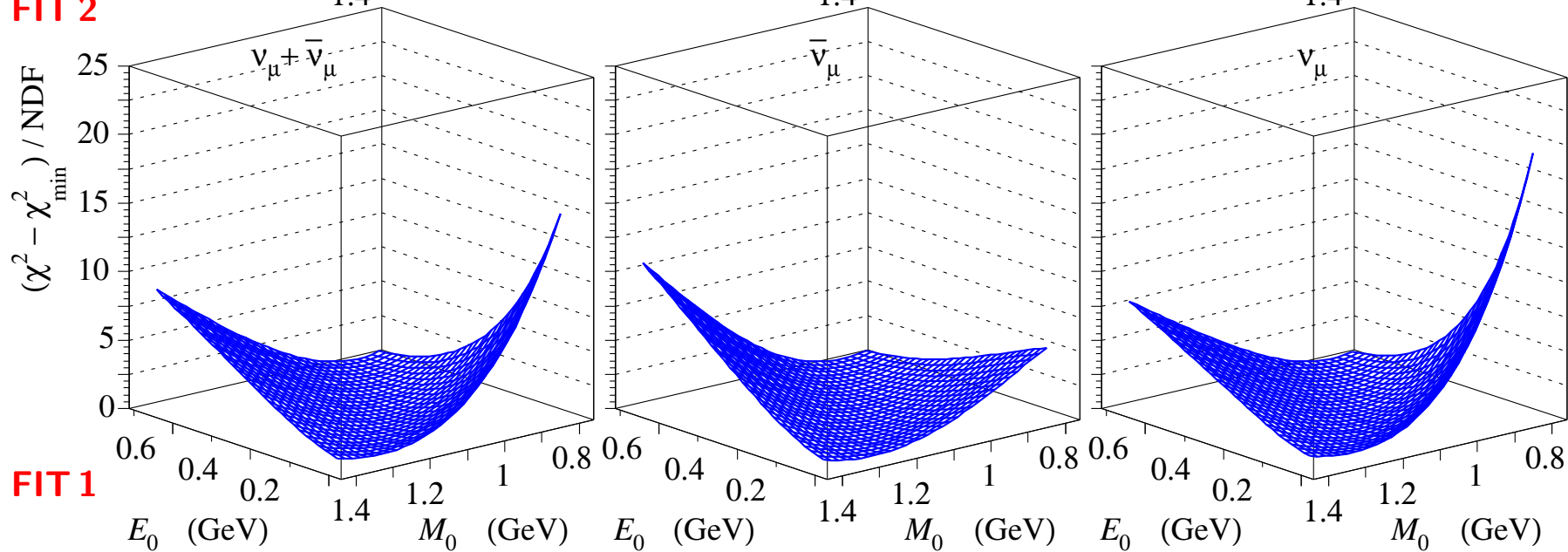


Error contours for the parameters M_0 and E_0 obtained from the global fits for ν (a), $\bar{\nu}$ (b), and $\nu + \bar{\nu}$ (c) CCQE data, performed *without anchoring of M_0* (FIT 1, greater areas) and *with anchoring of M_0* (FIT 2, smaller areas); see slide 74. The inner and outer contours for these fits indicate the 68% and 95% C.L. regions, respectively.

The shapes of $(\chi^2 - \chi_{\min}^2)/\text{NDF}$ for FIT 1 and FIT 2 are shown in the next slide. ↓

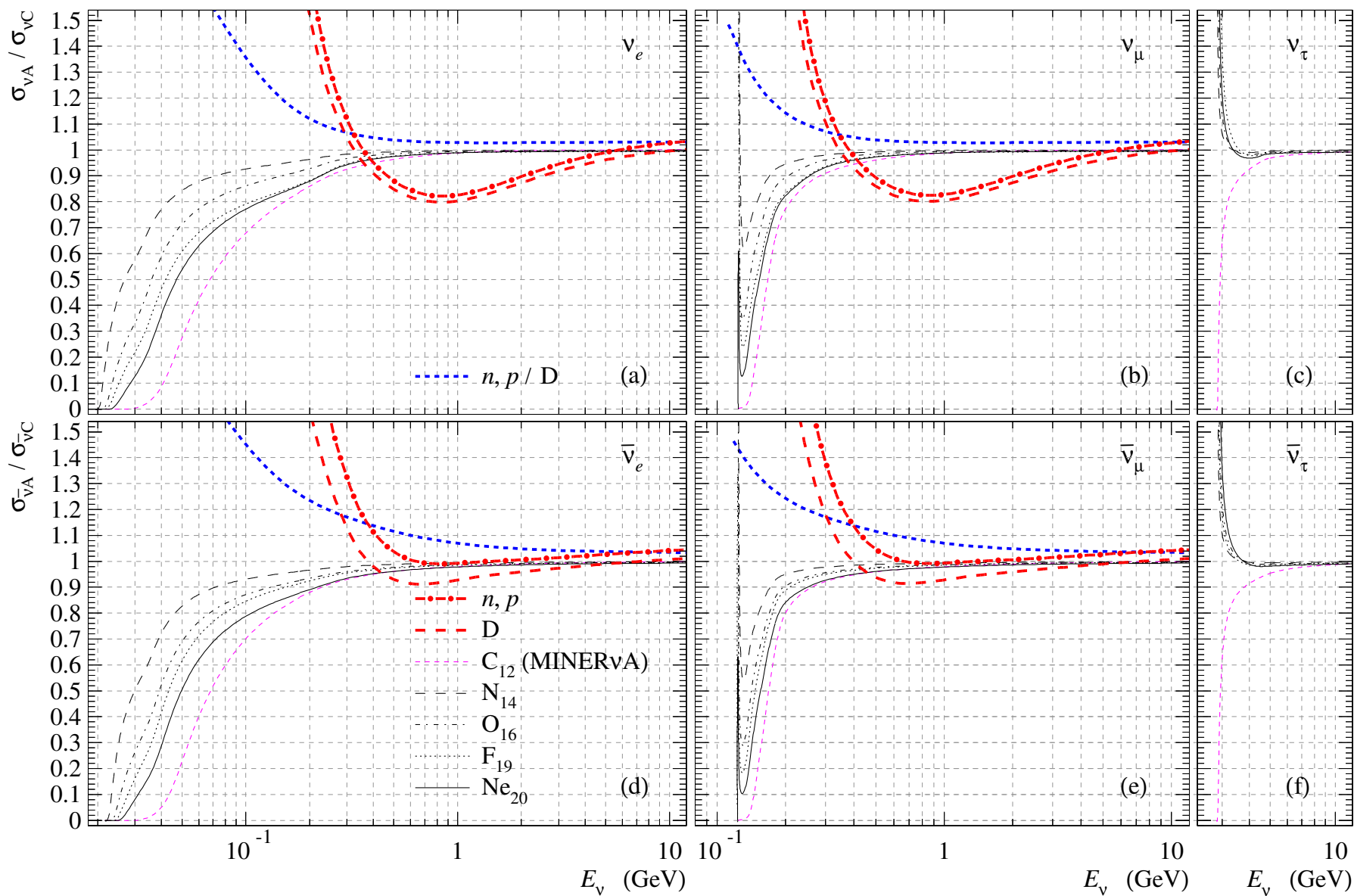


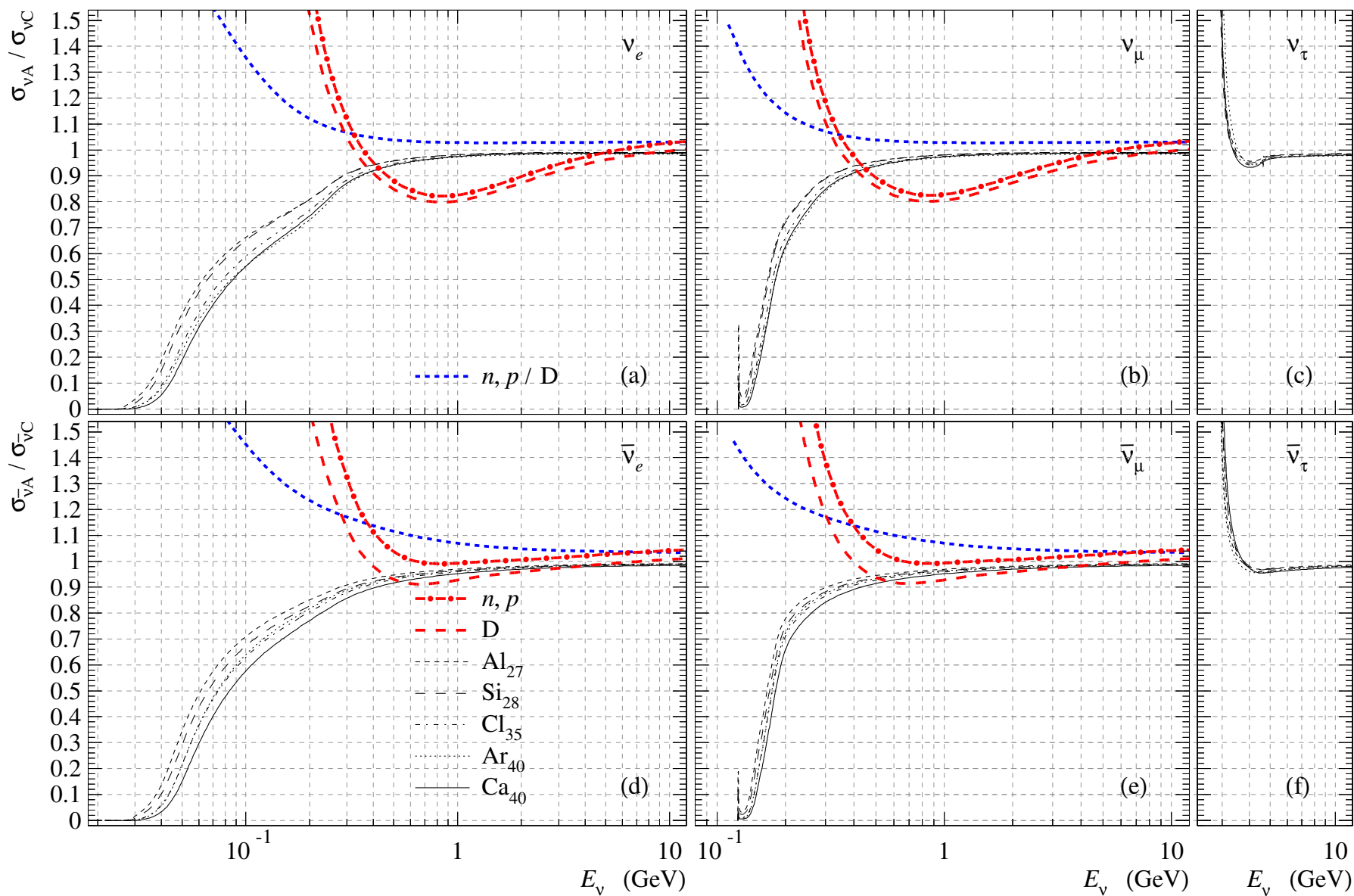
FIT 2

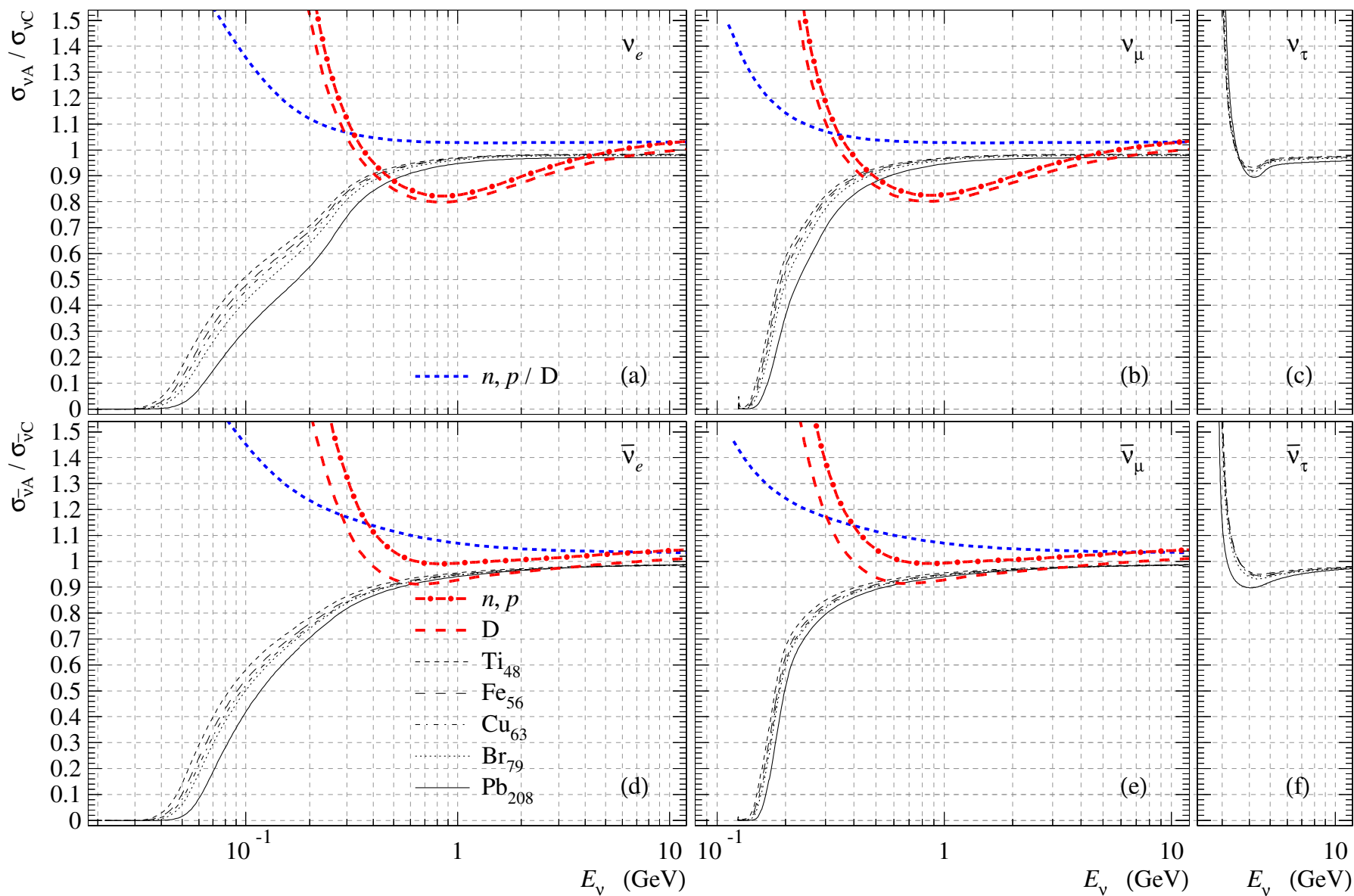


FIT 1

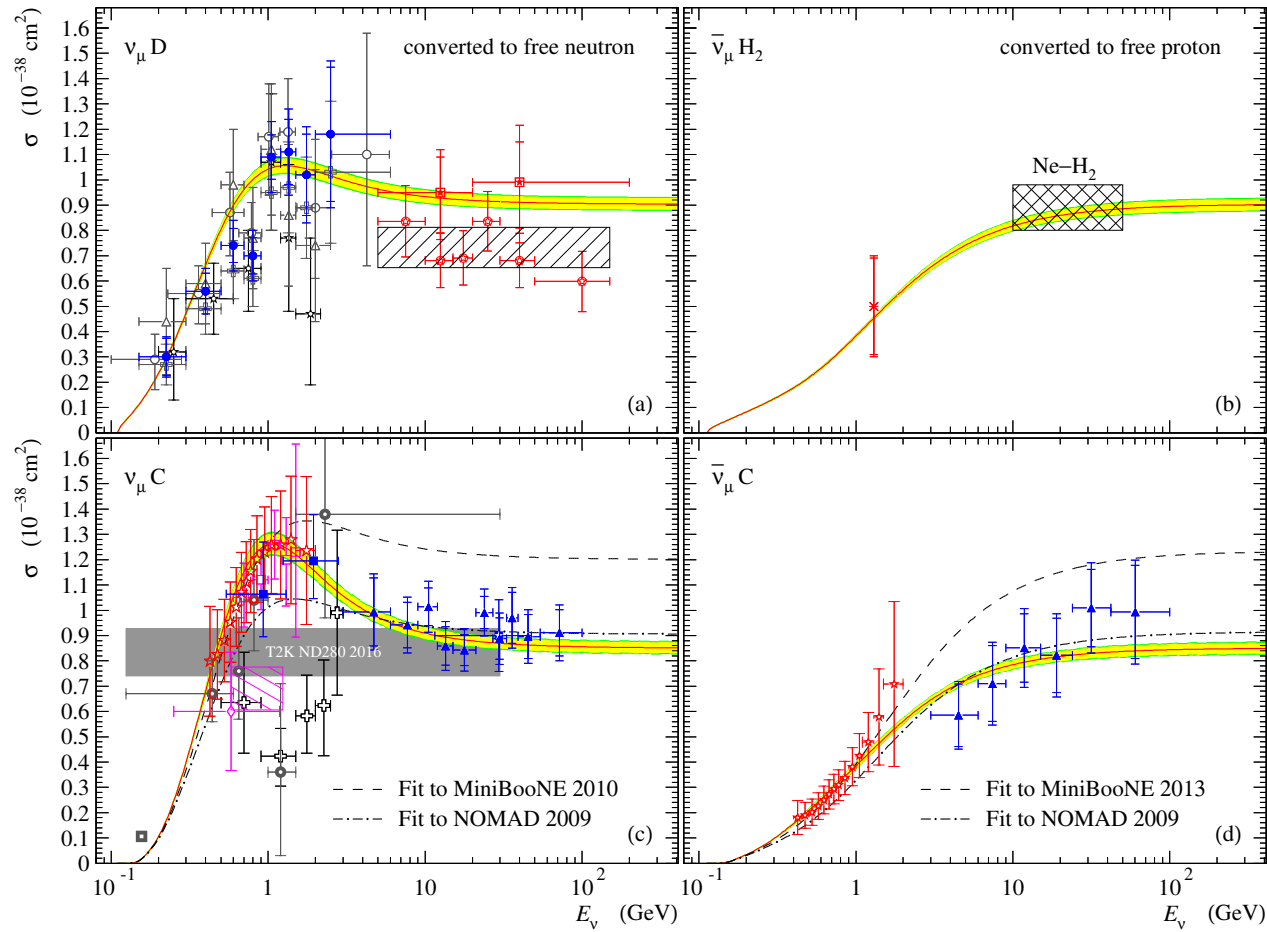
Nuclear effects

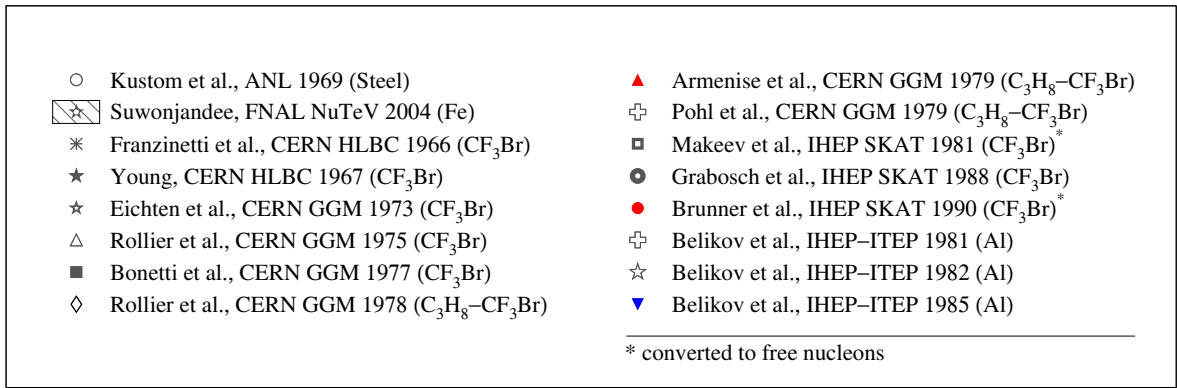
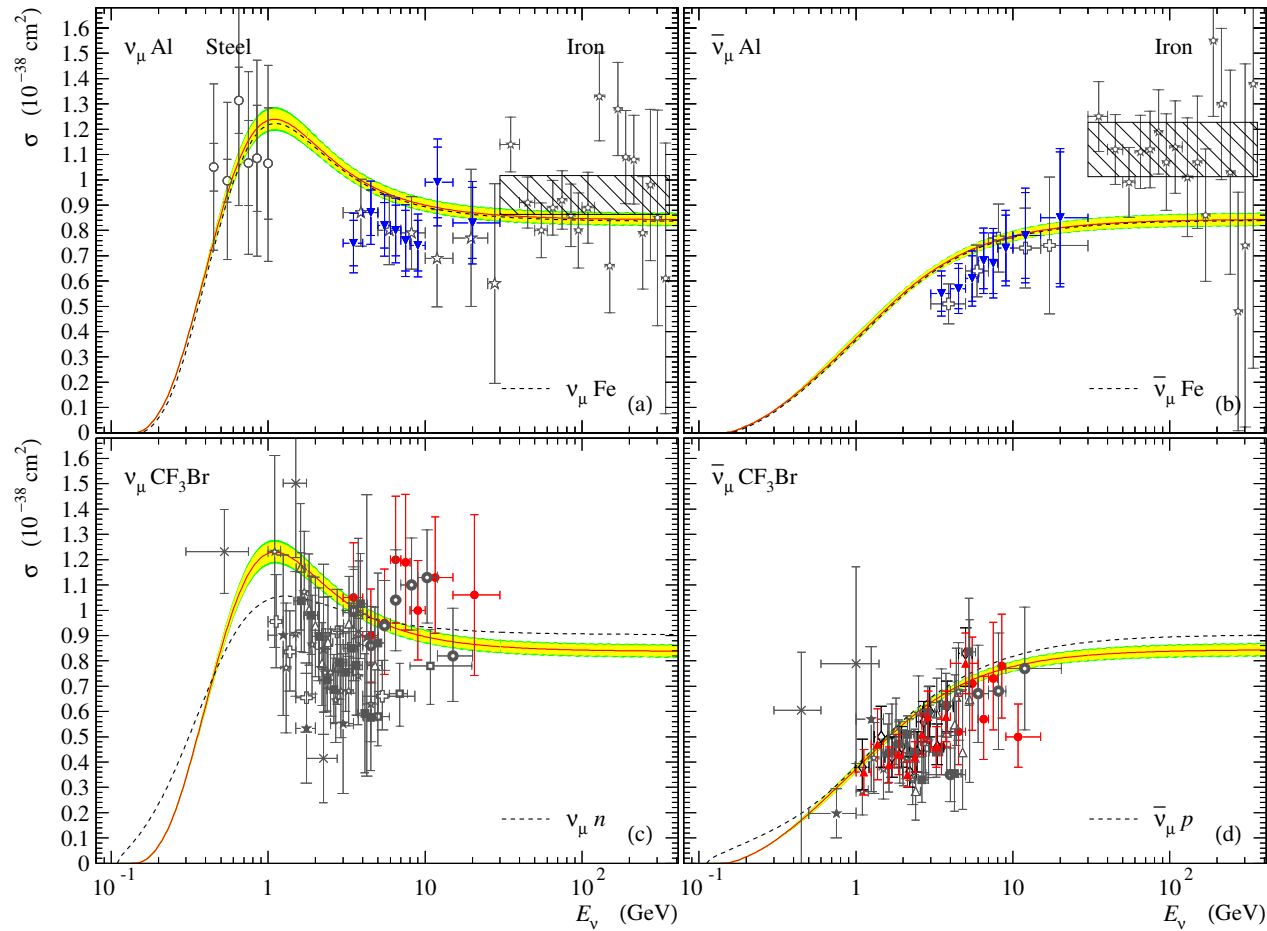


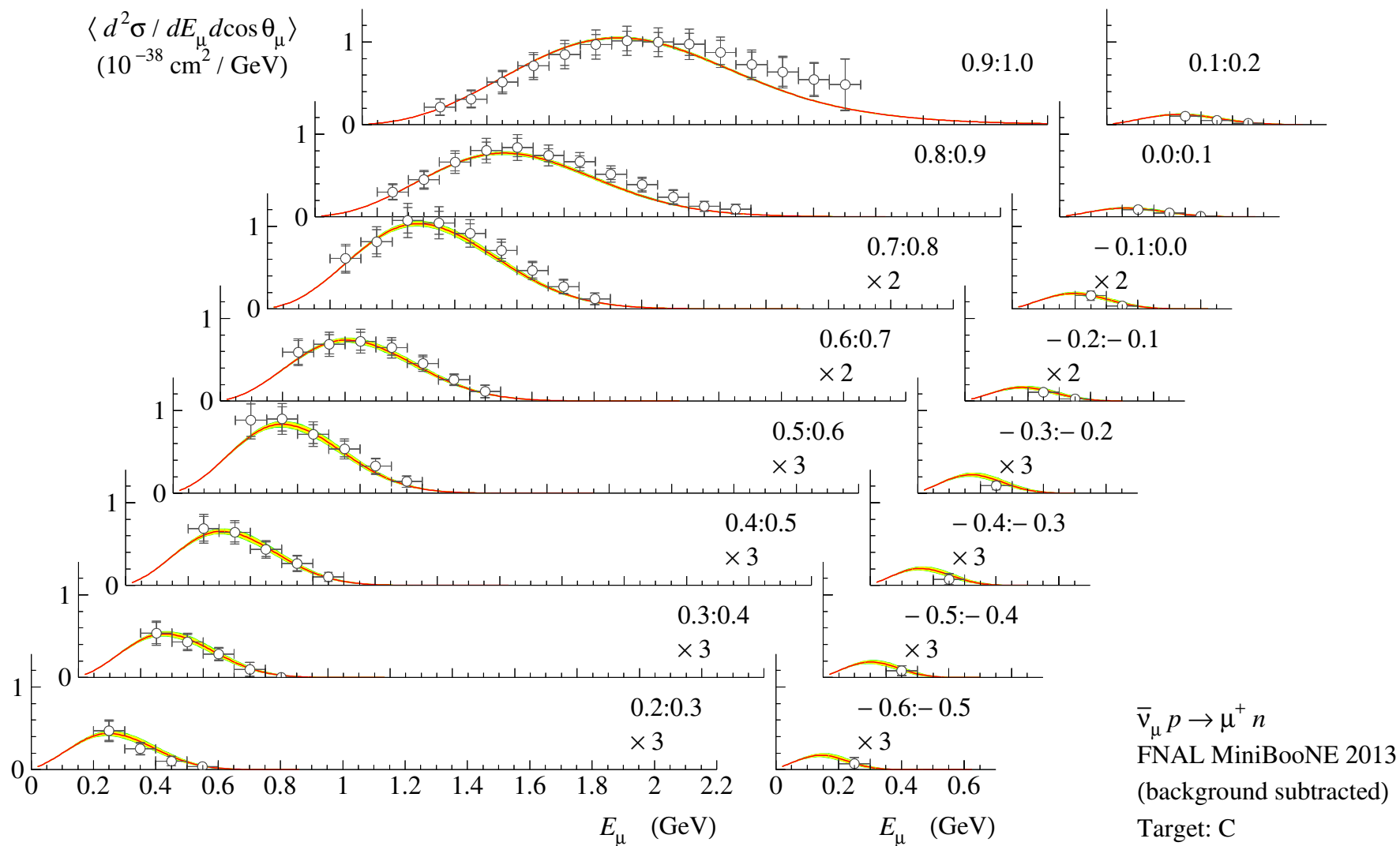




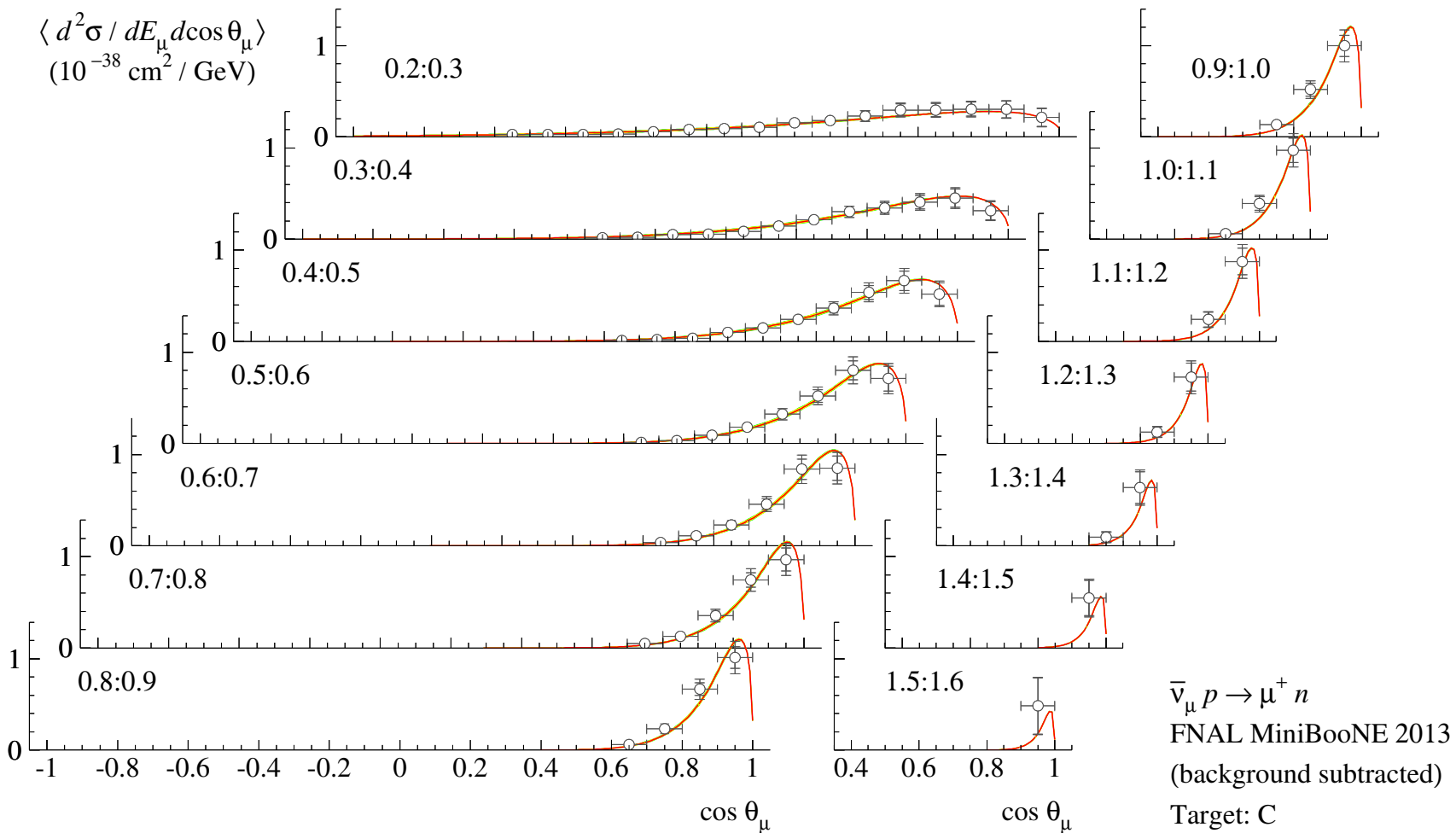
Comparison with data (a few more examples)



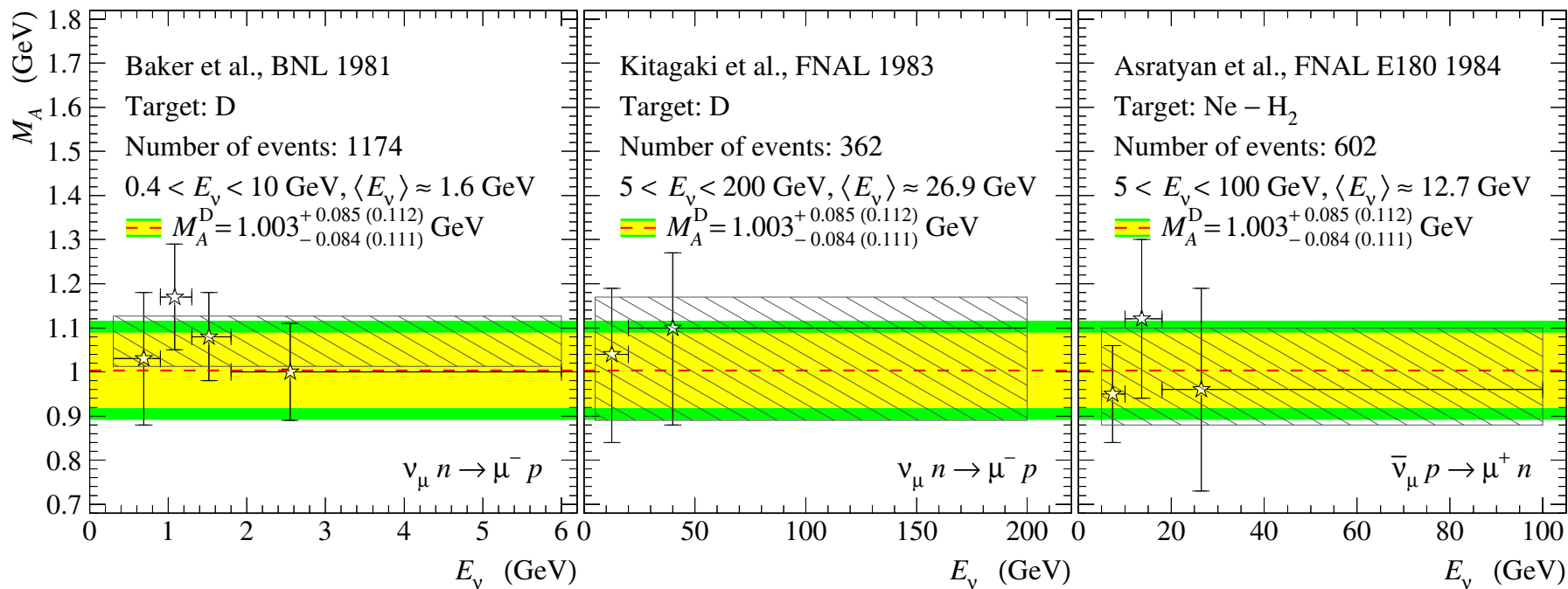




See note in slide 19.



See note in slide 19.

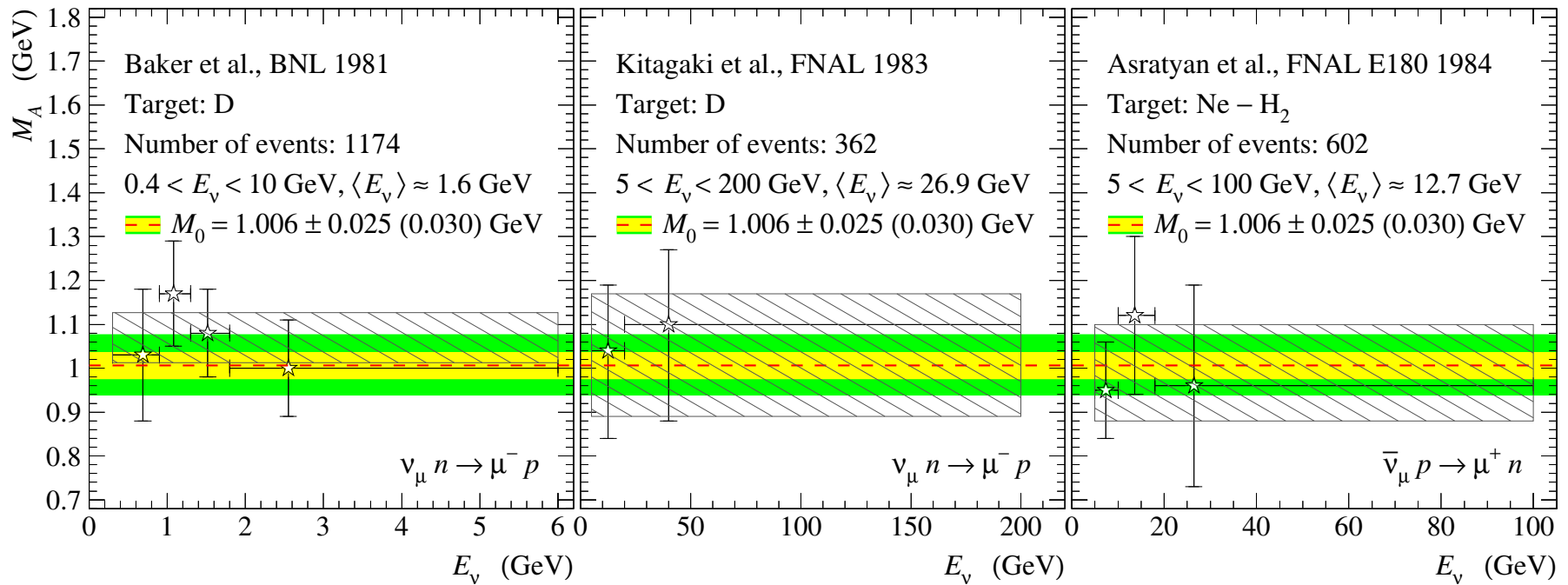


Current axial mass, M_A vs. neutrino energy measured for the $\nu_\mu n \rightarrow \mu^- p$ reaction with the deuterium filled detector at BNL [11]. Rectangle denotes the average value of M_A obtained by the authors of the experiment for the mean neutrino energy $\langle E_\nu \rangle = 1.48 \text{ GeV}$.

Current axial mass, M_A vs. neutrino energy measured for the $\nu_\mu n \rightarrow \mu^- p$ reaction with the deuterium filled detector at BNL [16]. Rectangle denotes the average value of M_A obtained by the authors of the experiment for the whole neutrino energy range at the mean energy of $\langle E_\nu \rangle = 26.9 \text{ GeV}$.

Current axial mass, M_A vs. antineutrino energy measured for the $\bar{\nu}_\mu p \rightarrow \mu^+ n$ reaction with the Ne-H₂ filled detector in the FNAL experiment E180 [17, 18]. Dashed rectangle denotes the average value of M_A obtained by the authors of the experiment for the whole energy range at the mean energy of $\langle E_\nu \rangle = 15.4 \text{ GeV}$.

Dashed line and shaded bands in each panel represent the best-fit value of M_A^D and corresponding 1σ and 2σ uncertainties, obtained in our global fit to the deuterium and hydrogen CCQE data.

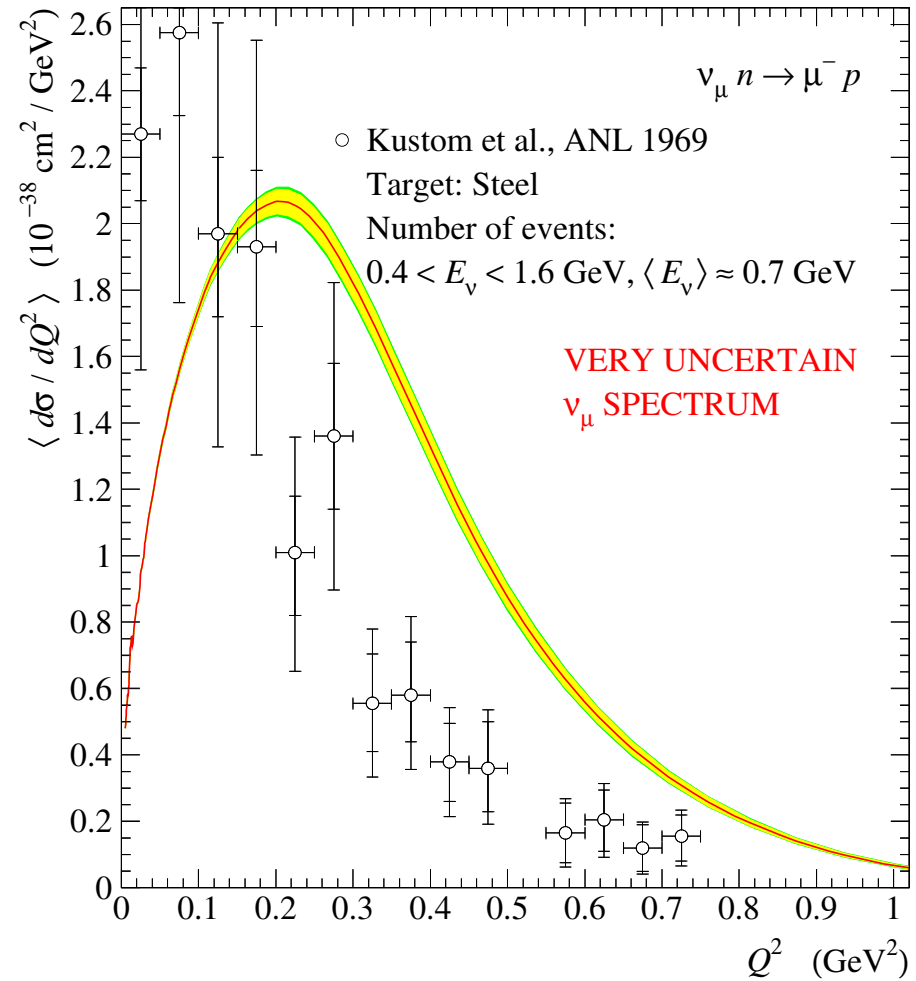
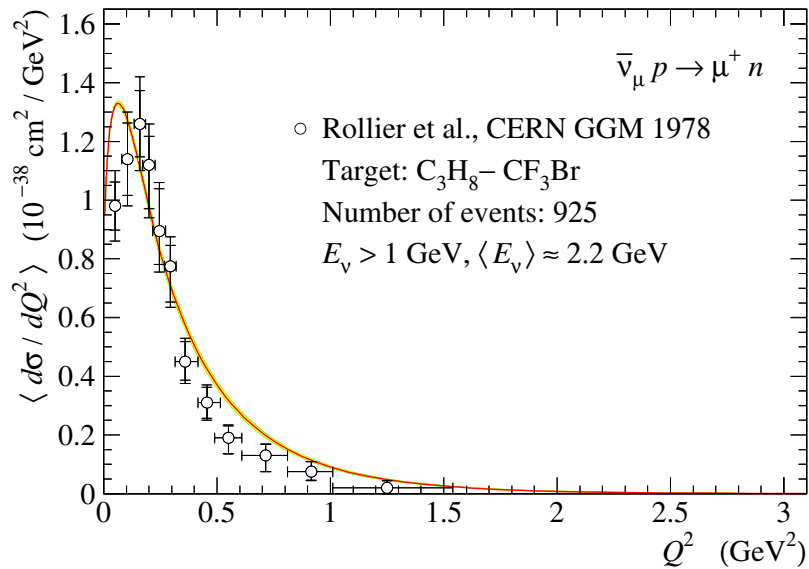


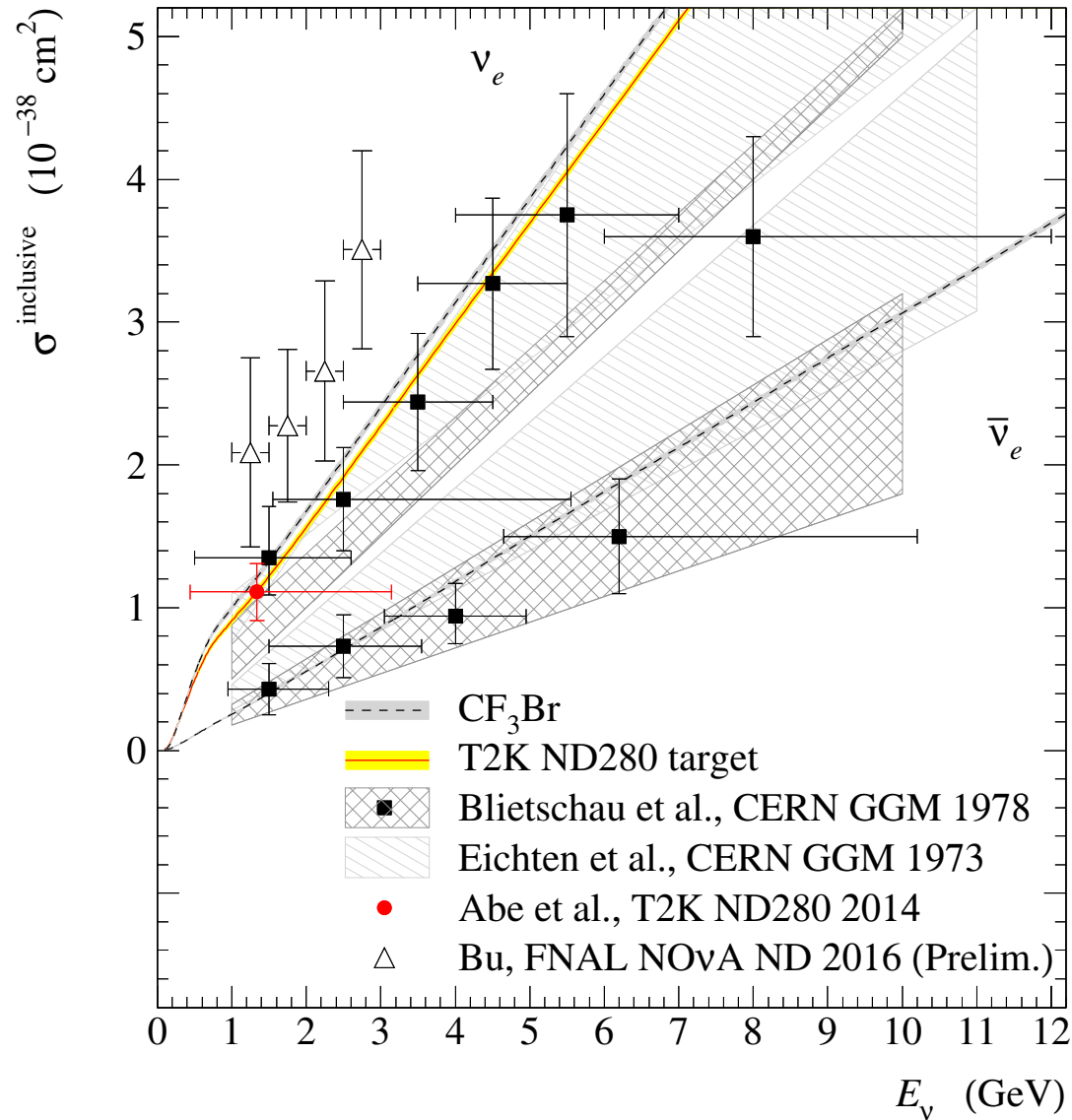
The same as in the previous slide except the lines and bands which now represent the best-fit value of the parameter M_0 (which can be identified with the current axial mass of the nucleon, M_A) and corresponding 1σ and 2σ uncertainties, obtained in our global fit to all CCQE data described in slide 69.

In all our fits, the nuclear corrections for the $\nu - d$ CCQE scattering were accounted for within the impulse approximation and by using the closure over the final dinucleon states and meson exchange current correction at low Q^2 ; the Reid hard core potential and Hulthen wave function for the deuteron were applied.^a

^aSee S.K. Singh and H. Arenhovel, "Pion exchange current effects in $\nu_\mu + d \rightarrow \mu^- + p + p$," Z. Phys. A **324**, 347 (1986) and references therein.

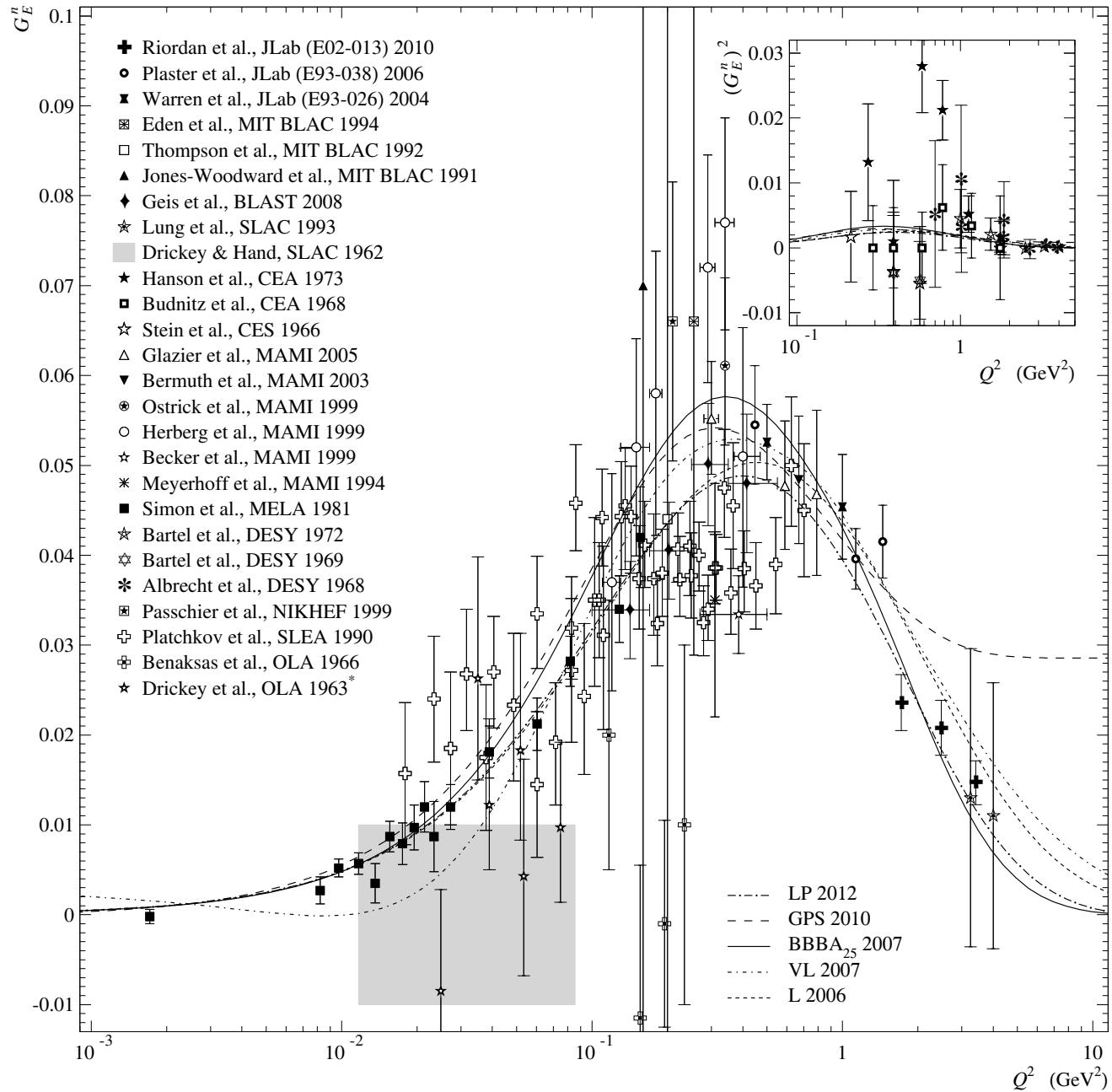
A fly in the ointment (examples of doubtful agreement)

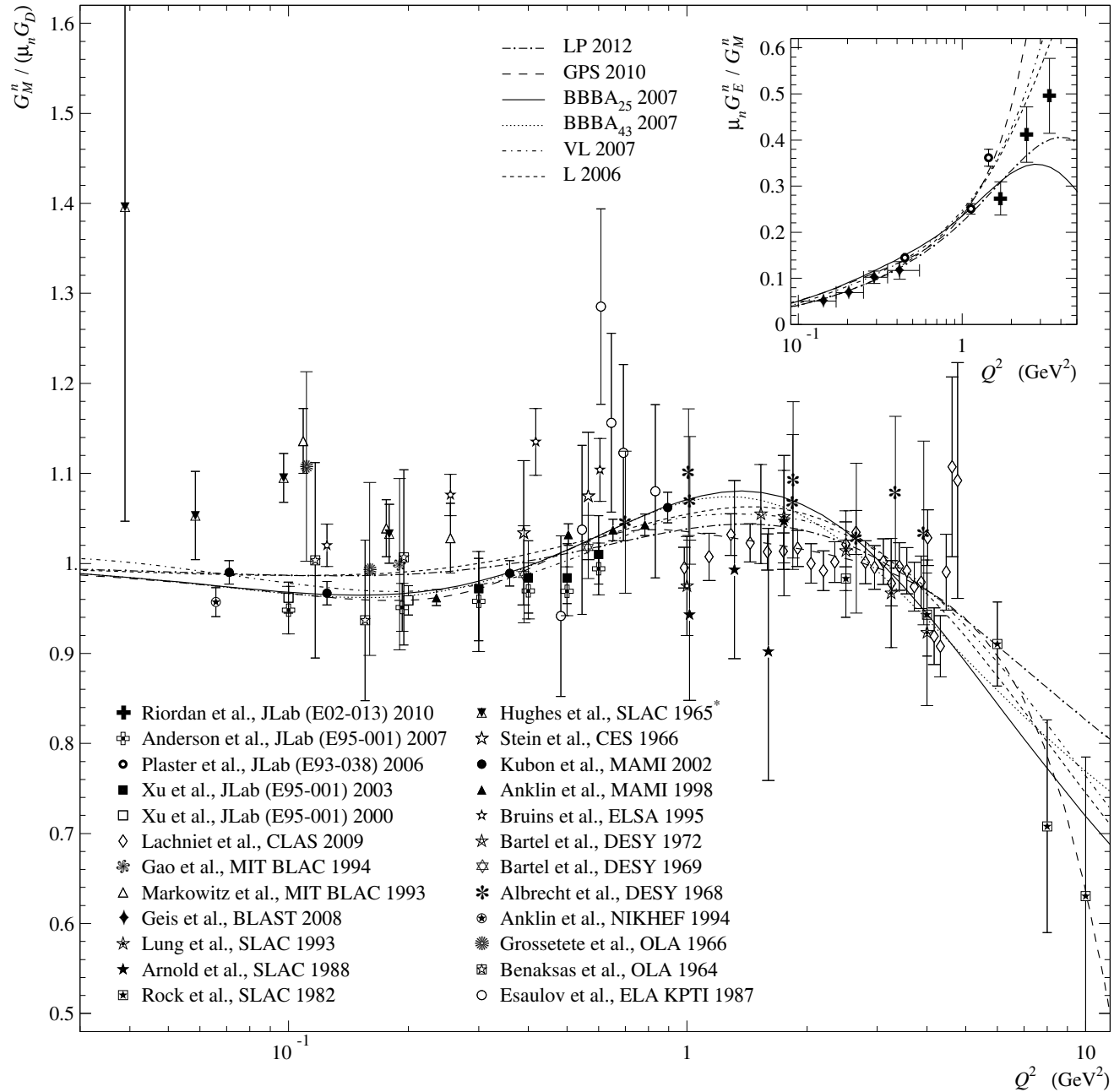


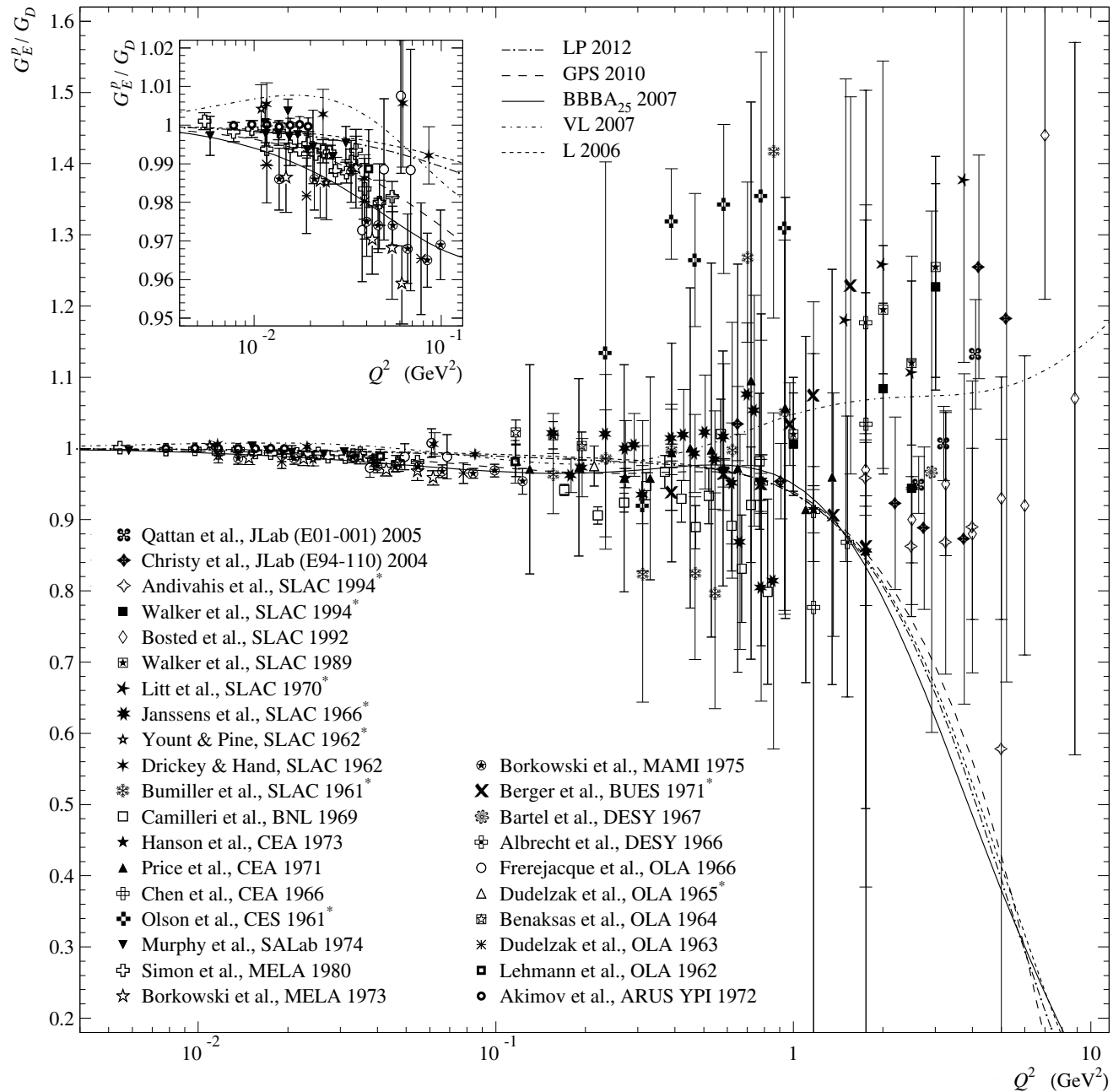


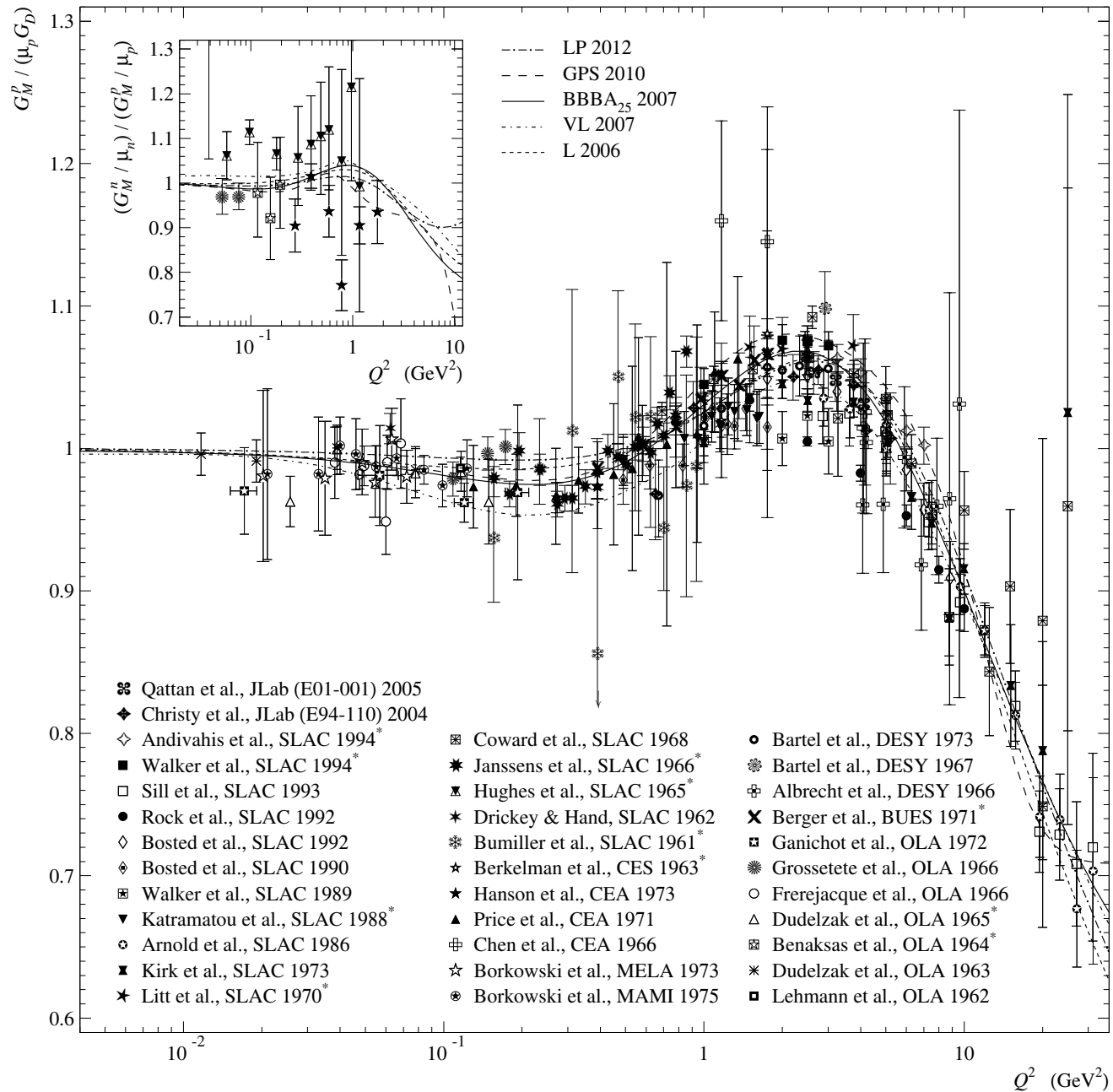
Total inclusive CC cross sections for ν_e and $\bar{\nu}_e$ at low energies with a bit surprising (*preliminary*) data from NO ν A Near Detector (X. Bu, arXiv:1601.01213 [hep-ex]).

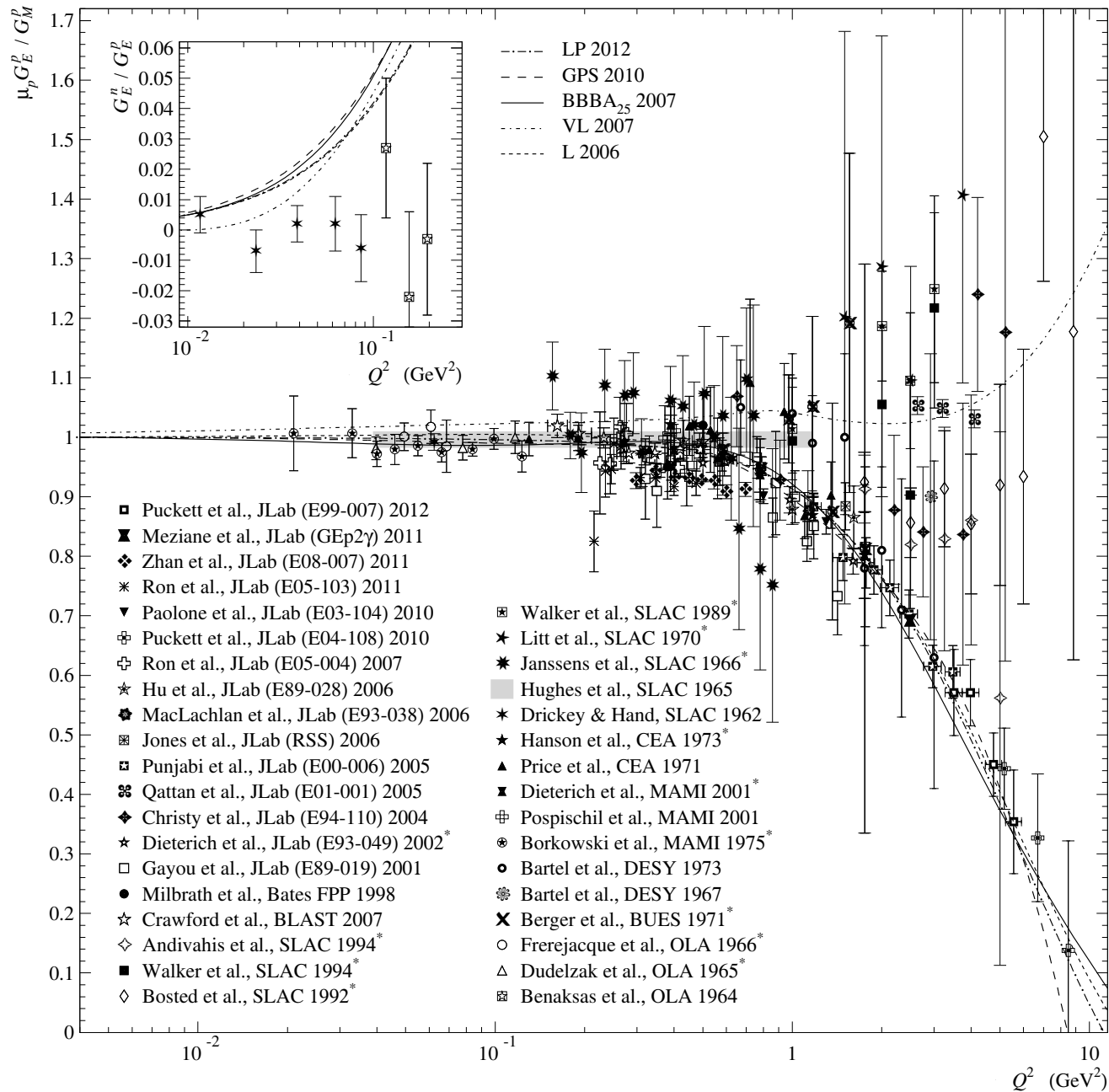
**Comparison of several models
for the nucleon electromagnetic
form factors with data**



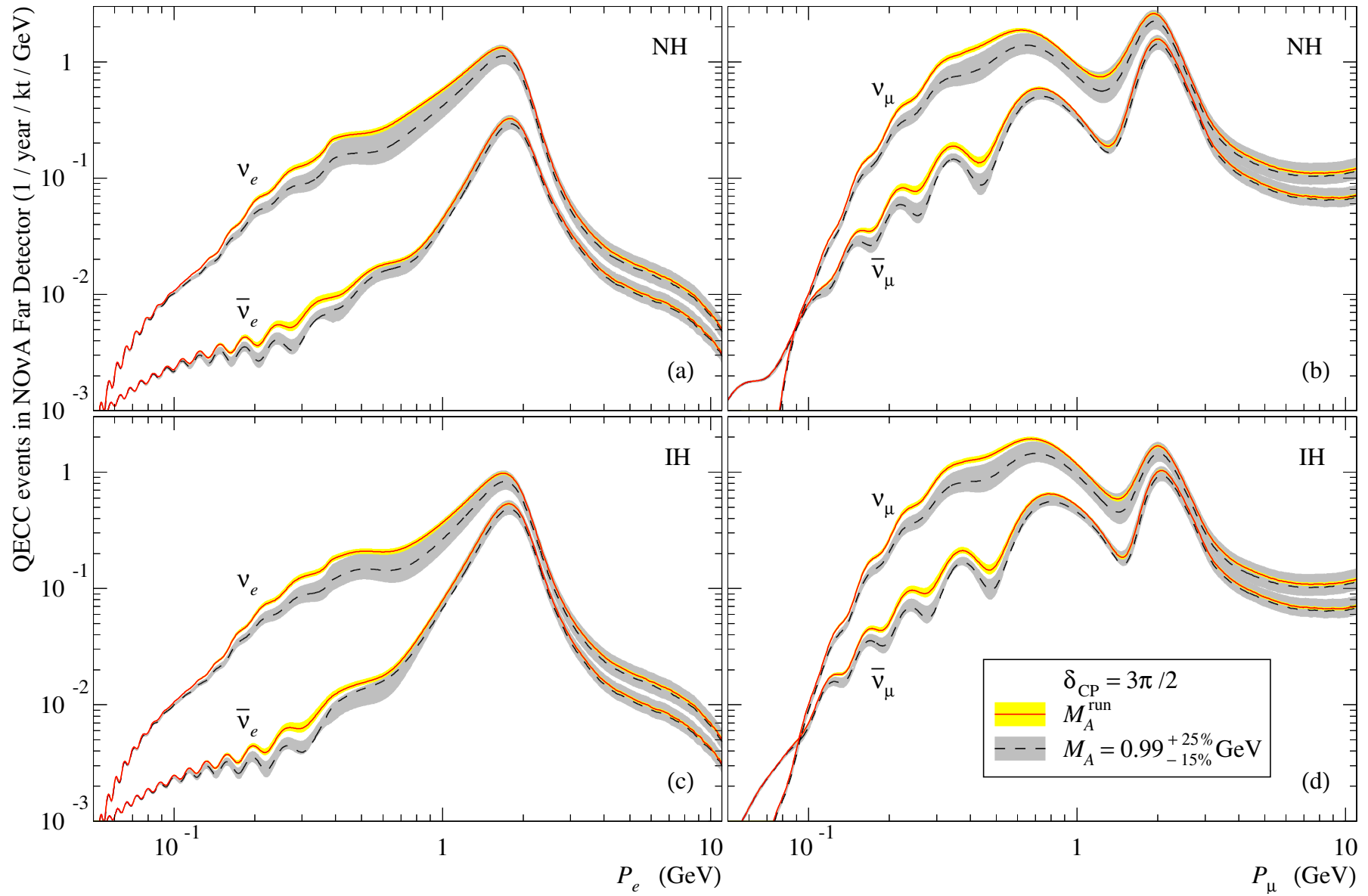




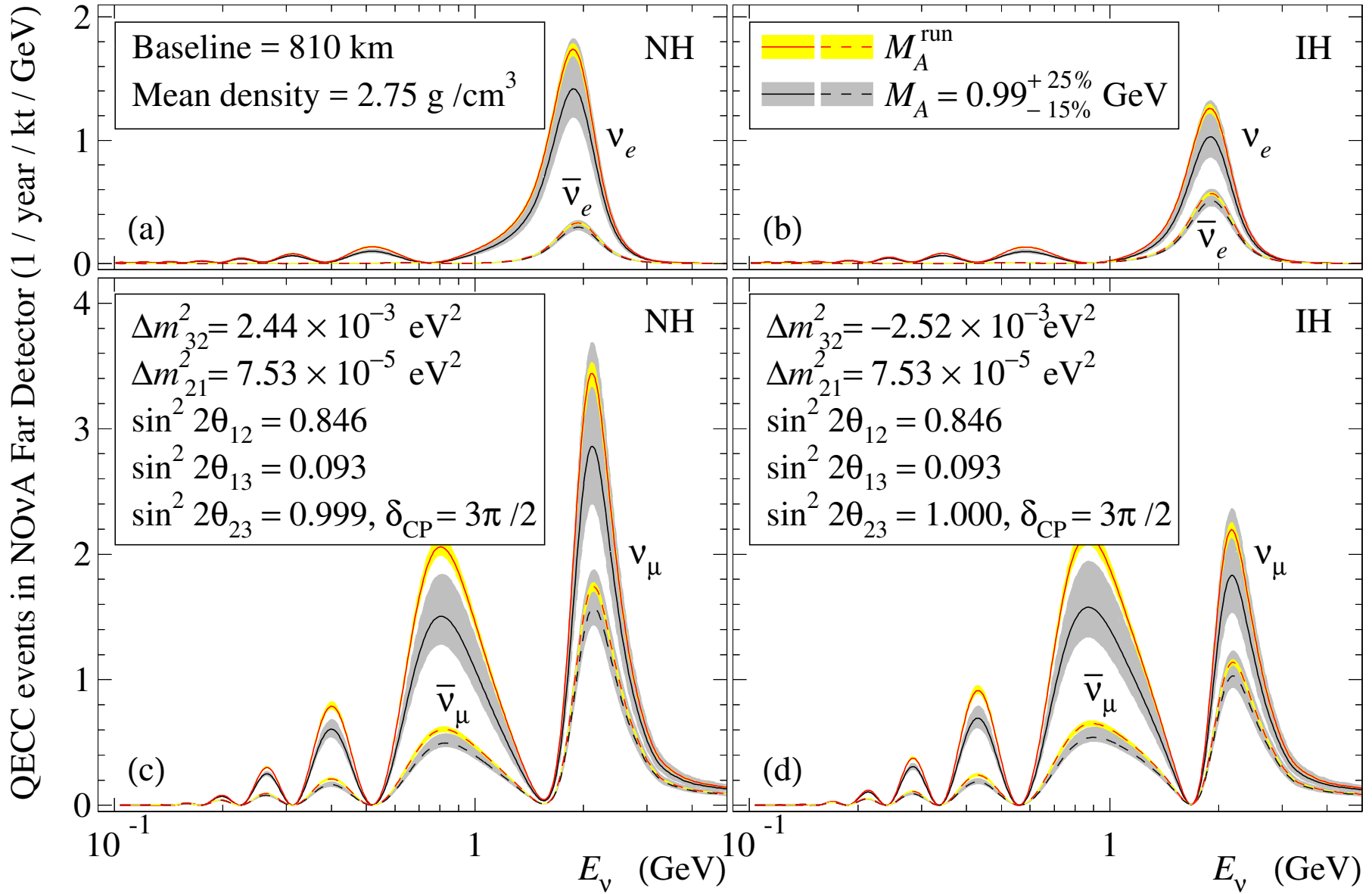




Some applications to NO ν A experiment



An application to NO ν A experiment (for detail, see Ref. [72]).



An application to NO ν A experiment (for detail, see Ref. [71]).

References

ANL EXPERIMENTS

- [1] W. A. Mann *et al.*, in: Proceedings of the 16th International Conference on High Energy Physics, National Accelerator Laboratory, Chicago-Batavia, Illinois, September 6–13, 1972, edited by J. D. Jackson and A. Roberts (National Accelerator Laboratory, Batavia, Illinois, 1973), paper #784.
- [2] W. A. Mann *et al.*, Phys. Rev. Lett. **31**, 844 (1973).
- [3] D. H. Perkins, in: Proceedings of the 1975 International Symposium on Lepton and Photon Interactions at High Energies, Stanford University, August 21–27, 1975, edited by T. W. Kirk (Stanford Linear Accelerator Center, Stanford, 1975), p. 571.
- [4] S. J. Barish *et al.* (ANL–Purdue Collaboration), preprints COO-1428-428, ANL-HEP-CP-75-38 (unpublished).
- [5] S. J. Barish *et al.*, Phys. Rev. D **16**, 3103 (1977).
- [6] R. A. Singer, in: Proceedings of the International Conference on Neutrino Physics and Astrophysics, “Neutrino’77,” Baksan Valley, USSR, June 18–24, 1977, edited by M. A. Markov, G. V. Domogatsky, A. A. Komar, and A. N. Tavkhelidze (Publishing office “Nauka”, Moscow, USSR, 1978), Vol. 2, p. 95.
- [7] K. L. Miller *et al.*, Phys. Rev. D **26**, 537 (1982).
- [8] R. L. Kustom *et al.*, Phys. Rev. Lett. **22**, 1014 (1969).

BNL EXPERIMENTS

- [9] A. M. Cnops *et al.*, in: Proceedings of the Topical Conference on Neutrino Physics at Accelerators, Oxford, UK, July 4–7, 1978, edited by A. G. Michette and P. B. Renton (Rutherford Lab, Chilton, 1978), p. 62. see also preprint BNL-24848, OG431, Brookhaven National Laboratory, 1978 (unpublished).
- [10] G. Fanourakis *et al.*, Phys. Rev. D **21**, 562 (1980).
- [11] N. J. Baker *et al.*, Phys. Rev. D **23**, 2499 (1981).
- [12] L. A. Ahrens *et al.*, Phys. Rev. D **31**, 2732 (1985); L. A. Ahrens *et al.* (Japan–USA Neutrino Collaboration), BNL-36726, CONF-850375-15, 1985.
- [13] L. A. Ahrens *et al.*, Phys. Lett. B **202**, 284 (1988).
- [14] T. Kitagaki *et al.*, Phys. Rev. D **42**, 1331 (1990)
- [15] K. Furuno *et al.*, A talk at the 2nd International Workshop on Neutrino-Nucleus Interactions in the few-GeV Region, (NuInt 2002), University of California, Irvine, December 12–15, 2002; KEK Preprint 2003-48, September, 2003 (unpublished). With reference to H. Sagawa, Ph.D. Thesis, Tohoku University, 1985 (unpublished); T. Kitagaki *et al.*, Phys. Rev. D **34**, 2554 (1986).

FNAL EXPERIMENTS

- [16] T. Kitagaki *et al.*, Phys. Rev. D **28**, 436 (1983).
- [17] A. E. Asratyan *et al.*, Yad. Fiz. **39**, 619 (1984) [Sov. J. Nucl. Phys. **39**, 392 (1984)].
- [18] A. E. Asratyan *et al.*, Phys. Lett. **137** B, 122 (1984).
- [19] V. V. Ammosov *et al.* (IHEP–ITEP–MPEI Collaboration), Z. Phys. C **36**, 377 (1987).
- [20] N. Suwonjandee, Ph.D. Thesis, University of Cincinnati, Cincinnati, 2004, FERMILAB-THESIS-2004-67, Fermi National Accelerator Laboratory, Illinois, 2004; UMI 31-20857 (unpublished).
- [21] A. A. Aguilar-Arevalo *et al.* (MiniBooNE Collaboration), Phys. Rev. Lett. **100**, 032301 (2008) [arXiv:0706.0926 [hep-ex]].
- [22] T. Katori, AIP Conf. Proc. **1189**, 139 (2009) [arXiv:0909.1996 [hep-ex]].
- [23] J. L. Alcaraz-Aunión and J. Walding, AIP Conf. Proc. **1189**, 145 (2009) [arXiv:0909.5647 [hep-ex]]; see also J. L. Alcaraz-Aunión, Ph.D. Thesis, University of Barcelona, Barcelona, 2010, FERMILAB-THESIS-2010-45, Fermi National Accelerator Laboratory, Illinois, 2010 (unpublished).
- [24] A. A. Aguilar-Arevalo *et al.* (MiniBooNE Collaboration), Phys. Rev. D **81**, 092005 (2010) [arXiv:1002.2680 [hep-ex]].
- [25] A. A. Aguilar-Arevalo *et al.* (MiniBooNE Collaboration), Phys. Rev. D **88**, 032001 (2013) [arXiv:1301.7067 [hep-ex]].
- [26] J. Chvojka, Ph.D. Thesis., University of Rochester, 2012, FERMILAB-THESIS-2012-22, Fermi National Accelerator Laboratory, Illinois, 2012 (unpublished).
- [27] G. A. Fiorentini *et al.*, Phys. Rev. Lett. **111**, 022502 (2013) [arXiv:1305.2243 [hep-ex]].
- [28] L. Fields *et al.*, Phys. Rev. Lett. **111**, 022501 (2013) arXiv:1305.2234 [hep-ex].

CERN EXPERIMENTS

- [29] M. M. Block *et al.*, Phys. Lett. **12**, 281 (1964).
- [30] H. Burmeister *et al.*, in: Proceedings of the Informal Conference on Experimental Neutrino Physics, CERN, Geneva, January 20–22, 1965, edited by C. Franzinetti, CERN Yellow Report No. 65-32, European Organization for Nuclear Research, Geneva, 1965, p. 25.
- [31] C. Franzinetti, Lecture given at the Chicago Meeting of the American Physical Society, Chicago, October 28, 1965, CERN Yellow Report No. 66-13, European Organization for Nuclear Research, Geneva, March 1966 (unpublished).
- [32] E. C. M. Young, Ph. D. Thesis, CERN Yellow Report No. 67-12, European Organization for Nuclear Research, Geneva, 1967 (unpublished).
- [33] A. Orkin-Lecourtois, C. A. Piketty, Nuovo Cim. **50 A**, 927 (1967).
- [34] M. Holder *et al.*, Nuovo Cim. A **57**, 338 (1968).
- [35] I. Budagov *et al.*, Lett. Nuovo Cim. **2**, 689 (1969).
- [36] T. Eichten *et al.*, Phys. Lett. **46 B**, 274 (1973).
- [37] M. Haguenaier (for the Aachen–Brussels–CERN–Paris–Milano–Orsay–London Collaboration), in: Proceedings of the 17th International Conference on High Energy Physics, London, July 1–10, 1974, edited by J. R. Smith (Rutherford High Energy Laboratory, Didcot, Berkshire, UK, 1975), p. IV-95.
- [38] M. Rollier (for the Aachen–Bruxelles–CERN–Ecole Polytechnique–Orsay–London Collaboration), in: Proceedings of the International Colloquium on High Energy Neutrino Physics, Paris, France, March 18–20, 1975, (Editions du CNRS, École Polytechnique, 1975), p. 349.
- [39] S. Bonetti *et al.*, Nuovo Cim. **38 A**, 260 (1977).
- [40] P. Musset and J.-P. Vialle, Phys. Rept. **39**, 1 (1978).
- [41] M. Rollier (for the Gargamelle Antineutrino Collaboration, Bari–Milano–Strasbourg–Torino–University College London), in: Proceedings of the Topical Conference on Neutrino Physics at Accelerators, Oxford, UK, July 4–7, 1978, edited by A. G. Michette and P. B. Renton (Rutherford Lab, Chilton, 1978), p. 68.
- [42] M. Pohl *et al.* (Gargamelle Neutrino Propane Collaboration), Lett. Nuovo Cim. **26**, 332 (1979).
- [43] N. Armenise *et al.*, Nucl. Phys. B **152**, 365 (1979).
- [44] D. Allasia *et al.* (Amsterdam–Bergen–Bologna–Padova–Pisa–Saclay–Torino Collaboration), Nucl. Phys. B **343**, 285 (1990).
- [45] S. K. Singh and E. Oset, Nucl. Phys. A **542**, 587 (1992).
- [46] A. Martinez de la Ossa Romero, arXiv:hep-ex/0703026.
- [47] V. V. Lyubushkin *et al.*, Eur. Phys. J. C **63**, 355 (2009) [arXiv:0812.4543[hep-ex]].
- [48] V. V. Lyubushkin, Ph. D. Thesis, JINR, Dubna, 2009 (unpublished).

IHEP EXPERIMENTS

- [49] S. V. Belikov *et al.* (IHEP–ITEP Collaboration), preprint IFVE 81-146 ONF SERP-E-45, Serpukhov, 1981 (unpublished).
- [50] S. V. Belikov *et al.*, Yad. Fiz. **35**, 59 (1982) [Sov. J. Nucl. Phys. **35**, 35 (1982)].
- [51] S. V. Belikov *et al.*, Z. Phys. A **320**, 625 (1985); S. V. Belikov *et al.*, Yad. Fiz. **41**, 919 (1985) [Sov. J. Nucl. Phys. **41**, 589 (1985)].
- [52] V. V. Makeev *et al.*, Pisma v Zh. Eksp. Teor. Fiz. **34**, 418 (1981) [JETP Lett. **34**, 397 (1981)].
- [53] H. J. Grabosch *et al.* (SKAT Collaboration), preprints PHE 86-11, Berlin-Zeuthen, 1986 and IFVE 86-221 ONF SERP-E-107, Serpukhov, 1986 (unpublished).
- [54] H. J. Grabosch *et al.*, Yad. Fiz. **47**, 1630 (1988) [Sov. J. Nucl. Phys. **47**, 1032 (1988)].
- [55] V. V. Ammosov *et al.*, Fiz. Elem. Chast. Atom. Yadra **23**, 648 (1992) [Sov. J. Part. Nucl. **23**, 283 (1992)].
- [56] J. Brunner *et al.* (SKAT Collaboration), Z. Phys. C **45**, 551 (1990).

K2K & T2K EXPERIMENTS

- [57] T. Kikawa (on behalf of the T2K collaboration), XXIV Workshop on Weak Interactions and Neutrinos, September 16 – 21, 2013, Natal, Brazil.
- [58] D. Hadley (for the T2K Collaboration), PoS(EPS-HEP 2013)008.
- [59] K. Abe *et al.*, Phys. Rev. D **87**, 092003 (2013) [arXiv:1302.4908 [hep-ex]].
- [60] R. Gran *et al.* (K2K Collaboration), Phys. Rev. D **74**, 052002 (2006) [arXiv:hep-ex/0603034].

- [61] K. Abe *et al.* (T2K Collaboration), Phys. Rev. D **92**, 112003 (2015) [arXiv:1411.6264 [hep-ex]].
- [62] K. Abe *et al.* (T2K Collaboration), Phys. Rev. Lett. **113**, 241803 (2014) [arXiv:1407.7389 [hep-ex]].
- [63] K. Abe *et al.* (T2K Collaboration), Phys. Rev. D. **91**, 112002 (2015) [arXiv:1503.07452 [hep-ex]].
- [64] X. Espinal and R. Sánchez, AIP Conf. Proc. **967**, 117 (2007).
- [65] K. Nitta *et al.*, Nucl. Instrum. Meth. A **535**, 147 (2004) [arXiv:hep-ex/0406023].
- [66] M. H. Ahn *et al.* (K2K Collaboration), Phys. Rev. D **74**, 072003 (2006) [arXiv:hep-ex/0606032].
- [67] Y. Ashie *et al.* (Super-Kamiokande Collaboration), Phys. Rev. D **71**, 112005 (2005) [arXiv:hep-ex/0501064].
- [68] K. Abe *et al.* (T2K Collaboration), Phys. Rev. Lett. **56**, 1107 (1986); erratum – *ibid.* **56**, 1883 (1986).
- [69] K. Abe *et al.* (T2K Collaboration), Phys. Rev. D **93**, 112012 (2016) [arXiv:1602.03652 [hep-ex]].

Papers on M_A^{run} and its applications

- [70] L. D. Kolupaeva, K. S. Kuzmin, O. N. Petrova, and I. M. Shandrov, “Some uncertainties of neutrino oscillation effect in the $NO\nu A$ experiment,” Mod. Phys. Lett. A **31**, 1650077 (2016) [arXiv:1603.07451 [hep-ph]].
- [71] K. S. Kuzmin, V. A. Naumov, and O. N. Petrova, “Running axial mass of the nucleon for $NO\nu A$ experiment,” presented by O. N. Petrova at the 52’nd Winter School of Theoretical Physics “Theoretical aspects of Neutrino Physics”, 14–21 February 2016, Łańdek Zdrój, Poland. Accepted by Acta Phys. Polon. B (in press).
- [72] K. S. Kuzmin, V. A. Naumov, and O. N. Petrova, “Quasielastic interactions of neutrinos with nuclei in the empirical model of running nucleon axial mass,” presented by O. N. Petrova at the International Session-Conference of the Section of Nuclear Physics of PSD RAS, April 12–15, 2016, JINR Dubna. Accepted by Phys. Part. Nucl. (in press).
- [73] K. S. Kuzmin and V. A. Naumov, “Running axial-vector mass of the nucleon for a precise evaluation of the quasielastic (anti)neutrino–nucleus cross sections,” in preparation.